Export and Regulation of Auxin Transport by PGP/MDR-Type ABC Transporters

---

Dissertation

zur

Erlangung der naturwissenschaftlichen Doktorwürde

(Dr. sc. nat.)

vorgelegt der

Mathematisch-naturwissenschaftlichen Fakultät

der

Universität Zürich

von

Rodolphe Bouchard

aus

Frankreich

Promotionskomitee

Prof. Dr. Enrico Martinoia

Dr. Markus Geisler

Prof. Dr. Ueli Grossniklaus

Prof. Dr. Christian Fankhauser

Zürich, 2005

TABLE OF CONTENT

Summary

Auxin, chemically indole-3-acetic acid (IAA), is of critical importance for the plant livelihood. It is considered as plant hormone and modulates diverse processes in plants such as tropic responses to light and gravity, general shoot and root architecture, organ patterning, vascular development and growth in tissue cultures. From its main synthesis sites, shoot meristem and young leaves, auxin is transported through the whole plant. In the 1970s, a real headway in understanding the transport pathway of auxin was made. It was shown that similarly to other plant hormones auxin is transported via a non-polar transport pathway, the phloem transport, but - being specific to auxin - also via a polar, cell-to-cell transport pathway. Subsequently, a coherent model for the polar auxin transport (PAT) was postulated. This model relies on the asymmetrical distribution of auxin influx and efflux carriers. Along the next 30 years the generation of different auxin response deficient plant mutants and their further characterization allowed to demonstrate the importance of auxin concentration gradients in developmental processes such as apical dominance, organs development, gravi- and phototropisms, as well as identification of auxin influx and efflux transporters. Based on their polar localization, growth defects observed in their mutants, to date members of the PIN-shaped (PIN) protein family are suggested to mediate auxin efflux.

The auxin transport deficiency-related phenotype of the loss-of-function mutation of the putative FK506-binding protein (FKBP) *FKBP42* gene, encoding for the immunophilin-like TWISTED DWARF1 (TWD1), constituted the starting point of this work. A more conceivable link to auxin transport was proposed when the *in vivo* and *in vitro* interaction of TWD1 with two closely related ABC transporters, PGP1 and PGP19, suggested auxin transport components, was demonstrated. The *twd1* phenotype suggested TWD1 to function as a regulator of the transport activity of associated PGPs.

The implication of PGP1 and PGP19 in auxin transport, primarily suggested by the auxin response deficient-like phenotype of the *pgp1*, *pgp19* and more particularly *pgp1pgp19* mutant plants, was further demonstrated by measurement of auxin transport activity on intact plant tissues and on the cellular level. The polar

localization of PGP1 in the mature root, the demonstration of PGP1 auxin transport activity either in heterologous systems or plant systems, confirmed PGP1 as an auxin exporter mediating basipetal root auxin transport. The stronger phenotype of the *pgp19* plant mutant in comparison with *pgp1* mutant plant and measured auxin transport deficiencies on the plant level suggested PGP19 to function as well as auxin exporter

Having our original proposal in mind, the use of over-expressing plants as well as co-expression of TWD1 and PGP1 in yeast and mammalian expression systems allowed demonstrating and confirming TWD1 as a regulator of PGP1- mediated auxin transport activity.

In summary, we identified P-glycoprotein-like ABC transporters as novel auxin transporters. Moreover, we have established a completely new mechanism of P-glycoprotein regulation via protein-protein interaction with FKBP-type immunophilins.

Zusammenfassung

Auxin, chemisch Indolylessigsäure (IAA) ist von entscheidender Bedeutung für das Wohlergehen der Pflanze. Es gilt als Pflanzenhormon und moduliert verschieden pflanzliche Prozesse, wie Tropismen zum Licht oder gegen die Schwerkraft, die Architektur des Sprosses und der Wurzel, die Gliederung der Organe, die Organentwicklung und das Wachstum in Flüssigkulturen. Auxin wird von de Hauptsyntheseorten, dem Sprossmeristem und jungen Blättern, über die ganze Pflanze verteilt. In den 70er Jahren, wurden bahnbrechende Ergebnisse zum Verständnis der Transportwege von Auxin gemacht. Es wurde gezeigt, dass in Analogie zu anderen Hormonen, Auxin unpolar im Phloem transportiert wird, aber auch, spezifisch für Auxin, durch einen polaren Transport von Zelle zu Zelle. Entsprechend wurde ein stimmiges Modell für den so genannten polaren Transport von Auxin (PAT) postuliert. Dieses Modell basiert im Wesentlichen auf der unsymmetrischen Verteilung von Influx- und Efflux-Carriern von Auxin. Innerhalb der nächsten 30 Jahre untermauerte die Charakterisierung entsprechender Mutanten, die nicht auf Auxin reagieren, sowie die Identifizierung von Auxininflux- und Effluxtransportern, weiter die Bedeutung von Auxingradienten für verschiedene Entwicklungsprozesse, wie Apikaldominanz, Organtentwicklung und Gravi- und Phototropismus. Basierend auf ihrer weitgehend polaren Lokalisation und den Wachstumsdefekten ihrer Mutanten, gelten bis heute PIN-shaped (PIN) Proteine als Auxinexporter.

Der Ausganspunkt dieser Arbeit war der Auintransport defizitäre Phänotyp der putativen FK506-binding protein (FKBP) *FKBP42*-Mutante, die für ein Immunophilin-ähnliches Protein namens TWISTED DWARF1 (TWD1) codiert. Ein direkter Zusammenhang zum Auxintransport konnte hergestellt werden, als gezeigt wurde, dass TWD1 mit den ABC-Transportern PGP1 und PGP19, zwei vermutlichen Auxintransport-Komponenten, interagiert. Der Phenotype der *twd1* Mutante prädestinierte TWD1 als Regulator der beiden assoziierten PGPs.
Die direkte Beteiligung von PGP1 und PGP19 am Auxintransport, die ursprünglich auf den Phänotypen der *pgp1*, *pgp19*, und eindeutiger ausgeprägt, der *pgp1 pgp19* Mutanten basierte, wurde durch Messungen des Auxintransports an intaktem

Pflanzengwebe und auf zellulärer Ebene belegt. Für PGP1 wurde gezeigt, dass er polar in älteren Abschnitten der Wurzel lokalisiert ist, und, durch Expression in pflanzlichen und heterologen Expressionssystemen, dass er in der Tat Auxin transportiert, was darauf hinweist, dass PGP1 als Exporter im basipetalen Auxintransport funktioniert. Der ausgeprägtere Phänotyp von *pgp19* im Vergleich zu *pgp1* Pflanzen und Reduktionen im Auxintransport auf der Pflanzenebene, weisen darauf hin, dass PGP19 ebenfalls als Auxintransporter arbeitet.

Unser ursprüngliches Konzept im Hinterkopf, bestätigten Daten an Pflanzen, die PGP1 und TWD1 überexpremimierten, sowie an Hefen, die PGP1 und TWD1 koexprimierten, TWD1 als Regulator des PGP1-vermittelten Auxintransports.

Zusammengenommen ist es uns gelungen ABC-Transporter der P-Glycoprotein-Familie als Auxintransporter zu identifizieren. Darüberhinaus haben wir einen neuen Mechanismus zur Regulation von P-Glycoproteinen über Protein-Protein Interaktion mit FKBP-ähnlichen Immunophilinen etabliert.

I INTRODUCTION

The plant hormone auxin

Auxin, also known as IAA or indole-3-acetic-acid, is of critical importance for plant and human livelihood. This plant hormone modulates diverse processes in plants such as tropic responses to light and gravity, general shoot and root architecture, organ patterning, vascular development and growth in tissue culture. In the 19 th century, the term “auxin” was allocated to the hypothetic molecule modulating both shoot elongation toward light (Darwin, 1881) and root bending toward gravity (Ciesielski, 1872). The hypothetic molecule was later determined to be indole-3-acetic-acid (IAA) (Thimann, 1977).

The most abundant naturally occurring auxin is IAA. Synthetic plant growth regulators such as 1-naphtylacetic acid (1-NAA) and 2, 4-dichlorophenoxyacetic acid (2, 4-D) display auxin-like activities. The NAA isomer, 2-NAA, has little activity in bioassays and provides a control for auxin specificity in experiment using the active 1-NAA.

Besides the free active form, auxin can be conjugated to amino acids, peptides and sugars. Such bound auxin is often present in higher concentration compared to free auxin (Cohen, J.D and Bandurski, R.S., 1982).

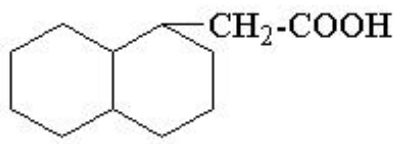

1-naphthylacetic acid (1-NAA)

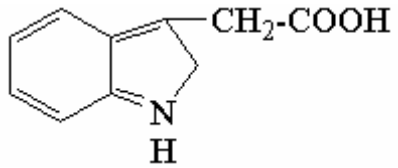

Indole-3-acetic acid (IAA)

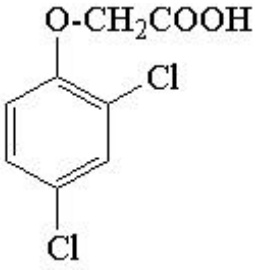

2,4-dichlorophenoxyacetic acid (2,4-D)

Figure 1. Structure of native and synthetic auxins

Auxin transport

Arabidopsis seedlings can synthesize IAA in the shoot apex, leaves, cotyledons and roots; young leaves having the highest biosynthetic capacity. In the 1920s, Cholodny and Went were independently trying to hypothesize how auxin moves from the shoot apex to the elongation zone of the root (Went, 1974). Transport of auxin to distant sites has been shown to be required for normal development.

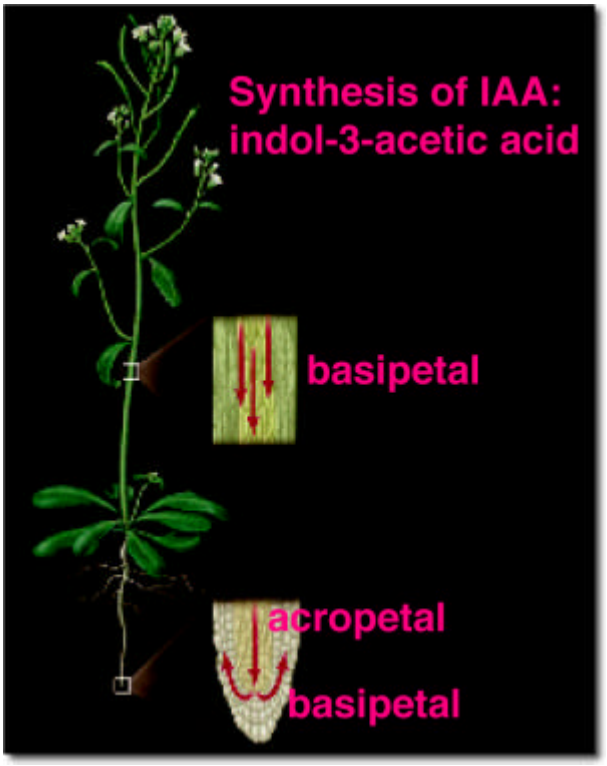

Figure 2: IAA transport in plant **(Jones, A.M., 1998, modified)**

Two main pathways describe the transport of auxin all along the plant (Figure 2). A fast and non-directional transport takes place in the phloem. This transport occurs in basipetal and acropetal directions and seems to correlate with transport of assimilate and inactive auxin conjugates. The second one, the so-called polar auxin transport (PAT) is slow and directional. PAT is specific for free auxin. The PAT stream runs basipetally from the shoot apex towards the base. In the shoot PAT was mainly detected in cambium and adjacent, partially differentiated xylem elements. Noteworthy, in the shoot, in contrast to the root, PAT also occurs in lateral direction. In the root, auxin stream continues acropetally towards the root apex, where a part of

auxin is basipetally redistributed towards the elongation zone through epidermis. PAT requires energy, is saturable and is sensitive to protein synthesis inhibitors. Moreover, PAT implies the existence at the cellular level of specific auxin transport proteins. In the middle of the 1970s a coherent model for auxin transport, was postulated the chemiosmotic hypothesis (Rubery and Sheldrake, 1974; Raven, 1975). This model relies on the asymmetrical distribution of auxin influx and efflux carriers (Figure 3).

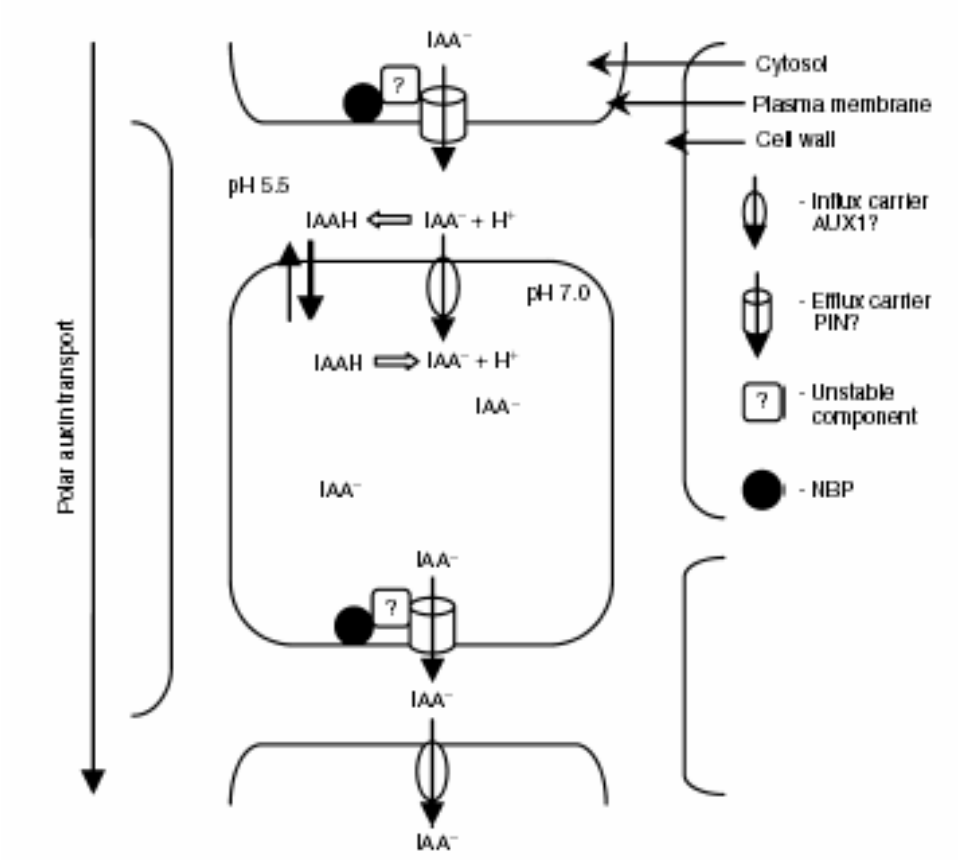

Figure 3: Putative cellular model of PAT (Friml and Wisnieswska, 2004)

Model of cell-to-cell or polar auxin transport. According to the chemiosmotic model, a membrane pH gradiant) maintained by plasma membrane H-ATPases) drives accumulation of IAA within cell. In the cytoplasm, some of the protonated auxin molecules dissociate and are "trapped" inside the cell and can only exit by efflux carrier systems. Asymmetry in the distribution of the efflux carrier results in a directional transport of auxin through the cell file. Efflux carrier is a protein complex containing efflux catalyst and NPA-binding protein (NBP) linked with an unstable component.

Almost 30 years were necessary to identify putative transport components of PAT. Use of chemicals, especially inhibitors of auxin efflux (NPA, 1-N-naphtylphtalamic acid; TIBA 2,3,5-triiodobenzoic acid) or auxin influx (1-NOA, 1-naphtoxyacetic acid; CHPAA, 3-chloro-4-hydroxyphenylacetic acid) allowed identifying candidate genes. The clear identification of components of PAT was mainly due to the screening of plant mutants displaying a deficiency in auxin response. From genetic screening and further characterization it was suggested that auxin efflux is facilitated by members of the PIN protein family (Friml, 2003; Friml and Palme, 2002).

PGP/MDR-like ABC transporters are involved in auxin transport

However several pieces of evidence suggested recently that two Arabidopsis ABC transporters of the MDR/PGP subclass, AtPGP1 and AtPGP19 (AtMDR1; hereafter referred to as AtPGP19), members of the MDR subfamily, are also affecting auxin efflux. AtPGP19 was originally identified by screening of genes differentially expressed in response to an inhibitor of anion channel activity (NPPB; 5-nitro-2-(3-phenylpropylamino)-benzoic acid) (Noh *et al*., 2001). As its closest homologue, AtPGP1, AtPGP19 binds NPA, relating both to the auxin export complex (Noh *et al*., 2001). The phenotype displayed by the *pgp19* single mutant and more especially by the *pgp1 pgp19* double mutant suggested that both PGPs are required for auxin transport in Arabidopsis. The demonstration of deficiency in basipetal auxin transport activity of *pgp19* and *pgp1 pgp19* reinforced the putative role of PGP19 in auxin transport (Noh *et al*., 2001).

ATP-binding cassette (ABC) transporters constitute one of the most abundant families of proteins. In 2003, more than 2000 ABC proteins were identified (Dassa E; 2003). An important characteristic of these proteins is that they share a highly conserved ATPase domain, the ABC, which has been demonstrated to bind and hydrolyze ATP, releasing energy for a wide number of biological processes. The amino acid sequence of this cassette displays three major conserved motifs: Walker A, Walker B and a specific signature motif, known as the ABC signature (also called linker peptide) starting with LSGG (Martinoia *et al*., 2002). It is important to note that the ABC signature motif allows classifying a protein as an ABC one.

ABC systems are involved not only in the import or export of a wide variety of substances, but also in many cellular processes and their regulation. Importers

represent the major part of prokaryotes transporters dependent upon a substrate-binding proteins, whose function is to provide bacteria with essential nutrients. Exporters are found in both prokaryotes and eukaryotes and are involved in extrusion of toxic substances, the secretion of extracellular toxins and the extracellular secretion of proteins (Fath and Kolter, 1993). A third type of ABC system is apparently not involved in a transport system but rather in cellular processes such as DNA repair, translation or regulation of gene expression (Bisbal *et al*., 2000; Chakraburtty, 2001; Tyzack *et al*., 2000).

All the transporters are composed of four structural domains: two very hydrophobic membrane-spanning domain or integral membrane domain (IM) and two hydrophilic cytoplasmic domains containing the ABC domain, peripherally associated with transmembrane domain on the cytosolic side of the membrane. The three different functional class previously mentioned display specific structure and domain organization.

Importers have in general the four domains encoded as independent polypeptides and they need for function an extracellular substrate binding protein. In most well characterized exporters, the transmembrane domains are fused to the ABC domains in several ways. However some systems with separated transmembrane domains and ABC domains have been reported to act as exporters although complete characterization of transport mechanism is awaiting. Prokaryote exporters also require accessory proteins. Systems involved in cellular processes other than transport do not have transmembrane domains and are composed of two ABC domains fused together.

As ATP is principally found in the cytosol, it served to define direction of the transport. Import is defined as the inwardly directed transport of a molecule into the cytosol. Export is, by contrast, the translocation of a molecule out of the cytosol even if its final location is an intracellular organelle.

Plants represent a large source of ABC proteins. The genome of the model plant Arabidopsis thaliana encodes for approximately 130 ABC proteins, distributed into 12 or more subfamilies. Arabidopsis is the first plant, indeed the first multicellular organism, whose ORFs have been systematically inventoried in their entirety. (Garcia *et al*., 2004; Martinoia *et al*., 2002; Sánchez-Fernández *et al*., 2001). The phylogeny of Arabidopsis ABC proteins is represented in Figure 4.

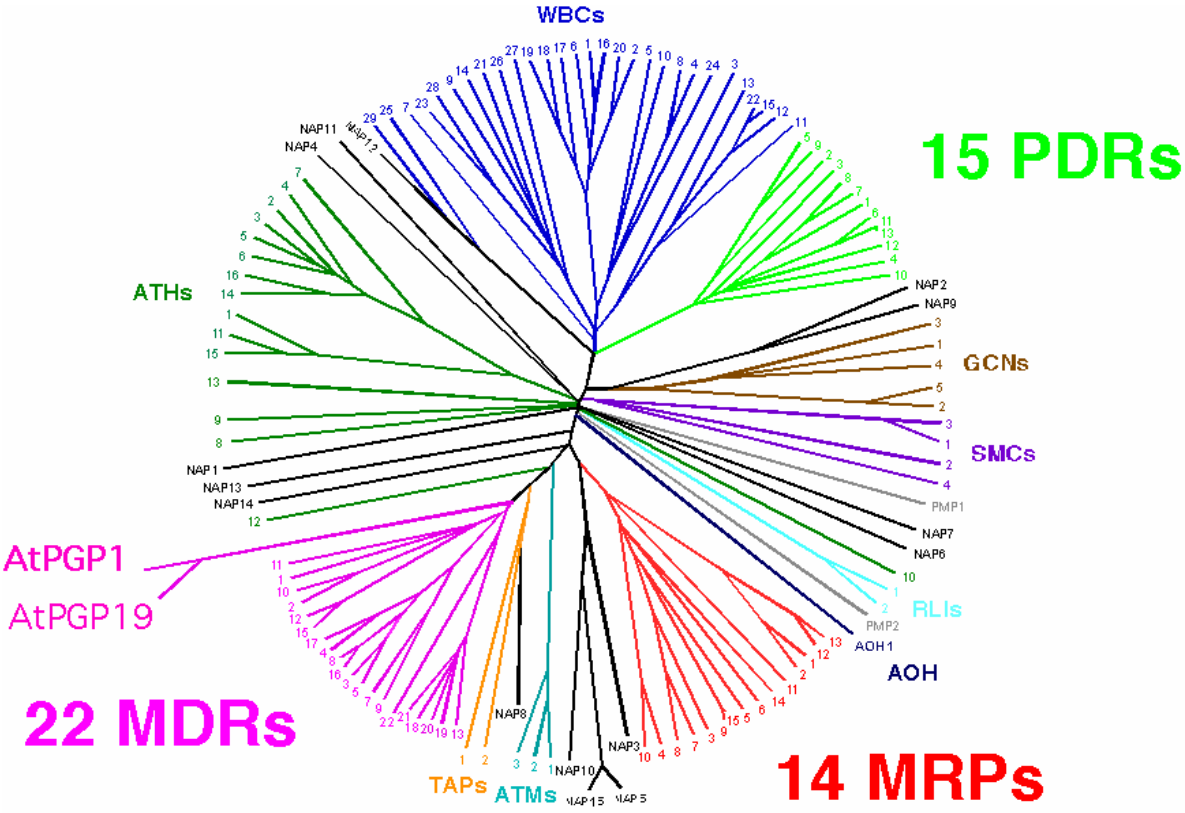

Figure 4: Phylogeny of Arabidopsis ABC transporters (taken from Sánchez-Fernandez et al., 2001, modified). Relevant AtPGPs, AtPGP1 and AtPGP19 (MDR1), are depicted.

12 subfamilies of Arabidopsis ABC proteins are assigned on the base of the protein size (full-, half- or quarter-molecule), orientation (forward or reverse), the presence or absence of idiotypic domain (transmembrane domain, linker domain), the overall sequence similarity. The subfamily name is attributed according to homology to an ABC protein previously described in other organisms. The only family that cannot be categorized in this way is the NAP family as any close resemblance with other Arabidopsis ABC proteins or homology to ABC proteins of other organism is displayed. Domain organization and composition of the 13 identified ABC Arabidopsis proteins is represented in Figure 5.

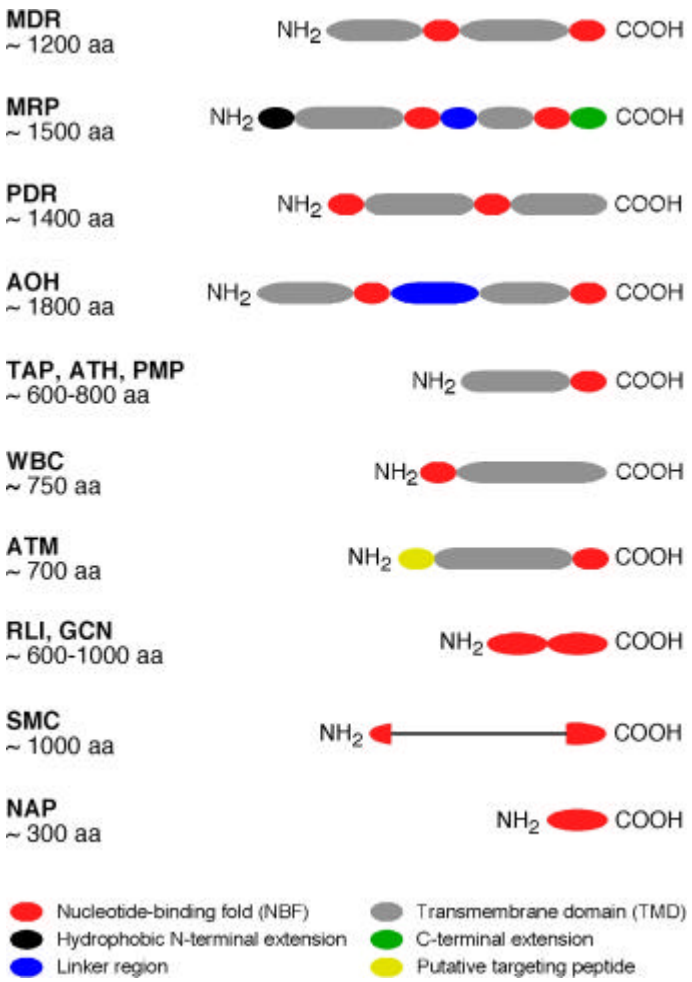

Figure 5: Domain organization of Arabidopsis ABC proteins (taken from Sánchez-Fernandez et al., 2001).

Studies focusing on functions fulfilled by ABC proteins revealed numerous as well as varied roles. Members of the MRP subfamily are implicated in detoxification process participating in vacuolar sequestration of many endogenous compounds which would be toxic whether they were not stored in a compartment separate from the cytosol (Martinoia *et al*., 2002). A common characteristic of MRPs is the preferential transport activity for organic anions. Besides detoxification of xenobiotic such as GS-conjugate herbicide, MRPs may mediate antimicrobial compound storage, protection from oxidative stress, cell pigmentation and chlorophyll catabolism. *At*MRP5 could be considered as an abroad MRP by order of its implication in signal transduction pathway (Gaedeke *et al*., 2001).

The PDR subfamily, the second of so-called full-size ABC transporters, contains 13 members for which the yeast PDR5 protein is the prototype. Two plant PDRs have been described, TUR2 and NpABC1, which are suspected to mediate excretion or mobilization of toxic metabolites and extrusion of sclareolide derivates, respectively (Jasinski *et al*., 2001; Smart and Fleming, 1996).

Noteworthy is the role of AtPMP2, member of the PMPs subclass, a representative of the half-molecule transporters. AtPMP2 has been shown to be responsible for import into the peroxysome of CoA-conjugated compound. Two of them, IBA-CoA and 2, 4-D CoA, after ß-oxydation will provide IAA and 2, 4-D, respectively.

The MDR subfamily is the second largest subfamily with 22 members (21 expressed genes and one pdeudogene) and the largest of the full-size ABC transporter family. The *Arabidopsis* MDR gene, *AtPGP1* was the first plant ABC gene to be cloned (Dudler and Hertig, 1992). In between several members of this subclass have been since cloned from Arabidopsis and other plant sources (Davies *et al*., 1996; Noh *et al*., 2001; Wang *et al*., 1997). Independent investigations carried out to elucidate the role of *AtPGP1* (Sidler *et al*., 1998) and *AtMDR1* (*AtPGP19* in Figure 4, Noh *et al*., 2001) in plant development, gave at a first glance contradictory results, but clear evidences that both ABC proteins are involved in plant development. Sidler *et al*. (1998) showed that control of PGP1 expression affects light-intensity dependent hypocotyls elongation. In contrast Noh *et al*. (2001) reported that contribution of PGP1 alone on morphology is minor considering the similarity of wild type and *pgp1* phenotype, aside developmental stage and light conditions. A more crucial role was attributed to *AtPGP19*. *pgp19* single mutant, and even more double mutant *pgp1 pgp19*, in comparison to wild type display characteristic traits of mutants deficient in

auxin response. Phenotype differences were correlated to measurements of auxin transport activity. Deficiency in basipetal transport activity was highlighted for *pgp19* and *pgp1 pgp19*, reinforcing the idea that *AtPGP19* may exert a prominent role in auxin transport in comparison to *AtPGP1*. The more pronounced auxin transport deficiency of *pgp1 pgp19* mutant and the NPA binding activity of both AtPGP1 and AtPGP19, led to the proposal that auxin transport is mainly affected by *AtPGP19*. The authors proposed for *AtPGP1* to have a similar role as *AtPGP19* but to be expressed to a lower level hiding *AtPGP1* activity.

Mammalian MDR/PGPs functionally interact with immunophilins

ABC transporters have been shown to mediate cytotoxic drug resistance in mammalians. Activity studies using the murine MDR3 ABC-type transporter suggested that yeast immunophilin FKBP12 was required for proper function of this ABC transporter (Hemenway and Heitman, 1996). FKBP12 was also shown to be a regulatory subunit of integral membrane Ca^{2+} channels. In each case the FKBP12-dependent regulation is independent of its PPIase (*cis-trans* peptidyl-prolyl-isomerase) activity (Hemenway and Heitman, 1996, Timmerman *et al*., 1995).

The immunophilins encompasses two major ubiquitous protein families: the FK-506 binding proteins, or FKBPs, and the cyclosporinA-binding proteins, or cyclophilins. (Romano *et al.,* 2005). These proteins were discovered by identification of soil organism. Among these *Tolypocladiun inflatum* was shown to synthesize a cyclic undecapeptide named cyclosporine A (CsA), which showed antifungal and microbial activities. A couple of years later the cyclosporine A was approved for prevention of organ transplant rejection. This led to a search for the cellular receptor of this potent immunosuppressive drug. Fischer *et al*. (1984) identified a highly abundant and a specific 18 kDa protein as the receptor of cyclosporine A. They named this protein cyclophilin. In 1989 two groups found that cyclophilin was also responsible for cytosolic *cis-trans* peptidyl-prolyl isomerase (PPIase) activity. In the same time a fungal polypeptide named FK506, related to the antifungal agent rapamycin, was shown to possess similar pharmalogical properties as cyclosporine. FK-506 and rapamycin were later shown to bind a protein named FK-506 binding protein (FKBP). As cyclophilins FKBPs display a PPIase activity despite the little primary sequence similarity. These two categories of proteins, cyclophilins and FKBPs are collectively named immunophilins. Immunophilins are responsible for suppression of immune T

cell response upon drug binding. Newly synthesized proteins, in order to be functional, have to be converted from their primary linear structure to the active tertiary structure, this protein maturation occurs through folding processes. The folding of globular single-domain polypeptides occurs on a second-millisecond time scale, whereas isomerization of the imidic peptide bond preceding proline residues in an amino acid sequence, also known as a peptidyl-prolyl bond, is a slower, rate-limiting step in the folding process. Prolyl bonds occur in both cis and trans conformation. *cis trans* peptidyl-prolyl isomerases (PPIase) catalyze the rapid isomerization of prolyl bonds from cis to the trans conformation. This enzymatic activity is shared by both FKBPs and cyclophilins.

Immunophilins are ubiquitous proteins. *Escherichia coli* possesses at least six immunophilin-like protein, *Saccharomyces cerevisiae* contains 12 immunophilin isoforms which are localized throughout the cell and have been shown to be dispensable for viability of yeast cell (Dolinski *et al*., 1997). However, the different cyclophilins and FKBPs have been shown to modulate (or being part of) signal transduction pathway and metabolic pathway.

Immunophilins are also present in multicellular organisms. *Drosophilla melanogaster* and *Caenorhabditis elegans* possess 20 immunophilins isoforms, including ubiquitous single-domain and multiple domain isoforms. In *C. elegans* the cyclophilin CYP3 may function as a stress responsive protein and may act as a foldase folding newly synthesized structurally proteins during larval development (Dornan *et al*., 1999). The NinaA cyclophilin of *D.melanogaster* is thought to be a putative chaperone acting in trafficking of rhodopsin (Dornan *et al*., 1999). Furthermore Drosophila FKBP59 is thought to modulate channel activity of the TRPL cation channel (Goel *et al*., 2001).

In mammalians, immunophilins have been studied in details first, in respect to their immunosuppressive activity, but later on interest was carried on their function in absence of their drug ligand. An important single domain immmunophilin, FKBP12, has been shown to associate and modulate the activity of major intracellular Ca^{2+} release channels. FKBP12 in association with the transforming growth factor-ß (TGF-ß) acts as a physiological regulator of cell cycle (Chen *et al*., 1997).

Plant immunophilins control plant development

In plants the discovery of the first immunophilins dates to 1990s. Sequencing of the Arabidopsis genome allowed the identification of 29 cyclophilin isoforms and 23 FKBP isoforms (He *et al*., 2004; Romano *et al*., 2004, Figure 6).

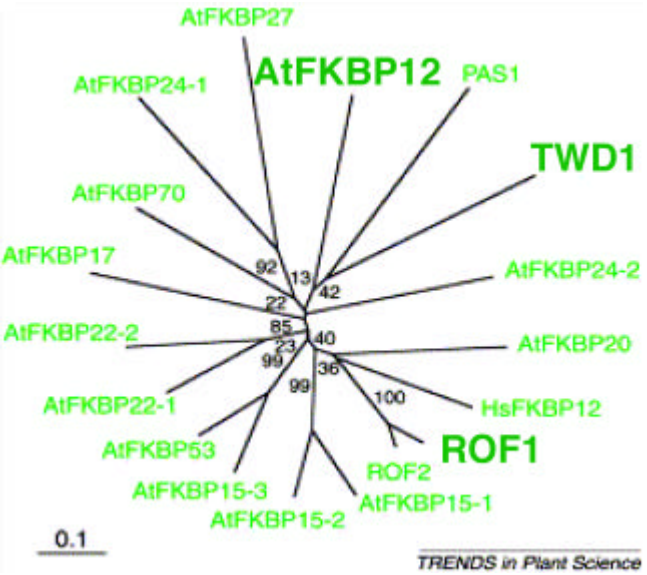

Figure 6: Phylogeny of plant FKBPs (taken from Faure et al. 2001). Relevant FKBPs for this work are printed in bold.

FKBPs localized in the chloroplast have been shown or are supposed, through their chaperone activities, to regulate activity of chloroplast proteins. Furthermore, several studies have pointed out FKBPs as potential actors in plant development. To date, three multi-domains FKBPs have been shown to be putative component of signal transducing pathways analogous to those already described in the animal system. One such functional parallel is the previously described Hsp90 complex, which is known to form functional scaffold of the steroid receptor complex in humans and has been shown to be present in plant (Pratt *et al*., 2001). *In vitro* experiment demonstrated that wheat germ lysate FKBP73 and FKBP77 are able to associate with the mammalian p23 and plant Hsp90 via its TPR domain, suggesting that multi-protein components of this chaperoning mechanism are likely to be conserved between animal and plant kingdom (Reddy *et al*., 1998).

More direct evidence illustrating the role of immunophilins in plant development comes from screens for genes involved in cell division and differentiation. Those

mutants were selected for their hypertrophic growth of aerial tissue when they are grown on medium containing cytokinin. One such class of mutant, named *pasticcino* or *pas* in relation of their excessive accumulation of sugars, encompasses 3 members (Faure *et al*., 1998). *pas* mutants display severe developmental defects throughout the growth stages: embryo formation is altered at the heart stage where cotyledon primordial is initiated, cotyledons do not form correctly, leading to a flat apex, seedlings possess short, thick hypocotyls and misshaped cotyledons and mature plants display abnormal rosettes with multiple shoots (Vittorioso *et al*., 1998). Root development is also affected, primary root is short and any or rare secondary roots are developing. *pas* mutants show altered response to exogenous cytokinin but is not deficient in cytokinin synthesis. The phenotype observed in *pas1* mutants is caused by mutation in the PPIase coding region. FKBP72 possess three FKBP-like domains and three TPR domains. Expression of meristematic homeobox genes KNAT2 and KNAT6 and SHOOT MERISTEMLESS is higher in *pas1* (Harrar *et al*., 2001). Enhanced expression of these genes is consistent with an enlarged meristematic zone that can be mimicked by cytokinin addition. The cytokinin induction of primary cytokinin response markers ARR1 and ARR6 is enhanced and prolonged in *pas* mutants, suggesting that PAS function to repress cytokinin response. Furthermore down-regulation of the primary auxin response genes IAA4 and IAA1 in *pas* mutants suggests an alteration in auxin response.

Additional evidence for implication of multidomain FKBP proteins in plant development comes from the characterization of mutants showing strong developmental abnormalities (Kamphausen *et al*. 2002, Pérez-Pérez *et al*., 2004). These mutants are known as *twisted dwarf1* (TWD1) and is allelic to *ultracurvata2* (UCU2, Pérez-Pérez *et al*., 2004); the phenotype is attributed to disruption of the AtFKBP42 gene. Plants lacking AtFKBP42 display a pleiotropic phenotype which includes dwarfism and helical rotation of a number of organs. These plants show severely distorted roots and stems, have small flowers with occasional homeotic transformation resulting in a partial reduction in fertility. The AtFKBP42 protein consists of an N-terminal inactive PPIase domain, one TPR domain containing three motifs, a putative calmodulin-binding domain and a C-terminal transmembrane domain (Kamphausen *et al*. 2002). AtFKBP42 is a membrane-anchored protein localized on the plasma and vacuolar membrane (Kamphausen *et al*., 2002).

In the present work it is shown that the immunophilin-like protein TWD1 (AtFKBP42), physically interacts with two ABC transporters, AtPGP1 and AtPGP19. It is demonstrated that PGP1 owns an auxin transport activity in both heterologous expression system and *in planta*. Furthermore, evidence is provided that TWD1 modulates activity of the ABC transporter AtPGP1. This suggests that a functional AtPGP1/TWD1/AtPGP19 is essential for efficient auxin efflux controlling plant development.

My contribution to publications where I am not a first author is as follows:

Markus Geisler[*], H. Üner Kolukisaoglu[†¶], Rodolphe Bouchard[*], Karla Billion[†], Joachim Berger[†°], Beate Saal[†], Nathalie Frangne[+], Zsuzsanna Koncz-Kálmán[‡], Csaba Koncz[‡], Robert Dudler[*], Joshua J. Blakeslee[**], Angus S. Murphy[**], Enrico Martinoia[*††] and Burkhard Schulz[†‖††](2003) TWISTED DWARF1, a unique plasma membrane-anchored immunophilin-like protein, interacts with *Arabidopsis* multidrug resistance-like transporters AtPGP1 and AtPGP19. *Molecular Biology of the Cell* **14**: 4238-4249.

In this work I performed the experiments concerning the yeast two hybrid analysis following the screening of an Arabidopsis cDNA library. I also did the cloning of AtPGP1 and AtPGP19 in yeast and plant vectors.

Markus Geisler[1, 5], Joshua J. Blakeslee[2,5], Rodolphe Bouchard[1], Ok Ran Lee[2], Vincent Vincenzetti[1], Anindita Bandyopadhyay[2], Boosaree Titapiwatanakun[2], Wendy Ann Peer[2], Aurélien Bailly[1], Elizabeth L. Richards[2], Karin F. K. Ejendal[3], Aaron P. Smith[2,4], Célia Baroux[1], Ueli Grossniklaus[1], Axel Müller[5], Christine A. Hrycyna[3], Robert Dudler[1], Angus S. Murphy[2,6], and Enrico Martinoia[1] (2005) Cellular efflux of auxin catalyzed by the Arabidopsis MDR/PGP transporter AtPGP1. *Plant Journal* **44**:179-94.

In this work I performed all yeast transport assays and some protoplast transport assays.

II TWISTED DWARF1, a unique plasma membrane-anchored immunophilin-like protein, interacts with *Arabidopsis* multidrug resistance-like transporters AtPGP1 and AtPGP19

Markus Geisler[*], *H. Üner Kolukisaoglu*[†¶], *Rodolphe Bouchard*[*], *Karla Billion*[†], *Joachim Berger*[†°], *Beate Saal*[†], *Nathalie Frangne*[+], *Zsuzsanna Koncz-Kálmán*[‡], *Csaba Koncz*[‡], *Robert Dudler*[*], *Joshua* J. Blakeslee[**], Angus S. Murphy[**], Enrico Martinoia[*††] and Burkhard Schulz[†||††]

* Institute of Plant Biology, University of Zürich, Zollikerstr. 107, CH 8008-Zürich Switzerland

† Universität zu Köln, Botanisches Institut II, Max-Delbrück-Laboratorium, Carl-von-Linné-Weg 10, D-50829 Köln, Germany

+ INRA-UMR, Reproduction et Développement des Plantes, Allée d'Italie 46 , 69364 Lyon Cedex 07, France

‡ Max-Planck-Institut für Züchtungsforschung, Carl-von-Linné-Weg 10, D-50829 Köln, Germany

** Purdue University, Department of Horticulture and Landscape Architecture, 1165 Horticulture Building West, Lafayette, IN 47907-1165

° present address: Max-Planck-Institut für Biophysikalische Chemie, Am Faßberg 11, D-37070 Göttingen, Germany

¶ present address: Universität Rostock, Biowissenschaften - Pflanzenphysiologie, Albert-Einstein Str. 3, D-18051 Rostock, Germany

|| present address: University of Tübingen, ZMBP-Pflanzenphysiologie, Auf der Morgenstelle 5, D-72076 Tübingen, Germany

†† Corresponding authors:
Enrico Martinoia, Institute of Plant Biology, University of Zürich, Zollikerstr. 107, CH 8008-Zürich Switzerland
Tel. +41 1 634 8222
Fax +41 1 634 8204

E-mail: enrico.martinoia@botinst.unizh.ch

Burkhard Schulz, University of Tübingen, ZMBP-Pflanzenphysiologie, Auf der Morgenstelle 5, D-72076 Tübingen, Germany
Tel. +49 7071 29 76667
Fax +49 7071 29 5135
E-mail : burkhard.schulz@zmbp.uni-tuebingen.de

RUNNING TITLE : Immunophilin-ABC transporter interaction

KEY WORDS
FKBP-like protein, protein-protein interaction, ABC transporter, membrane protein

This article was published in *Molecular Biology of the Cell* (2003) **14**: 4238-4249

ABSTRACT

Null-mutations of the *Arabidopsis* FKBP-like immunophilin *TWISTED DWARF1 (TWD1)* gene cause a pleiotropic phenotype characterised by reduction of cell elongation and disorientated growth of all plant organs. Heterogously expressed TWD1 does not exhibit *cis-trans*-peptidylprolyl isomerase (PPIase) activity and does not complement yeast FKBP12 mutants, suggesting that TWD1 acts indirectly via protein-protein interaction. Yeast two-hybrid protein interaction screens with TWD1 identified cDNA sequences that encode the C-terminal domain of *Arabidopsis* multidrug-resistance-like ABC transporter AtPGP1. This interaction was verified *in vitro*. Mapping of protein interaction domains shows that AtPGP1 surprisingly binds to the N-terminus of TWD1 harboring the *cis-trans* peptidyl-prolyl isomerase-like domain and not to the tetratrico-peptide repeat domain, which has been shown to mediate protein-protein interaction. Unlike all other FKBPs, TWD1 is shown to be an integral membrane protein that co-localizes with its interacting partner AtPGP1 on the plasma membrane. TWD1 also interacts with AtPGP19 (AtMDR1), the closest homologue of AtPGP1. The single gene mutation *twd1-1* and double *atpgp1-1*/*atpgp19-1* (*atmdr1-1*) mutants exhibit similar phenotypes including epinastic growth, reduced inflorescence size, and reduced polar auxin transport, suggesting that a functional TWD1-AtPGP1/AtPGP19 complex is required for proper plant development.

INTRODUCTION

Parvulins, FK506 binding proteins (FKBPs) and cyclophilins represent three structurally unrelated classes of immunophilins known to function as *cis-trans*-peptidylprolyl isomerases (PPIases; Schiene and Fischer, 2000). The latter two are distinguished by their ability to bind different immunosuppressant drugs, either FK506/rapamycin or cyclosporin A (CsA). These products of soil-borne microorganisms are used to treat and prevent graft rejection in organ transplantation. Cyclophilin-CsA and FKBP12-FK506 complexes bind to calcineurin (PP2B), a Ca^{2+}, calmodulin-regulated Ser/Thr-specific protein phosphatase, and thereby blocking Ca^{2+}-dependent signalling (Cardenas *et al*., 1999; Harrar *et al*., 2001) leading to inhibition of T-cell activation. Additionally, CsA and FK506 play a role in reversing multidrug resistance (MDR) in several types of cancer by inhibiting the efflux of anticancer drugs (Cardenas *et al*., 1999).

Small FKBPs such as FKBP12 are thought to modulate signal transduction pathways (Harrar *et al*., 2001). FKBP12 functions as physiological regulator of the cell cycle. Cells from FKBP-deficient (FKBP12-/-) knock-out mice are arrested in G1 phase of the cell cycle (Aghdasi *et al*., 2001).

High molecular weight FKBPs are composed of one or more FKBP12-like domains and can be distinguished from their smaller counterparts by the presence of a tetratrico-peptide repeat (TPR) domain (Das *et al*., 1998, Pratt *et al*., 2001), and a C-terminus that in most cases contains a putative calmodulin-binding domain (Harrar *et al*., 2001). Mammalian FKBP52, the best investigated example, is associated with hsp90 by its TPR domain in the native steroid hormone receptor complex (Silverstein *et al*., 1999) but plant high-molecular weight FKBPs bind plant hsp90 via the same TPR interaction as the mammalian homologues (Pratt *et al*., 2001; Kamphausen *et al*., 2002).

A recent proteomic investigation of *Arabidopsis* thylakoid lumen proteins describes 22 annotated FKBP-like proteins with predicted molecular weight from 12kDa to 72kDa in the entire genome (Schubert *et al*., 2002). While yeast seems to be viable without immunophilins (Dolinski *et al*., 1997), drastic phenotypes have been associated with mutations in individual plant immunophilins. Loss-of-function mutations in the cyclophilin40 homolog of *Arabidopsis* lead to reduction in number of juvenile leaves (Berardini *et al*., 2001). The *Arabidopsis* T-DNA mutant *pasticcino1*

(*pas1*), which lacks a 72kDa FKBP is characterized by ectopic cell division, abnormally developed cotyledons and leaves, fusion of tissues and impaired root development (Faure *et al*., 1998; Vittorioso *et al*., 1998). The *Arabidopsis* FKBP42 mutant *twisted dwarf1* (*twd1*), results in a drastic reduction of cell elongation combined with a disoriented growth behavior (see Figure 1). Genetic analysis of *twd1* null mutant demonstrates that TWD1 plays an important role in brassinosteroid reception or signal transduction (Schulz *et al*., submitted).

We show here that TWD1 interacts with the MDR-like proteins AtPGP1 and AtPGP19, both members of the ABC transporter superfamily. AtPGP1 was the first MDR-like ABC transporter identified in *Arabidopsis* (Dudler and Hertig, 1992). Based on the AGI sequence data (AGI, 2000), 22 members of the AtMDR subfamily have been annotated in the *Arabidopsis* genome (Martinoia *et al*., 2002; Sanchez-Fernandez *et al*., 2001). Like TWD1, AtPGP1 and AtPGP19 seem to be directly involved in plant growth processes. Downregulation of *AtPGP1* by antisense inhibition causes a reduction of hypocotyl elongation in seedling grown under low light, whereas *AtPGP1* overexpression leads to enhanced hypocotyl and root elongation (Sidler *et al*., 1998). Recently, Noh *et al*. (2001) and Murphy *et al*. (2002) have provided biochemical and genetic evidence suggesting that AtPGP1 together with its closest homologue AtMDR1, identified hereafter as AtPGP19 according to the nomenclature of Martinoia *et al*. (2002), are involved in polar auxin transport and auxin-mediated development: auxin transport was greatly impaired in hypocotyls of *atpgp19* and *atpgp1 atpgp19* double mutants and both proteins tightly bind the auxin transport inhibitor 1-naphtylphtalamic acid (NPA*). atpgp1-1/atpgp19-1* (*mdr1-1*) double knock-out mutants exhibit epinastic cotyledons, shortened and curved hypocotyls in the dark, curled rosette leaves and dwarfed light-grown plants which strikingly resemble *twd1* mutants.

FKBPs have been suggested to function as regulators of MDR-like ABC transporters (Cardenas *et al*., 1994), but any attempts to demonstrate a direct association with FKBP-like immunophilins have failed so far (Hemenway and Heitman, 1996; Mealey *et al*., 1999).

Here we show, that TWD1 forms a protein-protein complex via the C-terminus of the ABC transporter AtPGP1 and that both co-localize and associate on the plasma membrane.

MATERIALS AND METHODS

Plant growth conditions.

Seedlings were grown on 0.5 x MS medium (Duchefa, Haarlem, The Netherlands) containing 1% sucrose under continuous light. Plants grown on soil were grown under white light (photon flux rate 100 µmol m^{-2} s^{-1}; 8h light/16h dark cycle at 20°C).

Yeast two-hybrid analysis.

The coding region of the *TWD1* gene from codon 1 to 337 was amplified by PCR (BUSUP: 5' gga aaa acc atg gat gaa tct ctg gag cat caa act c, BUSdownB: 5'gga aaa agg atc ctt agc tct ttg act tag cac cac c) and cloned in frame via *Nco*I and *Bam*HI restriction sites into pAS2, generating a protein fusion between TWD1 and the GAL4 DNA-binding domain (pAS2-BusB). The bait construct pAS2-BusB was used to screen an Arabidopsis cell suspension cDNA library inserted into pACT2 (Nemeth et al. 1998). Fast growing colonies were selected on SD plates lacking leucine, tryptophan and histidine with 50 mM 3-amino-1, 2, 4-triazole and ß-gal positive clones were sequenced.

To identify the interaction domain of the TWD1 protein, subclones of pAS2BusB were constructed. The PPIase-like domain (aa residues 1 – 163) and TPR domain omitting the membrane anchor (aa residues 163 – 337) of TWD1 were fused to the Gal4 BD of vector pAS2 (Clontech, Palo Alto, CA).

The nucleotide sequences encoding the C-termini of AtPGP10 (MIPS code At1g10680, bp 2812-3681), AtPGP13 (At1g27940, bp 2872-3735), AtPGP14 (At1g28019, bp 2876-3744) and AtPGP19 (At3g28860, bp 2893-3756) were cloned by two-step RT-PCR. Therefore, total RNA from *A. thaliana* (Wassilewskija ecotype) grown in liquid culture under mixotrophic conditions was prepared using the RNA Plant Mini Kit (Qiagen, Hilden, Germany). cDNA was generated from 1 µg of RNA using the M-MLV Reverse Transcriptase, RNase H^- Point Mutant DNA Polymerase (Promega, Madison, WI) and the following gene-specific primers located in the 3` untranslated region of the genes: AtPGP10: 5' ttc ctt tca aga atg aat agc, AtPGP13: 5' gtg tcc aga tat tcc tga cac, AtPGP14: 5' tag ata ttc cca aca caa tcg, and AtPGP19: 5' cat agt tca gtc tta tgt tcc. The C-termini were inserted into pACT2 after PCR amplification using Vent DNA Polymerase (New England Biolabs, Frankfurt, Germany), and the following primers (UP/LP): AtPGP10: 5' acg gaa ttc tgg gtg aag

tgt tgg ctc tag/ 5’ acg ctc gag tta agg atg atg gcg ctg ccg, AtPGP13: 5’ acg gaa ttc tgt cgg aaa cgc ttg ctt tga/ 5’ acg ctc gag tca cag tac ttc ttg aag act c, AtPGP14: 5’ acg gaa ttc tgg cgg aaa cgc ttg cgt taa cc/ 5’ acg ctc gag tca cac cgc ttc ttg aag act c, AtPGP19: 5’ acg cca tgg aaa ctc tca gtc ttg ctc ctg/ 5’ acg gga tcc tca aat cct atg tgt ttg aag c. AtPGP2 (At4f25860) was amplified by PCR from the plasmid Y97 using the primers (UP/LP): 5’ acg gaa ttc tgg aga cat tgg ctc tag ctc cg/ 5’ acg ctc gag tta agg ttg ttg ctg ctg ctg. All RT-PCR products were sequenced to verify the absence of mistakes.

For interaction analysis, three to five independent transformants of two independent constructs were tested for HIS auxotrophy and LacZ (ß-galactosidase) reporter activity. Single colonies were resuspended in 1 ml of sterile water and 5 µl each were spotted on SD plates lacking leucine, tryptophan and histidine containing 25 mM 3-amino-1, 2, 4-triazole. Another 5µl were spotted on plates with selective media supplemented with 30µg/ml 5-bromo-4-chloro-3-indolyl-α-D-galactopyranoside (X-α-Gal). Growth was judged after 3 days. ß-galactosidase activity was quantified by liquid culture assay using standard protocols.

Recombinant expression of the TWD1- and AtPGP1 protein.

PCR-amplified *TWD1* (Primers: JOE1: 5´ cgg gat ccc agg ttg att tgg gaa ata atg g and 6118: 5' ggg ggt aga tct ttc acg ttg) was restricted with *Bam*HI and *Bgl*II and inserted into the *Bam*HI-site of pQE31 (Qiagen, Hilden, Germany). Restriction of the PCR product with *Bam*HI and *Ssp*I removed the putative membrane anchor and the resulting fragment corresponding to aa residue 1 to 324 was ligated into *Bam*HI and *Sma*I digested pQE31 (pTWD1-3). TWD1-3 peptides as N-terminal $RGSH_6$ tagged fusions were purified on Ni-NTA agarose (Qiagen, Hilden, Germany) under native conditions and dialyzed twice against 50 mM MOPS pH 7.0. Immunodetection of TWD1-3 on Western blots was performed with polyclonal antiserum against TWD1-1 peptide (see section Immunocytochemistry and confocal fluorescence microscopy analysis).

The insert of clone pACT2-4F12 encoding the C-terminus of AtPGP1 was cut out from the two-hybrid vector using *Bgl*II sites flanking the insert and ligated in-frame into the *Bam*HI site of pQE32 (Qiagen, Hilden, Germany). The resulting peptides were expressed as an N-terminal 6xHis-tagged fusion protein in *E.coli* strain BL21D3

pLysC (Stratagene, La Jolla, CA) and immunoprobed with polyclonal antiserum against AtPGP1-1 peptide (Sidler et al., 1998).

***In Vitro* binding assay**s.

Ni-NTA-affinity purified TWD1-3 peptides were immobilized to affigel-10 beads (Biorad, Hercules, CA) as recommended by the manufacturer. Matrix-bound TWD1-3 (1µg) was incubated for 1h at 4°C with cleared *E.coli* supernatants from cells overproducing the C-terminus of AtPGP1, H^+-ATPase AHA2 (expressed from plasmid pMP900, Fuglsang *et al.,* 1999) or vector control lysates diluted twice with binding buffer (50mM MOPS pH 7.4, 100mM NaCl, 10% (v/v) glycerol, 2mM $CaCl_2$, 2mM $MgCl_2$). After washing of the matrix-protein complex with binding buffer, the bound proteins were eluted by boiling the matrix with probe buffer and equal volumes of bound and non-bound protein were detected by Western blot analysis using monoclonal anti-$RGSH_6$, anti-penta His (both from Qiagen, Hilden, Germany) and anti-ACA4N27 (Geisler *et al.,* 2000) recognizing the PGP1 C-terminus, TWD1-3 and the GST fused to the AHA2 C-terminus, respectively. Individual bands were quantified using the Scion Image software 1.63 (http://www.scioncorp.com).

Membrane fractionation.

Equal volumes of *Arabidopsis* microsomes, separated by continuous sucrose gradient centrifugation, were blotted onto nitrocellulose membranes and probed with anti-AHA3 antiserum (no. 762; 1: 3000), anti-V-ATPase antiserum (2E7; 1: 200), anti-BIP antiserum (tobacco BIP; 1: 5000) anti-AtPGP1 antiserum (1: 1000) anti-TWD1 antiserum (1: 1000) and monoclonal antibodies anti-HA (clone 12CA5; 1: 3000, Roche Diagnostics, Basel, Switzerland) and anti c-myc (clone 9E10; 1: 3000, Roche Diagnostics) as described in Geisler *et al*., 2000.

Plasma membranes were purified by one-step aqueous two-phase partitioning of *Arabidopsis* microsomes in a 6.2% (w/w) dextran T500/PEG4000 phase system containing 3mM KCl and 5mM potassium phosphate buffer pH 7.8. *Arabidopsis* microsomes were prepared from 75g of a 4 days old cell suspension culture (cell line T87) grown in the dark (Axelos *et al*., 1992).

Transgenic plants.

Arabidopsis plants, ecotype Columbia, were transformed with an expression construct for a hemagglutinin (HA)-tagged TWD1 protein. Therefore, the entire open reading frame of TWD1 was amplified by PCR (TAGfor1: 5' gac ctc gag gtt aac aat ggc tta and TAGrev1: 5' cgc gga tcc gga gcg taa tca ggt aca tcg) and inserted into the *Bam*HI site of cloning vector pRTΩ-NotI (Überlacker and Werr, 1996). To fuse the 9 aa long HA1-tag to the TWD1 peptide, the construct was digested with *Xho*I and *Bam*HI to remove the ?-sequence from tobacco mosaic virus which was replaced by an HA1-tag with compatible ends (pRTΩ-NotI3/4T). The cassette containing the CaMV 35S promoter and the HA-tagged TWD1 gene was excised with *Asc*I and inserted after Klenow fill-in into the blunted *Hind*III site of binary vector pPTV-BAR (Schulz *et al*., submitted). The resulting binary construct pPTV3/4/2T was used to transform *Arabidopsis* via vacuum infiltration using Agrobacterium strain GV3101. BASTA resistant transformants were selected on soil and a line containing a single copy T-DNA was selected by Southern blot hybridization (our unpublished results).

Immunocytochemistry and confocal fluorescence microscopy analysis.

For TWD1 antiserum production, a partial peptide (TWD1-1) comprising the first 187 aa of TWD1 was cloned into pET3-His, expressed as a 6xHis-tag version in *E.coli* strain Bl21DE3 (Stratagene) and purified under denaturing conditions by Ni-NTA agarose chromatography. The purified protein was subjected to preparative SDS-PAGE and the eluted band was used for antiserum production performed by BioGenes Inc. (Berlin, Germany) using standard protocols.

Protoplasts from leaves of HA-TWD1 expressing plants were prepared, fixed and immunocytochemistry was performed as described in Geisler *et al*., 2000. Incubations with monoclonal anti-HA high affinity antibody (clone 12CA5; Roche, Rotkreuz, Switzerland) and secondary anti-mouse antibody coupled to FITC (Jackson Immuno Research Laboratories, West Grove, USA) were performed for 1h with a 1:100 dilution. FITC and TRITC fluorescence was detected with the corresponding filter sets and stored images were colored as green (FITC) or false colors (TRITC) using Adobe PhotoShop 5.5 (Adobe Systems Inc., San Jose, USA).

Co-immunoprecipitation.

Immunoprecipitations were carried out using the Seize X Protein G Immunoprecipitation Kit and the imidoester crosslinker DTBP according to the manufacturer (Pierce, Rockford, USA). Approximately 500µg of Arabidopsis microsomes, prepared as described above, were crosslinked at 4°C and membrane proteins were solubilized using 2% (v/v) TX-100. Cleared lysates were loaded on anti-AtPGP1 columns made by binding and crosslinking of the antiserum to Protein G. After washing, bound proteins were eluted, separated by PAGE in the presence or absence of DTT and probed against anti-TWD1 antisera.

TWD1 affinity chromatography.

Solubilized microsomal proteins were prepared from 6d light-grown HA-TWD1 over-expressing seedlings and separated by anion exchange chromatography as described previously (Murphy *et al*., 2002) with the exception that the phase separation enrichment of plasma membrane proteins and preliminary gel permeation chromatography steps were eliminated and the solubilization buffer contained 50 µM naphtylphtalamic acid (NPA) where noted. After SDS-PAGE, Western blots were prepared utilizing anti-HA-epitope (Sigma, St. Louis MO) and alkaline phosphatase-conjugated goat anti-rabbit polyclonal antibodies, and visualized with Lumiphos (Roche, Indianapolis IN) reagent.

Separately, native HA-tagged TWD1 was purified from microsomal membrane proteins of HA-TWD1 over-expressing plants solubilized with 50 µM NPA (see above) utilizing immobilized anti-HA affinity resin (Roche, Indianapolis IN). After extensive washing with PBS, solubilized microsomal proteins were incubated with the affinity matrix for 4h at 4°C, and washed extensively with PBS. Immobilized proteins were then eluted with 30µM NPA in PBS and visualized by SDS PAGE and Western blotting with a polyclonal anti-PGP1 antibody (Sidler *et al*., 1998) and goat anti-rabbit antibody as above.

Auxin transport assays.

Auxin transport assays were conducted on intact light grown seedlings as described previously (Noh *et al*., 2001; Murphy *et al*., 2000), with the following exceptions: seedlings (WS wild-type, twd1-1, atpgp1-1, atpgp19-1, and atpgp1-1/atpgp19-1) used in the transport assays were grown in light on 1% phytagar plates containing 0.25 x MS (pH 5.2) and 1% sucrose until hypocotyl lengths reached 5 mm. Prior to assay, 10 seedlings were transferred to vertically discontinuous filter paper strips saturated in 0.25 x MS and allowed to equilibrate for 1.5 hours. Auxin solutions used to measure transport were made up in 0.25% agarose containing 2% DMSO and 25 mM MES (pH 5.2). Using microscope-guided micromanipulators, 0.1µl microdroplet containing 500 nM unlabelled IAA and 500 nM ^{3}H-IAA (specific activity 25 Ci/mmol, American Radiochemical, St. Louis, MO) was placed on the apical tip of seedlings. Seedlings were then incubated in the dark for 5 h. Following incubation, the upper hypocotyls and cotyledons were removed, and a 2-mm section centered on the root-shoot transition zones was harvested, along with a 4 mm basal section of each root.

RESULTS

Loss-of-function mutation of the *Arabidopsis* FKBP-like immunophilin *TWISTED DWARF1 (TWD1)* gene results in dramatic differences in growth and organ development in comparison to wild-type. The pleiotropic mutant phenotype is characterised by reduction of cell elongation and disorientated growth of nearly all plant organs. Leaves and cotyledons of twd1-1 show epinastic growth, hypocotyls are shorter and root growth is reduced in the light, but enhanced in the dark. Cell elongation in twd1-1 plants is severely impaired which results in a dwarf phenotype (see Figure 7; Schulz *et al*., submitted).

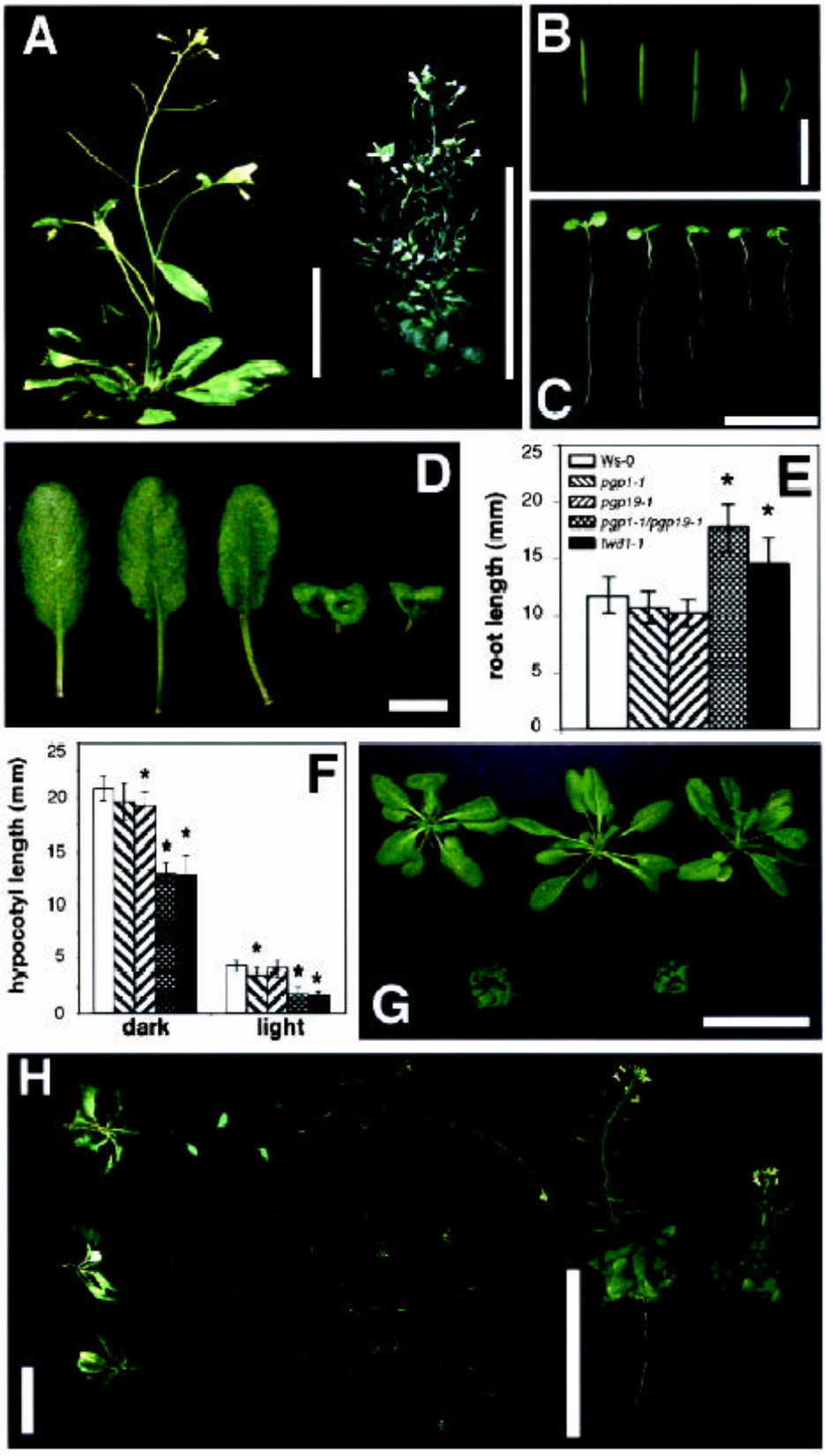

Figure 7. The twisted dwarf1 (twd1) mutant displays a pleiotropic developmental phenotype resembling atpgp1-1/atpgp19-1 (atmdr1-1) double mutants

Figure 7. The twisted dwarf1 (twd1) mutant displays a pleiotropic developmental phenotype resembling atpgp1-1/atpgp19-1 (atmdr1-1) double mutants (cont.)

A. Phenotype of soil-grown wild-type (left) and *twd1-1* (right) plants at maturity. Bars, 5 cm.

B. Siliques of wild-type, pgp1-1, pgp19-1, pgp1-1/pgp19-1 and twd1-1 (from left to right) plants showing disoriented growth behavior. Bars, 1 cm.

C. Light grown seedlings 5 d after germination. From left to right: wild-type, atpgp1, atmdr1 (atpgp19), mdr1/pgp1, twd1.Bar, 1 cm.

D. Rosette leaves of wild-type, pgp1-1, pgp19-1, pgp1-1/pgp19-1 and twd1-1 (from left to right) plants. Double mutant and twd1-1 show strongly reduced leaf expansion and strong epinastic growth behavior. Bar, 1 cm.

E. Dark-grown seedlings of pgp1-1/pgp19-1 (mdr1-1) and twd1-1 plants have longer roots. Seedlings were grown on plate in darkness and root lengths. Root lengths were measured with a ruler (> 10 seedlings) after 8 days and are presented as means plus standard deviations. Plant growth being statistically different (Mann-Whitney U test, $p > 0.05$) compared to wild-type control plants is indicated by an asterisks.

F. Seedlings of *atpgp1-1*/*atpgp19-1* (*atmdr1-1*) and *twd1-1* plants have longer hypocotyls. Seedlings were grown on plate in darkness or continuous white light. Hypocotyl lengths were measured with a ruler (> 10 seedlings) after 8 days and are presented as means plus standard deviations. Plant growth being statistically different (Mann-Whitney U test, $p > 0.05$) compared to wild-type control plants is indicated by an asterisks.

G. Phenotype of soil-grown plants after 40 d of culture. Upper panel from left to right: wild-type, *atpgp1-1*, *atpgp19-1* (*atmdr1-1*), lower panel: *atpgp1-1*/*atpgp19-1* (*atmdr1-1*) double mutant, *twd1-1*. Bar, 5 cm.

H. Reduced apical dominance in *atpgp1-1*/*atpgp19-1* (*atmdr1-1*) and *twd1-1* plants. Plants (left panel from top to bottom: wild-type, *atpgp1-1*, *atpgp19-1* (*atmdr1-1*); right panel from left to right: *atpgp1-1*/*atpgp19-1* (*atmdr1-1*) and *twd1-1*) were cultured on soil for 70 d. Note the size bars differ between left and right panels.

Isolation of AtPGP1 as a TWD1-interacting protein

Heterologously expressed TWD1 does not exhibit a PPIase activity (Kamphausen *et al*., 2002) and does not complement yeast FKBP12 shown by its inability to restore the sensitivity towards rapamycin, which is caused by disruption of the FKBP12 gene in yeast (data not shown). Therefore, we assumed that TWD1 acts indirectly via protein-protein interactions.

Screening of an *Arabidopsis* cDNA library made from suspension culture with the entire cytosolic domain of TWD1 as bait (BusB, TWD1 amino acid (aa) residues 1-337, Figure 8B) resulted in more than 1,800 His-auxotrophic clones. 48 ß-galactosidase-positive prey clones were sequenced and six out of those encoded C-terminal peptides of multidrug resistance-like ABC transporter (ABCB1) AtPGP1 (Dudler and Hertig, 1992; Martinoia *et al*., 2002). Colony hybridization with these cDNA clones revealed that approximately 7% of all clones harboured *AtPGP1*-like sequences. The specificity of TWD1 interaction with AtPGP1 was confirmed using unrelated CBL1 and CIPK proteins (Shi *et al*., 1999) as positive and GAL4-binding domain (BD) or activation domain (AD) alone not interacting with TWD1 or AtPGP1 as negative controls, respectively (Figure 8A).

All TWD1-interacting AtPGP1 prey constructs coded for the C-terminus of AtPGP1 carrying the C-terminal nucleotide binding fold covering the Walker A and B boxes and the intermediate ABC signature (Martinoia *et al*., 2002; Rea *et al*., 1998). Similar galactosidase activities with all *AtPGP1* clones suggest that a peptide of 237 aa (aa residues 1049 - 1286) is sufficient for interaction.

Interaction with AtPGP1 is mediated by the PPIase-like domain of TWD1

To assess whether the TPR domain – a 34aa long protein-protein interaction motif (Das *et al*., 1998; Owens-Grillo *et al*., 1996; Pratt *et al*., 2001) localized in the C-terminal part of TWD1 - was responsible for the interaction with AtPGP1, we generated GAL4-BD fusions covering the PPIase-like (aa residues 1 - 163) and the TPR domains (aa residues 163 - 337) of TWD1. Surprisingly, AtPGP1 interacted only with the N-terminus containing the PPIase-like domain, but not with the TPR domain containing part of TWD1 (Figure 8B) as can be judged from the ß-galactosidase activity test on colonies as well as growth on plates lacking histidine.

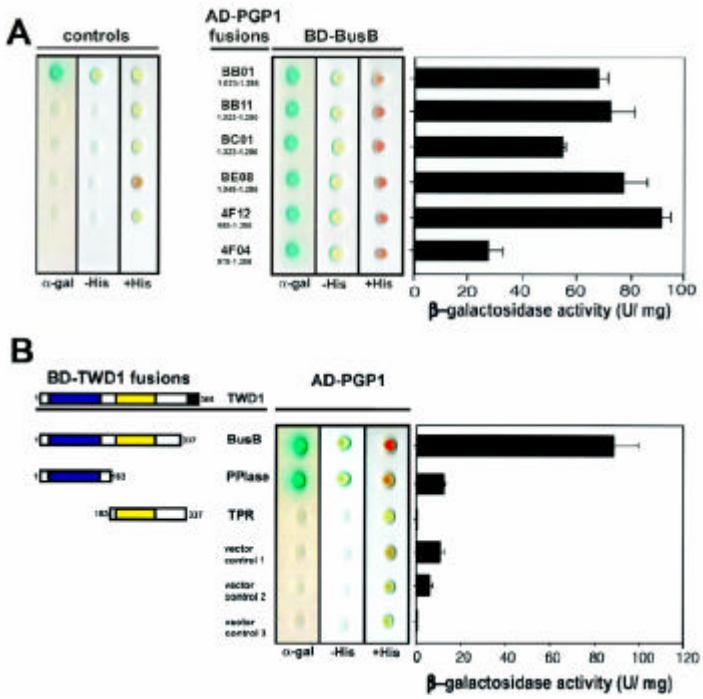

Figure 8. Analysis of TWD1-AtPGP1 interaction

A. Interaction between TWD1 (BD-BusB) and six AtPGP1 clones fused to the GAL4 activation domain (AD) isolated in a yeast 2-hybrid screen. Controls are from top to bottom: pGBT9.BS-CBL1/ pGAD-CIPK (positive control), pGBT9.BS vector/ pGAD vector, BD-BusB/ AD vector, BD vector/ AD-4F12 and AD vector/ BD vector (negative controls).

B. The PPIase-like domain of TWD1 is responsible for the interaction with AtPGP1. The PPIase-like and the TPR-domain of TWD1 as GAL4 binding domain (BD) fusions were tested against activation domain AD-PGP1 fusion (clone 4F12). Colored boxes represent the following putative functional domains: blue, *cis-trans*-peptidyl proly isomerase domain; yellow, tetratrico-peptide repeat; black, membrane anchor.

Transformants were analyzed for histidin auxotrophy and LacZ (ß-galactosidase) reporter activity. Single colonies were spotted on selective media plates supplemented with X-α-Gal. LacZ reporter activities were quantified by liquid culture assays and are displayed as units per mg protein; error bars represent standard deviations from three to five independent transformants.

Very recently, both AtPGP1 and its closest homolog AtPGP19 (AtMDR1) were co-purified by NPA affinity chromatography (Murphy *et al*., 2002) and have been implicated in polar auxin transport (Noh *et al*., 2001; Luschnig 2002). To test whether the C-terminus of AtPGP19 was also able to bind to TWD1, we generated GAL4-AD fusions of a homologous stretch of AtPGP19 (aa residues 965 – 1252). AtPGP19 interacted specifically with TWD1 in the yeast two-hybrid system, while the C-termini of related multidrug-resistance ABC transporters AtPGP2, AtPGP10, AtPGP13 and AtPGP14 did not (Figure 9A). ß-galactosidase and HIS-auxotrophy assays suggest similar strengths of interaction for AtPGP1 and AtPGP19 with the TWD1 construct

BusB. However, the interacting domain of AtPGP19 could not be mapped clearly to either the PPIase-like or TPR domain of TWD1 (Figure 9B).

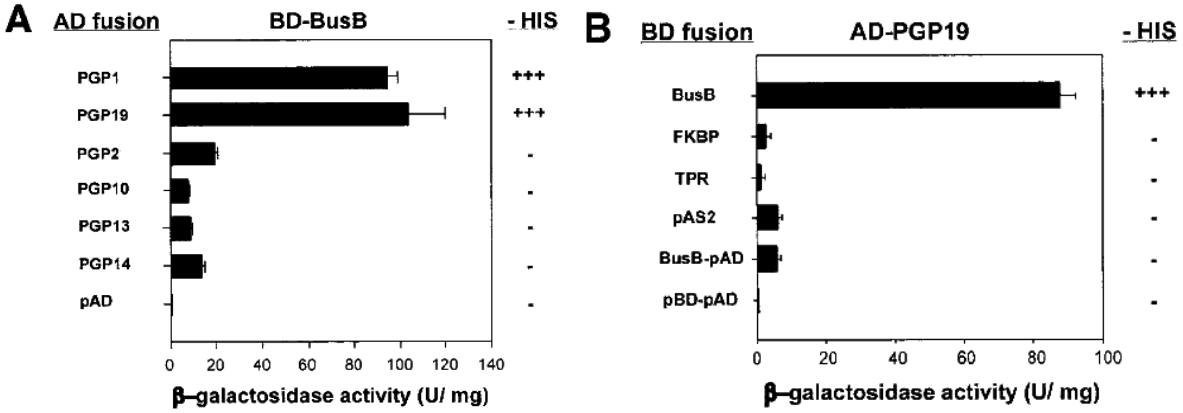

Figure 9. The entire TWD1 protein is essential for interaction with AtMRP19

A. TWD1 interacts specifically with AtPGP1 and AtPGP19

TWD1 fused to a GAL4 binding domain (BD-Bus) was tested for interaction with AD fusion of AtPGPs that are closely related to AtPGP1. See Material and Methods for accession numbers.

B. Mapping of TWD1 domains that interact with AtPGP19. TWD1 fragments fused to a GAL4 binding domain (BD) tested for interaction with AD-PGP19 are represented by boxes and correspond to Fig. 2. Activation of histidine growth reporter (growth on –HIS) is indicated by + and -; LacZ reporter activities are displayed as units per mg protein. Error bars represent standard deviations from three to five independent transformants.

In vitro protein interaction assay

To verify the two-hybrid data in vitro, AtPGP1 peptide 4F12 was expressed in E. coli shown as Coomassie stain and Western detection using anti-$RGSH_6$ (Figure 9C, lane 2 and 6). TWD1-3 (aa residue 1 – 337) was affinity purified on Ni-NTA agarose (Figure 10C, lane 1 (Coomassie stain) and lane 5 (Western detection using anti-penta His)) and immobilised on affigel beads. The TWD1 affinity matrix was able to quantitatively sediment the AtPGP1 C-terminus of 42 kDa from soluble E.coli extracts shown by Western analysis of corresponding amounts of bound (P) and unbound fractions (SN). Monoclonal anti-$RGSH_6$ and anti-penta His were used to recognize the PGP1 C-terminus and TWD1-3, respectively (Figure 10C, lanes 9 and 10). This high ratio (100%) indicates the specificity of TWD1-AtPGP1 interaction. As eukaryotic glycoproteins are not glycosylated when expressed in E.coli, this result suggests that the interaction of TWD1 with AtPGP1 is dependent on primary amino acid sequence interactions rather than interactions of TWD1 with carbohydrate moieties.

Using the same pair of antisera, no AtPGP1 protein was detected in bound fractions of controls in which a vector control lysate (Figure 9C, lane 11), or the empty affigel resin (Figure 10B, lane 15) was used. As a specific control, we tested the C-terminus of plasma membrane H^+-ATPase AHA2, which binds to 14-3-3 proteins (Fuglsang *et al.,* 1999). The AHA2 C-terminus (aa residues 850 - 948) that was expressed as GST fusion of around 30 kDa and immunodetected with anti-ACA4N27 antiserum (Geisler *et al.,* 2000) recognizing the GST did not bind to the TWD1 matrix (Figure 10C, lane 13).

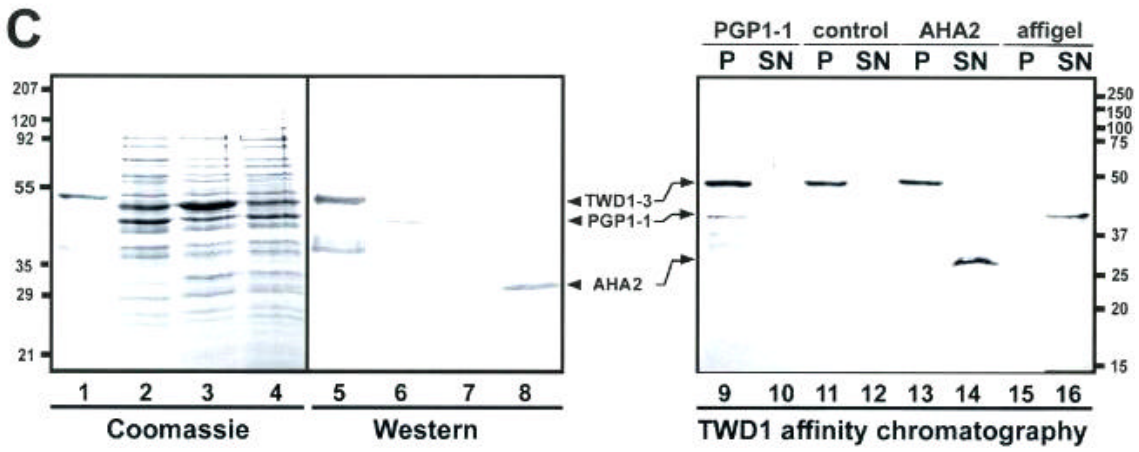

Figure 10. Analysis of TWD1-AtPGP1 interaction

C. Ni-affinity purified TWD1-3 (lane 1 and 5) and cleared total *E.coli* lysates containing the expressed C-termini of AtPGP1 (lane 2 and 6), the vector control (lane 3 and 7) and the C-terminus of *Arabidopsis* H^+-ATPase AHA2 (lane 4 and 8) were visualized as Coomassie Blue stain (left panel) and immunoprobed (middle panel) as described in MATERIALS AND METHODS. A TWD1 affinity matrix was incubated with cleared *E.coli* lysates containing the expressed C-termini of AtPGP1, the vector control or the Cterminus of Arabidopsis H-ATPase AHA2. As negative control, empty affigel beads were incubated with the AtPGP1-1 lysate. Equal volumes of matrix-eluted (P) as well as unbound proteins (SN) were separated by PAGE, and immunoprobed using the antisera described above (see MATERIALS AND METHODS).

TWD1 and AtPGP1 form a complex on the plasma membrane

The C-terminus of TWD1 contains a hydrophobic α-helical region (residue 339 - 357) with the potential to form a membrane anchor predicted by hydrophobicity analysis. To demonstrate that TWD1 is indeed a membrane-anchored protein, the TWD1 protein was N-terminally tagged with a HA-epitope and expressed in transgenic plants. Pellets of microsomal membrane fractions prepared from HA-TWD1 expressing plants were treated either with chaotropic agent KSCN, high salt, carbonate or TX-100. TWD1 could only be released from microsomes by solubilization with high concentrations (1% v/v) of the detergent TX-100 (Figure 11A) indicating that TWD1 is in fact a membrane anchored, rather than peripheral membrane protein.

AtPGP1 has been localized in the plasma membrane (Sidler *et al*., 1998), suggesting that TWD1 resides as well on the plasma membrane. To test this assumption, membranes prepared from *Arabidopsis* plants overexpressing a HA-epitope tagged form of TWD1 were separated by linear sucrose gradient density centrifugation. Both polyclonal anti-TWD1 antiserum and a monoclonal anti-HA antibody detected HA-TWD1 (48 kDa) in fractions 10-13 (sucrose concentrations of 34% and 44%) of the sucrose gradient (Figure 11B). TWD1 co-localized with the plasma membrane marker H^+-ATPase AHA3 and AtPGP1 (same distribution of peak fractions 11-14, Figure 11B). Markers for other membranes, such as the vacuolar V-ATPase subunit B or BIP, an ER-specific marker, cross-reacted with other fractions. Anti-TWD1 recognized additionally a smaller 40 kDa protein; detection of this protein with the monoclonal anti-HA antibody suggested that it represents a degradation product of TWD1.

To confirm these data, microsomal membranes from wild-type *Arabidopsis* suspension cultures were separated by aqueous two-phase partitioning. Efficient partitioning of internal cell membranes to the bottom phase and plasma membranes to the top phase was ascertained by Western blotting using antisera against the vacuolar V-ATPase, plasma membrane-bound AtPGP1, and H^+-ATPase (Geisler *et al*., 2000) revealing no cross contamination of both membrane types (Figure 11C). A protein band corresponding to the expected size of TWD1 was detected in the top fraction of phase partitioning with anti-TWD1 antisera confirming its plasma membrane location (Figure 11C).

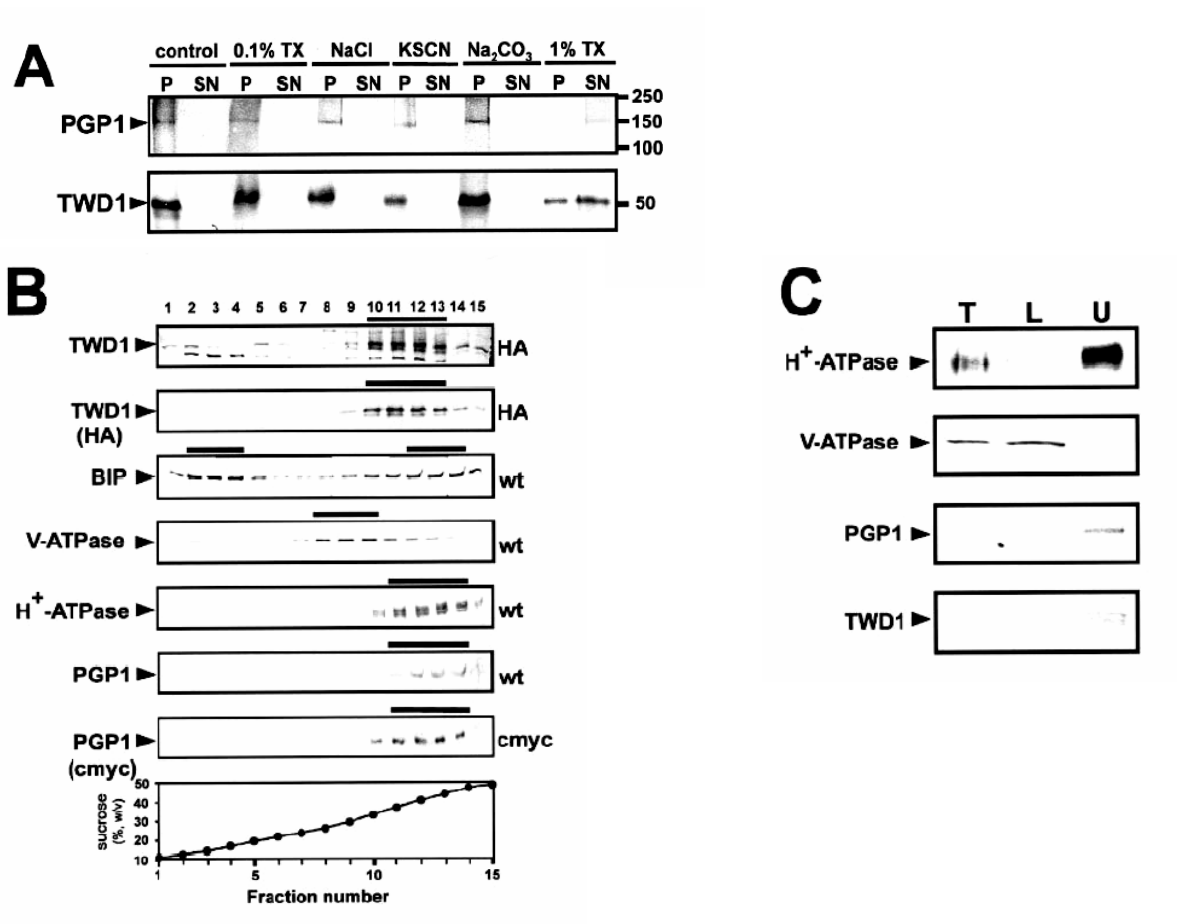

Figure 11. TWD1 is a plasma membrane-anchored protein

A. Microsomal fractions expressing an HA-epitope-tagged version of TWD1 or a c-Myc epitope-tagged version of AtPGP1 were treated with 0.1% TX-100, 2M NaCl, 1M KSCN, 200mM Na_2CO_3 or 1% TX100. Membranes were pelleted, supernatants were precipitated with TCA and subjected to PAGE. TWD1 and AtPGP1 were detected using anti-HA and anti-c-Myc antibodies.
B. Microsomes of wild-type (wt) and transgenic Arabidopsis plants ectopically expressing c-Myc- or HA-epitope-tagged AtPGP1 (c-Myc) and TWD1 (HA), respectively, were subjected to linear sucrose density gradient fractionation. Fractions were immunoprobed against given marker enzymes as described in (Geisler et al., 2000). Transgenic plant material was probed additionally against anti-c-Myc (c-Myc) and anti-HA (HA), respectively. Immunopositive peak fractions are highlighted by bars.
C. Microsomal fractions obtained from aqueous two-phase partitioning of Arabidopsis suspension culture were probed with anti-TWD1 and anti-AtPGP1 antisera. Efficient partitioning of total microsomes (T, 10 µg of protein) to the lower phase (L, 10 µg of protein) or to the upper phase (U, 5 µg of protein) was ascertained by Western blot analysis using antisera against the marker proteins vacuolar V-ATPase and the plasma membrane-bound H^+-ATPase.

These biochemical fractionation data were supported by cellular immunolocalisation of HA-TWD1 protein in transgenic plant cells by laser scanning microscopy. Protoplasts from leaves were treated with anti-HA antibody, which was decorated with a FITC-conjugated secondary antiserum. Optical sections showed that transgenic protoplasts were FITC labeled at the periphery (green in Figure 12A, C), which is consistent with a plasma membrane localization of TWD1. Protoplasts treated only with the secondary antiserum revealed no background (data not shown)

and wild-type material treated with both antibodies resulted in only very faint peripheral background (Figure 12E).

Subsequent recording of chlorophyll autofluorescence using TRITC filter settings showed that this fluorescence is limited exclusively to the chloroplasts (red in Figure 12B), which revealed no peripherical fluorescence around the protoplasts. Superimposed false green and red images represent images obtained with FITC and TRITC filters.

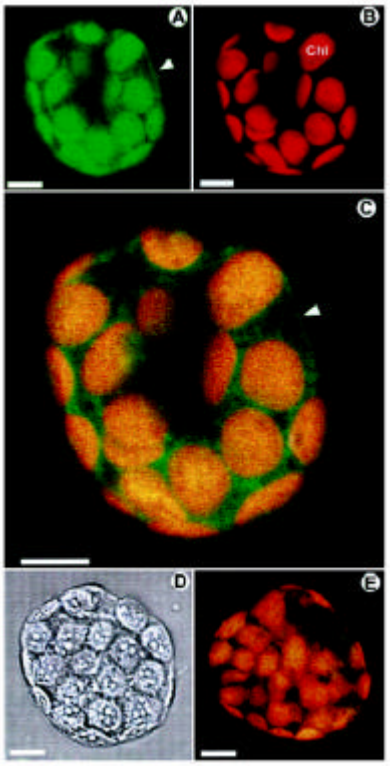

Figure 12: Immunolocalization of TWD1 in the plasma membrane

A. Fluorescence of a protoplast from HA-TWD1 plants immunoprobed with anti-HA antibody recorded with FITC filter settings.

B. The same protoplast sample detected with TRITC filter settings.

C. Superimposing of A. and B.

D. The same protoplast as in A. and B. in bright field illumination.

E. Superimposing of fluorescence of wild-type protoplast treated as described (A) using FITC and TRITC filter settings. Images **A – C**, **E** represent internal optical sections generated by Laser scanning confocal microscopy. Note that green fluorescence in the chloroplasts (Chl) is not due to FITC fluorescence but to green coloring of chlorophyll autofluorescence of chloroplasts. Arrowheads mark the fluorescence of the plasma membrane. bars, 10 µm.

A different strategy to detect TWD1-AtPGP interaction in plant cells was followed by showing that on the one hand TWD1 is excluded from solubilized microsomal protein preparations separated by anion exchange chromatography after treatments with NPA (Figure 13A). On the other hand, using HA-TWD1 protein, isolated from overexpressing plants as a ligand to anti-HA-epitope resin, we were able to immobilize AtPGP proteins from microsomal membrane preparations and visualize them using a polyclonal anti-PGP1 antibody (Sidler *et al*. 1998). NPA treatments elute AtPGP1 and AtPGP19 illustrating a specific interaction between TWD1 and those two transporters (Figure 13B). Identities of both upper bands was verified by MALDI analysis of tryptic fragments (results not shown) while the identity of a third band of lower molecular weight is unknown.

To demonstrate the TWD1/AtPGP1 complex *in vivo*, AtPGP1 was immunoprecipitated from solubilized wild-type membrane microsomes after crosslinking with thiol-cleavable DTBP (Figure 13C). Crosslinking was used, since strong detergent treatment is essential to solubilize both proteins from the plasma membrane. These treatments were expected to disrupt protein-protein interaction (Weixel and Bradbury, 2000). To prevent contamination of the eluate with the heavy chain of rabbit anti-AtPGP1 - running at similar size than TWD1 - the primary antibody was additionally immobilized to protein G by crosslinking. The absence of heavy chain antibodies was verified using only secondary antibodies detecting no band even after prolonged exposure (not shown).

Wild-type TWD1, which is slightly smaller than HA-TWD1 (Figure 13C, lane 1) was indeed detectable (Figure 13C, lane 3) using anti-TWD1 antiserum, suggesting co-precipitation with AtPGP1 (Figure 13C, lane 4). This was the case under reducing conditions (+DTT), which cleave the DTBP crosslinker. The intensity of a TWD1 band under reducing conditions was approximately ten times higher than under non-reducing conditions (not shown). This faint signal is not surprising as acidic elution of the complex can result in partial cleavage of sulfur double bonds of the crosslinker. No TWD1 could be detected in control experiments using empty protein G (Figure 13C, lane 2).

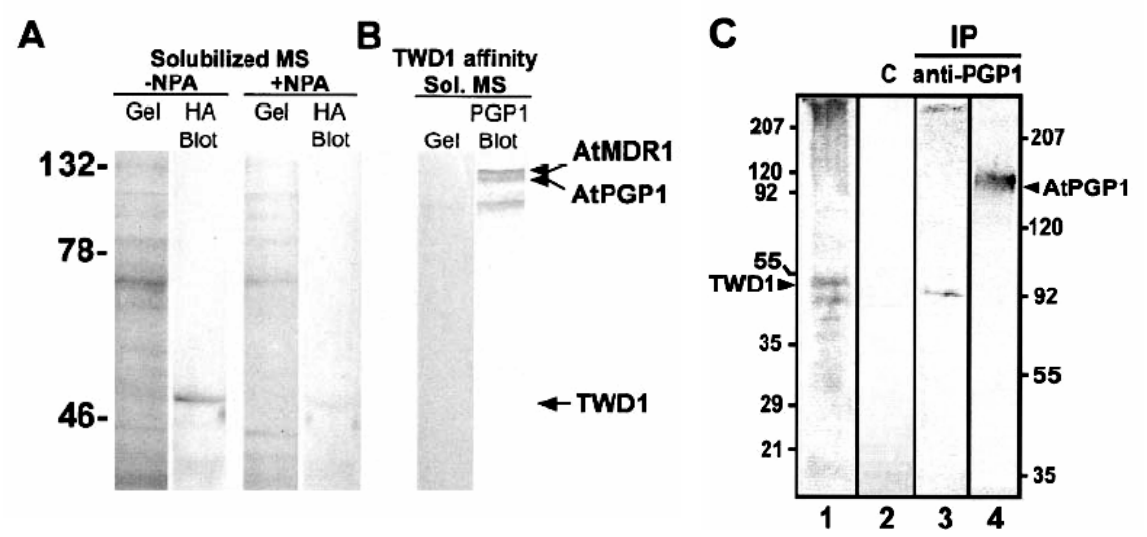

Figure 13. In vivo interaction between TWD1 and AtPGPs

A. TWD1 is excluded from microsomal fractions by naphtylphtalamic acid (NPA).

Microsomal proteins were solubilized in the presence and absence of NPA, fractionated by anion exchange chromatography and separated on SDS-PAGE gels. Western blots of these gels were probed with a monoclonal HA antibody (Sigma, St. Louis MO).

B. Co-purification of TWD1 and AtPGPs via TWD1 affinity chromatography.

HA-TWD1 protein, purified from overexpressing plants in the presence of NPA, was bound to anti-HA affinity resin. Solubilized microsomal proteins were incubated with this matrix and proteins were eluted after washing with PBS with 30µM NPA. Eluted proteins were separated on SDS-PAGE gels and AtPGPs were detected with a polyclonal anti-PGP antibody on Western blots.

C. Co-immunoprecipitation of TWD1 using anti-AtPGP1 antiserum

Membranes from Arabidopsis cell suspension culture were crosslinked with DTBP, solubilized using 2% TX-100 and immunoprecipitated using anti-AtPGP1 antiserum. Immunoprecipitated proteins were separated by 12.5% (lane 1 - 3) and 7.5% PAGE (lane 4) and probed with anti-TWD1 (lane 1 - 3) and anti-AtPGP1 (lane 4) antiserum, respectively. As negative control, unspecific binding of proteins to empty protein G was monitored (lane 2). Note that the size difference of the co-precipitated wild-type TWD1 in lane 3 having a slightly smaller weight than the HA-epitope-tagged TWD1 run in parallel (lane 1) is due to the lack of the HA-epitope. Molecular size markers on the left and right correspond to lanes 1 to 3, respectively; positions of TWD1 and AtPGP1 are indicated.

Polar auxin transport is reduced in twd1 and atpgp mutants

Measurements of polar auxin transport in hypocotyls of *atpgp19-1* (*atmdr1-1*) and *atpgp1-1* mutants shows reduction of auxin transport between 44% and 77%. This reduction in transport activity is more drastic in the double mutant *atpgp1-1*/*atpgp19-1* (*atmdr1-1*) where the transport is reduced to 24% of wild-type plants. Polar auxin transport in *twd1* mutants is reduced to 14% of wild-type plants even when no mutations in *AtPGP1* and *AtPGP19* are present (Figure 14). The methods used to measure auxin transport in this paper represent a refinement of those used in Noh et al. (2001) (see MATERIALS AND METHODS section).

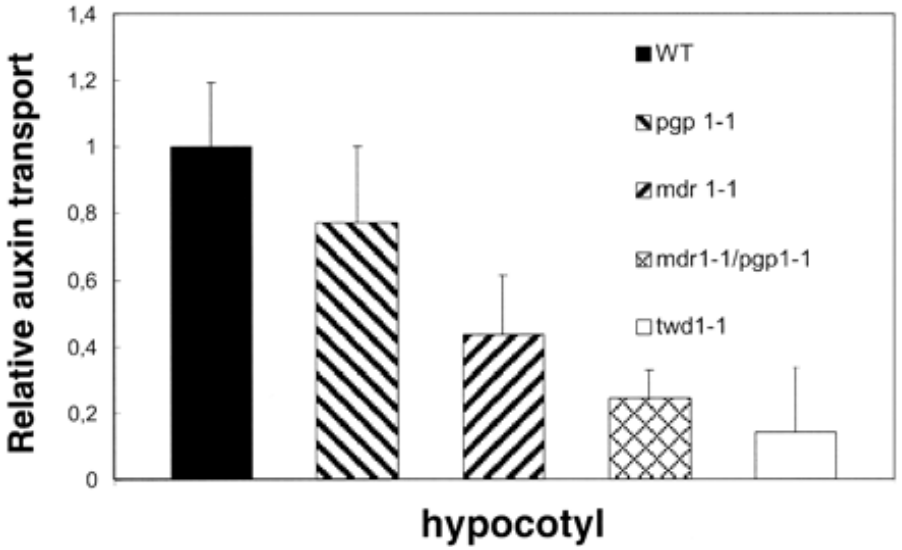

Figure 14. Relative auxin transport activity in hypocotyls of young seedlings

The ABC transporter mutation atpgp1-1 exhibits slightly reduced polar auxin transport under these conditions shown, whereas the atpgp19-1 (atmdr1-1) exhibits markedly reduced polar auxin transport. Auxin transport in the double atpgp1-1/atpgp19-1 (atmdr1-1) mutant was dramatically impaired. The twd1-1 mutant showed even less polar auxin transport activity.

DISCUSSION

Mutations in the *Arabidopsis TWD1* gene encoding a protein highly homologous to FK506-binding immunophilins cause a dramatic pleiotropic phenotype including epinastic cotyledons, a reduction of cell elongation and a disoriented growth behavior (see Figure 1; Schulz *et al*., submitted). As TWD1 does not exhibit PPIase activity (Kamphausen et al., 2002) or complement yeast FKBP12, we assumed that TWD1 action is mediated indirectly by protein-protein interaction. In a yeast two-hybrid screen we identified the *Arabidopsis* ABC transporter AtPGP1 as a TWD1-interacting partner. We provide several lines of evidence that AtPGP1 and AtPGP19 (AtMDR1) are relevant interacting partners of TWD1. Moreover, we collected indirect and direct proof that a functional complex of TWD1-AtPGP1/AtPGP19 is required for proper plant development: phenotypes observed for *twd1* and the *atpgp1-1*/*atpgp19-1* (mdr1-1) double mutant – but not of individual *atpgp1-1* or *atpgp19-1* mutants - resemble each other in early stages of development and auxin transport is severely reduced in *twd1-1* and *atpgp1*/*atpgp19* mutant hypocotyls.

Interaction with AtPGP1 is mediated by the PPIase-like domain of TWD1

Two-hybrid and *in vitro* analyses suggest that TWD1 specifically interacts with both AtPGP1 and AtPGP19 (AtMDR1). These ABC transporters were isolated by NPA-chromatography in a high-affinity NPA-binding fraction together with TWD1 (misannotated as a cyclophilin 5–like protein) and AtPGP2 as minority components (Murphy *et al*., 2002, Noh *et al.,* 2001). TWD1 does not interact with the C-terminus of any other AtPGP in a common sub-branch of a phylogenetic tree (Martinoia *et al.,* 2002), which emphasizes the specificity of interaction of TWD1 with AtPGP1 and AtPGP19.

Mapping of TWD1 motifs required for AtPGP1 binding demonstrated that AtPGP1 recognizes the N-terminal PPIase-like domain. This is an unexpected finding as the TPR domain is usually implicated in protein-protein interactions as observed for other FKBPs (Harrar *et al*., 2001, Das *et al*., 1998, Lamb *et al*., 1995). However, another exception is known: hFKBP52 was found to interact with dynein, FAP48 and PHAX via its PPIase-like domain (Chambraud *et al*., 1996; Chambraud *et al*., 1999). Mapping analysis revealed that AtPGP19 in contradiction to AtPGP1 requires additional TWD1 regions for interaction. Thus far all attempts to measure any PPIase

activity for TWD1 using synthetic peptide substrates have failed (Kamphausen *et al*., 2002). Additionally, TWD1 also failed to complement the yeast FKBP12 mutant (data not shown). Finally, we found no interference of FK506 in TWD1-AtPGP1 interactions by using either the yeast two-hybrid system or *in vitro* using TWD1-affinity chromatography.

These findings might not be surprising as 12 aa residues involved in high-affinity interactions between human FKBP12 and FK506 or rapamycin which are highly conserved in most mammalian and yeast FKBPs (Van Duyne *et al*., 1991) are poorly conserved in most plant FKBPs. Only four of the 14 residues are conserved in TWD1 (74Y, 85F, 87D, 132Y). Interestingly, FKBP12 from *Vicia faba* (75% conservation) also failed to mediate FK506 and rapamycin action in yeast (Schubert *et al*., 2002). Amino acid substitution presumably also abolishes drug binding and PPIase activity in human FKBP38 (Pedersen *et al.*, 1999).

In summary, our results support the possibility that a modified PPIase-like domain which is able to interact specifically with xenobiotic immunsuppressants in animal cells could have acquired the ability to interact with ABC transporters *i.e.* AtPGP1 and AtPGP19 in plants.

TWD1 is a unique membrane-anchored FKBP forming a complex with AtPGP1 in the plasma membrane

Various members of the FKBP subfamily in plants are expressed as soluble proteins in different intracellular compartments including the cytoplasm, ER and nucleus (Luan *et al*., 1996, Reddy *et al*., 1998). High-molecular weight FKBP73 and FKBP77 from wheat have been identified as part of a HSP90 hetero-complex *in vitro* (Reddy *et al*., 1998).

A database search identified C-terminal putative transmembrane domains additionally only in human and mouse FKBP38 as well as in Drosophila FKBP45, but TWD1 is the first immunophilin shown to be a membrane-anchored protein. Anchoring of TWD1 on the plasma membrane was demonstrated by fractionation of membrane preparations. Only high concentrations of Triton X-100 - but not gentle treatments, destroying hydrophilic or hydrophobic protein-protein or membrane-protein interactions - resulted in partial solubilization of the TWD1 protein (Figure 11A). The fact that solubilization was always incomplete indicates that additional

interactions (e.g. to AtPGP1/19) might contribute to TWD1 retention on the plasma membrane.

Membrane fractionation and confocal laser microscopy of transgenic plants expressing a HA-tagged version of TWD1 demonstrate that TWD1 is indeed localized on the plasma membrane (Figure 11B and 12). Despite its low abundance, we were able to confirm these results by detection of TWD1 in purified plasma membranes from wild-type plant material derived from aqueous two-phase partitioning (Figure 11B). Weak background fluorescence surrounded the chloroplasts in the protoplasts examined (green stain in Figure 12C). Immunoblotting of thylakoids and chloroplast inner envelope membranes isolated from plant material overexpressing HA-TWD1 never showed any signals (data not shown), which excludes a chloroplast localization of TWD1. In contradiction to our data, Kamphausen *et al*. (2002) immunolocalized TWD1 to the plasma membrane as well as to the tonoplast in plants overexpressing HA-TWD1 employing electron microscopy. In these plants but not in wild-type preparations, white unstructured areas were distinguishable that were discussed to occur from massive overproduction of a membrane protein.

On cross-linking, TWD1 could be detected in an immunoprecipitation assay using anti-AtPGP1. This result suggests a functional AtPGP1 and TWD1 protein complex on the plasma membrane (Figure 13C).

Possible physiological role of TWD1

Two plausible models offer explanations for the observed TWD1-AtPGP1/AtPGP19 interaction. The first hypothesis suggests that TWD1 is involved in proper folding or protein trafficking of AtPGP1 to the plasma membrane. Based on our results this option can be excluded because membrane fractionation showed a very similar distribution of AtPGP1 in twd1-1 mutant and wild-type plants (data not shown).

The second model hypothesizes that immunophilin-like proteins play a regulatory role in multi-protein complexes. TWD1 could thus function as a potential regulator of AtPGP1 and AtPGP19 transport activities by means of domain-specific protein-protein interactions. This model is supported by several studies: FKBP12 is a subunit and inhibits basal signaling of two intracellular calcium release channels, the inositol 1,4,5-trisphosphate and ryanodin receptor (Cameron *et al*., 1995; Timerman *et al*., 1995). It has also been suggested that FKBP12 regulates MDR-like ABC transporters (Hemenway and Heitman, 1996; Mealey *et al*., 1999). Interestingly, FKBP12-

dependent regulation of the ryanodine-sensitive Ca^{2+} channel and MDR3-mediated drug resistance is independent of FKBP12 PPIase activity (Hemenway and Heitman, 1996, Timerman *et al*., 1995). As TWD1 interacting clones of AtPGP1 and AtPGP19 cover the Walker A and B boxes of the C-terminal nucleotide binding fold involved in nucleotide binding and hydrolysis (Martinoia *et al*., 2002, Rea *et al*., 1998), it is conceivable that interaction of this domain with TWD1 affects ATP binding or hydrolysis.

The putative regulatory impact of TWD1 on AtPGP1 and AtPGP19 (AtMDR1) activity is hard to test at present because the *in vivo* substrate specificity of AtPGP1 and AtPGP19 (AtMDR1) must still be resolved (Thomas *et al*., 2000, Noh *et al*., 2001, Windsor *et al*. 2003). However, AtPGP1 and AtPGP19 have a direct or indirect role in polar auxin transport (Luschnig 2002) and the structural similarity between auxin and synthetic indolic substrates transported by mammalian MDR proteins is obvious (Nelson *et al*., 1998). Measurements of polar auxin transport in hypocotyls of the ABC transporter mutant *atpgp1-1* show a slight and somewhat variable reduction in transport, whereas auxin transport in *atmdr1-1* (*atpgp19*) is clearly reduced. The reduction of auxin transport is even more pronounced in the *atpgp1-1*/*atpgp19-1* (*atmdr1-1*) double mutant and could be interpreted as an additive effect of both mutations. The mutation in *TWD1* results in even greater reduction of polar auxin transport in hypocotyls, which indicates that TWD1 is necessary for the activity and interaction of both ABC transporters. A role for TWD1 in auxin transport regulation is also suggested by unsuccessful attempts to measure auxin transport in an AtPGP19 (AtMDR1) expressing heterologous yeast system (Noh *et al*., 2001; Murphy, unpublished data). TWD1 may be a specific regulator of putative auxin transporters or possibly also MDR-like ABC transporters (Muday and Murphy, 2002, Luschnig 2002). Such an interaction is further suggested by recent binding studies of *Arabidopsis* plasma membrane proteins to a matrix containing an immobilized form of the polar auxin transport inhibitor NPA (Murphy *et al*., 2002). In these studies, AtPGP1, AtPGP19 (AtMDR1), and small amounts of TWD1 co-purified in the same NPA-binding fraction (fraction IV). We could corroborate these data by modifying the experimental setup. By binding HA-epitope-tagged TWD1 protein that was isolated from plant material in the presence of NPA to an anti-HA-epitope matrix, we were able to show that AtPGPs solubilized from microsomal protein preparations bound to the TWD1 protein. This interaction could be disrupted by treatments with NPA.

Isolating TWD1 from microsomal preparations was successful only in the absence of NPA (Figure 13).

Importantly, in the previous NPA-affinity matrix experiments, only residual amounts of TWD1 were retained when the NPA used was immobilized via a critical carboxylic acid essential to its function as an auxin transport inhibitor (Murphy *et al*., 2002). In the experiments described herein, elution with conjugated, and therefore physiologically active, NPA appeared to disrupt all TWD1 - AtPGP interactions. This again, shows a specific and NPA-sensitive interaction of TWD1 with AtPGPs in the plant cell.

It is tempting to speculate that the similar phenotypes of *twd1-1* and *atpgp1-1*/*atpgp19-1* double mutants (Figure 8) are both the result of abnormal distribution of growth factors such as auxin. Strong growth effects on leaf lamina expansion (epinastic growth) and root length reduction support this assumption. If so, the absence of TWD1 would not allow the formation of a transport-competent complex, which involves ABC transporters of the PGP/MDR-subfamily.

ACKNOWLEDGEMENTS

We would like to thank Drs. H. Sze, A. Vitale and R. Serrano for providing antisera, J. Kudla for CBL1 and CIPK, K. Palme for Y97 and M.G. Palmgren for pMP900 plasmids. We are greatful to M. Meylan-Bettex and Dr. L. Bovet for the preparation of *Arabidopsis* thylakoid and inner envelope membranes and V. Vincenzetti for excellent technical assistance. We thank Drs. U.I. Flügge for continuous support and E. Spalding for sharing results prior to publication. Drs. N. Johnsson and R. Schmidt are greatly acknowledged for critical reading of the manuscript. This work was supported by the Swiss National Foundation, Deutsche Forschungsgemeinschaft (Schu/821-2), the European Community (LATIN, BIOTEC 4), and the Ministerium für Schule, Wissenschaft und Forschung des Landes NRW, Novartis and the Alexander von Humboldt-Foundation (Feodor-Lynen and Novartis fellowships to M.G.). A.S.M. and J.J.B. were supported by the National Science Foundation (NSF grant #0132803).

ABBREVIATIONS

FKBPs, FK506 binding proteins; PPIases, *cis-trans*-peptidylprolyl isomerases; MDR, multidrug resistance; CsA, cyclosporin A; TPR, tetratrico-peptide repeat; twd1, twisted dwarf1; ABC, ATP-binding cassette; ß-gal, ß-galactosidase; PGP, P-glycoprotein; NPA, naphtylphtalamic acid

III Cellular efflux of auxin mediated catalyzed by the Arabidopsis MDR/PGP transporter AtPGP1

Markus Geisler[1,5], Joshua J. Blakeslee[2,5], Rodolphe Bouchard[1], Ok Ran Lee[2], Vincent Vincenzetti[1], Anindita Bandyopadhyay[2], Boosaree Titapiwatanakun[2], Wendy Ann Peer[2], Aurélien Bailly[1], Elizabeth L. Richards[2], Karin F. K. Ejendal[3], Aaron P. Smith[2,4], Célia Baroux[1], Ueli Grossniklaus[1], Axel Müller[5], Christine A. Hrycyna[3], Robert Dudler[1], Angus S. Murphy[2,6], and Enrico Martinoia[1]

[1]Institute of Plant Biology, Basel-Zurich Plant Science Center, University of Zurich, CH-8007 Zurich, Switzerland

[2]Department of Horticulture, Purdue University, West Lafayette, IN 47907 USA

[3]Department of Chemistry, Purdue University, West Lafayette, IN 47907 USA

[4]Present address: Dept. of Genetics, University of Georgia, Athens, Georgia

[5]Lehrstul für Pflanzenphysiologie, Ruhr-Universität Bochum, D-44801 Bochum, Germany

[6]These authors contributed equally to this work.

[7]Corresponding author: Angus S. Murphy (TEL) 01-765-496-7956 (FAX) 01-765-494-0391 e-mail murphy@purdue.edu

This article was published in *The Plant Journal* (2005) **44**:179-94

SUMMARY

Directional transport of the phytohormone auxin is required for the establishment and maintenance of plant polarity, but the underlying molecular mechanisms have not been fully elucidated. Plant homologsorthologs of human multiple drug resistance/P-glycoproteins (MDR/PGPs) have been implicated in auxin transport, as defects in *MDR1* (At*PGP19)* and At*PGP1* result in reductions of growth and auxin transport in Arabidopsis (*atpgp1*, *atpgp19*), maize (*brachytic2*), and sorghum (*dwarf3*). Here we examine the localization, activity, substrate specify, and inhibitor sensitivity of AtPGP1. AtPGP1 exhibits non-polar plasma membrane localization at the shoot and root apices, as well as polar localization above the root apex. Protoplasts from Arabidopsis *pgp1* leaf mesophyll cells exhibit reduced efflux of natural and synthetic auxins with reduced sensitivity to auxin efflux inhibitors. Expression of At*PGP1* in yeast and in the standard mammalian expression system used to analyze human MDR-type proteins results in enhanced efflux of indole-3-acetic acid (IAA) and the synthetic auxin 1-naphthalene acetic acid (1-NAA), but not the inactive auxin 2-NAA. AtPGP1-mediated efflux is sensitive to auxin efflux and ABC transporter inhibitors. As is seen *in planta,* AtPGP1 also appears to also mediate some efflux of IAA oxidative breakdown products associated with apical sites of high auxin accumulation. However, unlike what is seen *in planta*, some additional transport of the benzoic acid is observed in yeast and mammalian cells expressing *AtPGP1,* suggesting that other factors present in plant tissues confer enhanced auxin specificity to PGP-mediated transport.

INTRODUCTION

Transport of the plant auxin indole-3-acetic acid (IAA) is best described by a chemiosmotic model in which plasma membrane ATPases generate a H^+ gradient between the neutral cytoplasm and the acidic extracellular space (Lomax *et al*., 1995). Cellular IAA uptake is mediated by lipophilic diffusion of IAAH augmented by tissue-specific gradient-driven H^+ symport activity (Lomax *et al*., 1985; Swarup *et al*., 2004). The same gradient motivates carrier-mediated efflux of cytoplasmic anionic IAA^-. The bias of auxin transport is attributed to highly regulated, polar-localized efflux complexes characterized by the PIN-FORMED (PIN) family of facilitator proteins (Friml and Palme, 2002). PINs have been shown to align with the auxin transport vector and to be necessary for normal polarized organ development and auxin movement (Benkova *et al*., 2003; Blilou *et al*., 2005; Galweiler *et al*., 1998; Palme and Galweiler, 1999;). Treatment with auxin efflux inhibitors (AEIs) phenocopies some *pin* mutant phenotypes (Friml and Palme, 2002). Additionally, some members of the PIN family exhibit vectorial relocation during tropic growth and function in the generation and maintenance of auxin sinks (Chen *et al*., 1998; Friml *et al*., 2002a,b; Muller *et al*., 1998).

Plant homologs of human multiple drug resistance/P-glycoproteins (MDR/PGPs) are numerous. The *Arabidopsis* PGP sub-family of ABC transporters is large, containing 21 members (five of which are highly homologous) (Jasinski *et al*., 2003; Martinoia *et al*., 2002). Structural characteristics of mammalian MDR/PGPs are well conserved in plant homologs, except in the predicted pore-facing helical domains thought to confer substrate specificity (Ambudkar *et al*., 2003). Analysis of expression patterns of the 21 members of the PGP subfamily using both the AREX and AtGENEXPRESS microarray databases, shows that members of the PGP family exhibit distinct yet overlapping expression patterns (http://www.arexdb.org/index.jsp; Schmid *et al*., 2005). PGPs have been implicated in auxin transport, as defects in *MDR1* (*AtPGP19)* and *AtPGP1* result in reduced growth and auxin transport of varying severity in Arabidopsis (*atpgp1*, *atpgp19*), maize (*brachytic2/zmpgp1*), and sorghum (*dwarf3/sbpgp1*) (Geisler *et al*., 2003; Multani *et al*., 2003; Noh *et al*., 2001). Further, auxin transport defects and dwarf phenotypes are more exaggerated in Arabidopsis double mutants, suggesting overlapping function (Noh *et al*., 2001). As gradient-driven anion efflux is sufficient to drive polar transport, it is not clear where

plasma membrane-localized MDR/PGP ATP binding cassette transporters fit into this scheme.

A mechanistic explanation of PGP function in auxin transport was suggested when, after fixation and detergent treatment, PIN1 was found to be mislocalized from the plasma membrane in xylem parenchyma cells of hypertropic Arabidopsis *atpgp19* hypocotyls, but not in *atpgp1* hypocotyls which do not exhibit altered tropic responses (Noh *et al*., 2003). These results suggest that PGPs might regulate transport by stabilizing plasma membrane efflux complexes, especially as PGPs are difficult to solubilize, are localized in detergent- resistant membrane microdomains (lipid rafts), bind the noncompetitive AEI 1-N-naphthylphthalamic acid (NPA), and are components of membrane complexes that can be dissociated by NPA treatment (Geisler *et al*., 2003; Murphy *et al*., 2002; Noh *et al*., 2001). It is important to characterize the transport activity of PGPs in order to understand their functional role in these complexes.

Here we characterize the AtPGP1 protein (hereafter referred to as PGP1), by examining PGP1 localization, activity, substrate specificity, and inhibition of activity. We confirm that PGP1 has an intermediate dwarf phenotype under short-day conditions and characterize other auxin-related phenotypes. We show that PGP1 exhibits non-polar subcellular localization at the shoot and root apices that is consistent with *PGP1* expression. We show that *pgp1* mutant protoplasts exhibit reduced IAA transport, substrate specificity, and reduced sensitivity to AEIs. We show that *PGP1* expressed in yeast and the standard mammalian cell expression system used to analyze human MDR-type proteins can mediate efflux of IAA and the synthetic auxin 1-NAA, but not the weak synthetic auxin 2-NAA. Further, PGP-mediated efflux is sensitive to auxin efflux and ABC-transporter inhibitors. *PGP1* expression in yeast also results in increased resistance to toxic indolic IAA analogs. Expression of *PGP1* in mammalian cells does not enhance the efflux of other classes of compounds that are common substrates for mammalian MDR-type transporters.

RESULTS

pgp1 exhibits subtle auxin-related phenotypes

While the growth phenotypes of *atpgp19* (hereafter referred to as *pgp19)* and the double mutant *pgp1 pgp19* are clearly visible in both short and long day conditions (Geisler *et al.*, 2003; Noh *et al.*, 20022001; Geisler et al., 2003), those of *pgp1* are not. Enhanced tropic bending observed in *pgp19* hypocotyls is not observed in *pgp1* hypocotyls (Noh *et al.*, 2003), and gravitropic defects are difficult to quantify in *pgp1* roots, largely because of greater variability in root gravitropic bending and root nutation compared to wild type (Noh *et al.*, 2003). Reduced hypocotyl growth reported in antisense *PGP1* transformants (Sidler *et al.*, 19989) was not observed in the *pgp1* mutant (Noh *et al*, 2001) and, in our hands and, under long day conditions, shoot and hypocotyl growth of *pgp1* mutants was difficult to distinguish from wild type (not shown). However, under shorter day conditions, mature *pgp1* exhibited an intermediate dwarf phenotype that is not as severe as *pgp19* (Figure 15A) and is consistent with intermediate reduction in the transport of ^{3} H-IAA from the shoot apex to the root-shoot transition zone previously observed in *pgp1* (Geisler *et al*., 2003).

A

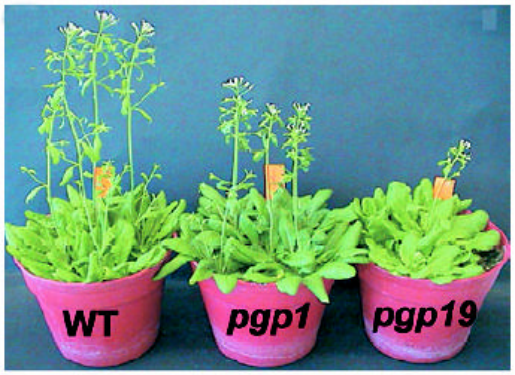

Figure 15. pgp1 mutants have a subtle phenotype.

A *pgp1* and *pgp19* mutants have a dwarf phenotype under short-day conditions.

However, since as previous assays utilizing higher concentrations of ^{14}C-IAA indicated slight increases in *pgp1* auxin transport levels (Noh et al, 2001),reported previously indicated slight increases in *pgp1* auxin transport levels under some coniditons (Noh et al, 2001), free IAA levels in hypocotyls and whole roots in 5-day *pgp1* and *pgp19* seedlings were determined (Figure 15B) and were found to be consistent with more recently published transport data (Geisler *et al.*, 2003).

Consistent with auxin levels observed in whole-root tissues, free IAA levels in *pgp19* primary root *tips* were severely reduced (62 ± 18.3 %of wild type). However, levels in *pgp1* root tips were lower than expected (38 ± 29.7 % wild type). A small increase in IAA leakage from *pgp1* (and not *pgp19*) root tips is also apparently a factor, as, like the flavonoid-deficient mutant *tt4* (Murphy *et al*, 2000; Peer *et al*, 2004), *pgp1* root tips exhibited enhanced leakage of radiolabeled IAA into the support media in assays of shoot- to- root polar ^{3}H-IAA transport (124 ± 9.4% of wild type levels).

B

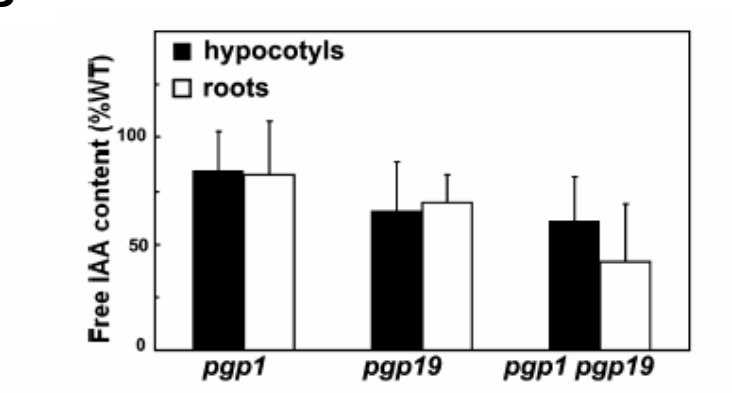

Figure 15 pgp1 mutants have a subtle phenotype

B. Free IAA content in 5-d seedlings. Values are mean ± SD from. 500 seedlings per replicate, n = 3.
WT values=100% ± 0.074 for hypocotyls, and 100% ±11.114 for roots.

Confirming these results, Pro$_{DR5}$:GUS expression of the auxin reporter construct Pro$_{DR5}$:GUS was reduced in *pgp1*, *pgp19*, and *pgp1 pgp19* compared with wild type, but was stronger in *pgp19* than in *pgp1*and *pgp1 pgp19* (Figure 15C). FurtherAdditionally, a stelar Pro$_{DR5}$:GUS signal observed in *pgp19* was not visible in *pgp1*, consistent with a lesser accumulation of auxin in *pgp1* root tips compared

withto *pgp19*. The reductions of Pro$_{DR5}$:GUS staining observed in *pgp* mutant root tips have been further confirmed in a recently published study showing reduced Pro$_{DR5}$:GUS expression in the root tips of independently generated *pgp1* and *pgp19* mutants (Lin and Wang, 2005).

IAA root basipetal transport in 5-day pgp1 seedlings

Pro$_{DR5}$:GUS results suggested that basipetal transport in *pgp1* and *pgp19* might be reduced at the root rip. Consistent with these results, export of radiolabeled IAA to the 2-mm segment proximal to the root tip in *pgp1* and *pgp19* was less than in the wild type (Figure 15D). Auxin transport to the next 2-mm segment was less than wild type in *pgp19* but not *pgp1*, consistent with stronger *PGP19* expression in non-apical tissues compared to *PGP1* (Noh *et al*., 2001; Sidler *et al*., 1998) and greater apparent auxin retention in *pgp19*, indicated by Pro$_{DR5}$:GUS (Figure15C).

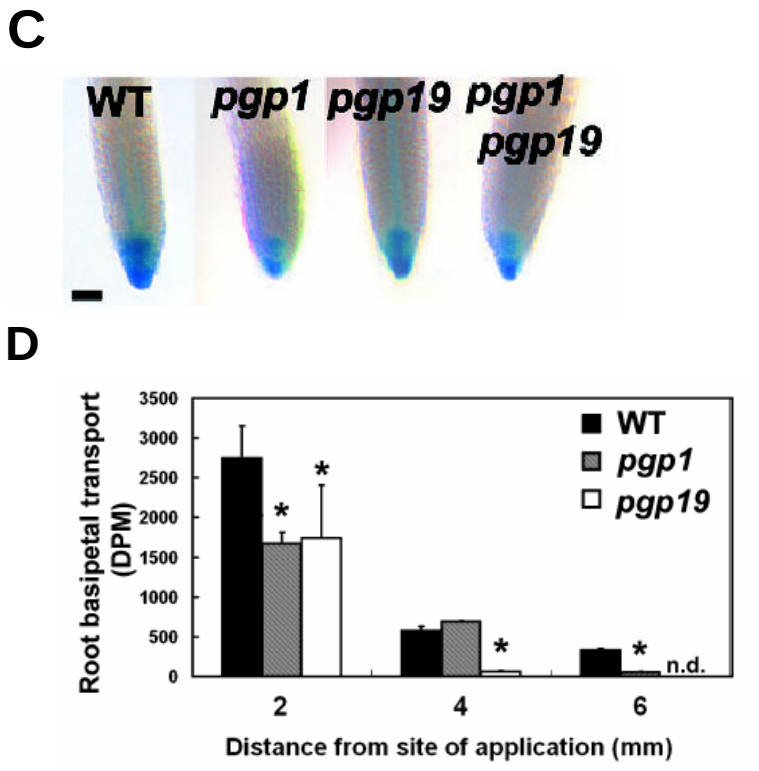

Figure 15. pgp1 mutants have a subtle phenotype.

C. Pro$_{DR5}$:GUS expression in 5-day seedling root tips. Bar, 0.1mm.

D. Basipetal ^{3}H-IAA transport from the root tip in 5-day seedlings. Values are mean ± SD from 10 seedlings each per replicate. n = 3.

As PIN1 and PIN2 were not mislocalized in *pgp1* root tips (Figure 16A-D), altered PIN localization cannot account for the altered auxin transport. Application of IAA >2mm above root tips of both *pgp* mutants resulted in only marginal reductions in transport compared with wild type (approximately 5% in *pgp19* and 14% in *pgp1*), suggesting limited PGP function in root basipetal transport in non apical tissues. However, wild type rates of basipetal auxin transport in these tissues are also much lower than apical transport rates, and decrease with distance from the root tip (data not shown). These results are similar to Pro_{DR5}:GUS activity and root basipetal transport reported in *agr1-5/pin2* root tips (Shin *et al*., 2005).

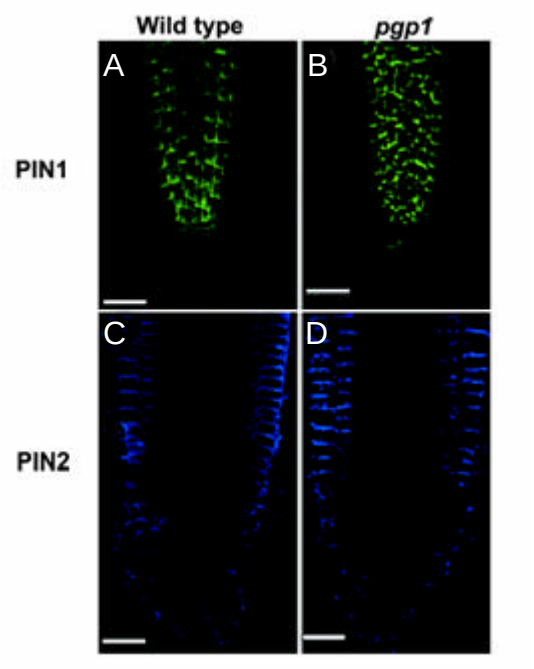

Figure 16. PIN1 & PIN2 localization is unaltered in pgp1 root tips.

A. PIN1 immunolocalization in 5-day wild type root tips.

B. PIN1 immunolocalization in 5- day *pgp1* root tips.

C. PIN2 immunolocalization in 5- day wild type root tips.

D. PIN2 immunolocalization in 5- day *pgp1* root tips. Bar, 125 µm.

PGP1 localization is non-polar at the shoot and root apices

Auxin transport profiles of *pgp1*and the strong expression of *PGP1* observed in light-grown root and shoot apices (Noh *et al*., 2001, Sidler *et al*., 1998) focused our attention on PGP1 function in these regions. Unlike *PGP19*, which is highly expressed in upper hypocotyls and throughout the root in light-grown seedlings (Noh *et al*., 2001), *PGP1* is expressed at lower levels in non-apical tissues in both light- and dark-grown seedlings (Geisler *et al*., 2003, Noh *et al*., 2001). Pro_{PGP1}:GUS enzyme and quantitative real-time-PCR assays confirmed that *PGP1* expression is strongest in root and shoot apices in dark-grown wild type seedlings (Table 1).

Table 1. Relative expression of AtPGP1 in 5-day wild type

Treatment	*AtPGP1*
Whole seedlings	
Light	1.00 ± 0.73
Light + NPA	0.60 ± 1.66
Dark	14.89 ± 0.98*
Dark + NPA	3.70 ± 1.69
Shoots	
Wild type	1.0 ± 0.8
Wild type + IAA	8.5 ± 1.4*
Roots	
Wild type	1.0 ± 0.9
Wild type + IAA	2.1 ± 0.9

NPA,1-N-naphthylphthalamic acid ; IAA, indole-3-acetic acid.

* Significantly different ($P < 0.05$), ANOVA followed by Tukey's post-hoc analysis.

Pro$_{PGP1}$:GUS visualization also confirmed previous reports of *PGP1* expression in lateral root primordia and apices (Sidler *et al.*, 1998; Figure 17C), as well as previously unpublished weaker expression in cortical cells of the mature root and endodermal cells at the upper border of the distal elongation zone (Figure 17E). *PGP1* expression in these tissues was further confirmed by examination of original *in situ* hybridization materials from Sidler *et al*. (1998) and microarray expression data in AREX (http://www.arexdb.org/index.jsp).

PGP1 proteins were immunolocalized utilizing a functional Pro$_{PGP1}$:PGP1-cmyc transformant (see Experimental procedures), and the localization patterns were compared with Pro$_{PGP1}$:GUS expression. PGP1 exhibits a strong non-polar localization in shoot and root apical cells as well as lateral root tips (Figure 17A, B, D). This suggests a role for PGP1 in non-directional auxin export from apical cells and suggests that PGP function may be additive to, or synergistic with, PIN protein function.

Interestingly, in root tissues above the distal elongation zone, an apparent polar PGP1 localization was observed in mature cortical cells and endodermal cells at the upper boundary of the distal elongation zone (Figure 17F), suggesting that PGP1 may function in polar or reflux auxin movement (Blilou *et al*., 2005) in these tissues. In endodermal cells, the localization was always basal. In cortical cells, the localization was predominantly basal, although an apical localization without any obvious pattern was observed in some cortical cells flanking the stele. No reorientation of the basal signals was observed after microdeposition of IAA at the shoot or root tip or along the root surface (see Experimental procedures), suggesting a developmental basis for apical or basal localization. Transformation of *pgp1* with Pro$_{PGP1}$:PGP1-cmyc complemented the mutant phenotype and restored wild-type auxin transport profiles (Figure 18C), and PGP1 protein localization was similar to that seen in transformed wild type (figure 17 G); PIN2 localization was not altered in transformants (Figure 17H). No signal was observed in wild type immunolocalizations utilizing only primary or secondary antibodies under any detergent-solubilization conditions, no signal was observed in transformant immunolocalizations utilizing secondary antibodies only (Figure S1).

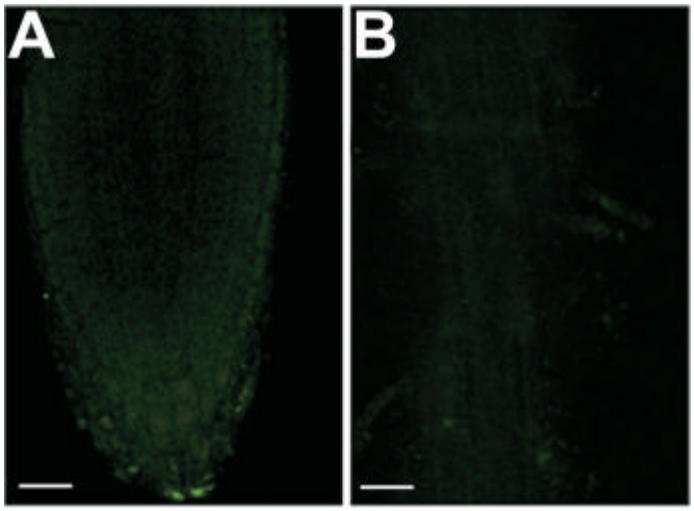

Figure S1 Anti-c-myc antibody controls

A No immunolocalization signal was observed in wild type root tips with the anti-c-myc antibody.

B No immunolocalization signal was observed in wild type mature roots with the anti-c-myc antibody. Bar, 125 µm.

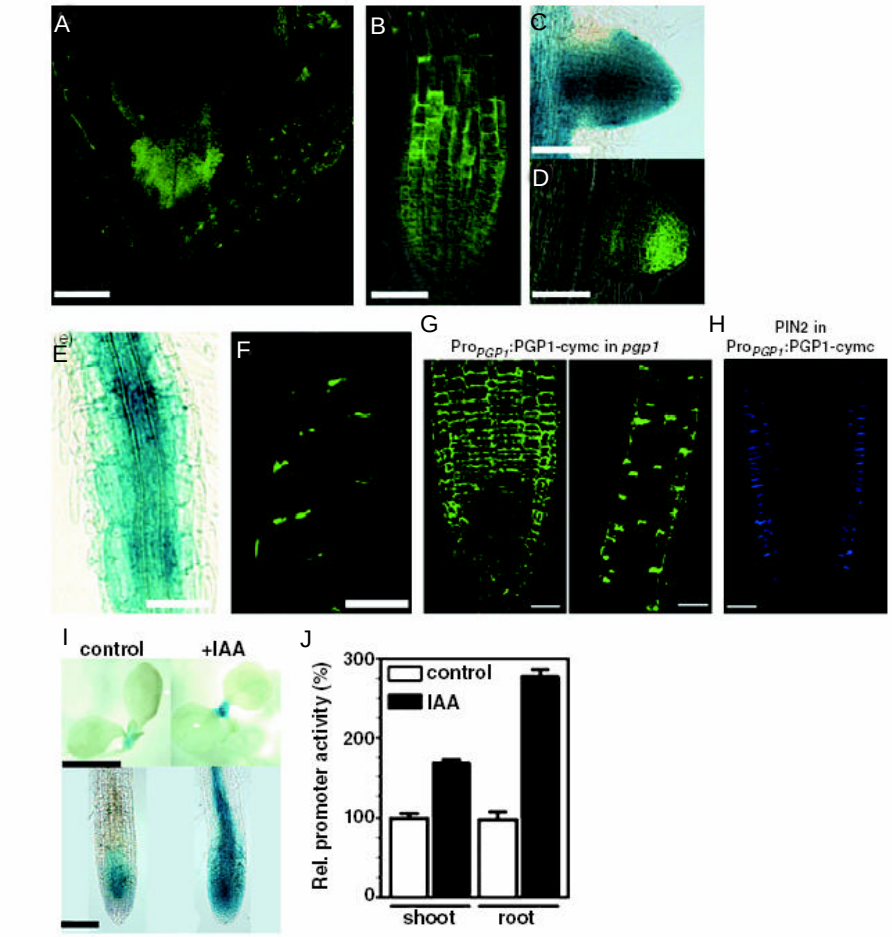

Figure 17. PGP1 localization in shoots and roots.

A. PGP1 localization is non-polar at the shoot apex in Pro$_{PGP1}$:PGP1-cymc 5-day seedlings. Bar, 100 µm.

B. PGP1 localization is non-polar at the root apex in Pro$_{PGP1}$:PGP1-cymc 5-day seedlings. Bar, 100 µm.

C. Pro$_{PGP1}$:GUS is expressed in the lateral root tip in 9-day seedlings. Bar, 100 µm.

D. PGP1 localization is restricted to the lateral root tip and a row of cells behind the lateral root tip in Pro$_{PGP1}$:PGP1-cmyc nine-day seedlings. Bar, 100 µm.

E. Pro$_{PGP1}$:GUS is expressed in the mature root of 5-d seedlings; seedling is overstained to visualize weak cortical GUS expression. Bar, 100 µm.

F. PGP1 localization is polar in the mature root of Pro$_{PGP1}$:PGP1-cymc 5-day seedlings. Bar, 100 µm.

G. When *pgp1* is transformed with Pro$_{PGP1}$:PGP1-cmyc, the localization of the protein is consistent with the localization of the *in situ* hybridization and Pro$_{PGP1}$:GUS expression previously published (Sidler *et al*., 1998) and that observed in wild type transformants. Bars, 125 µm and 70 µm, respectively.

H. PIN2 localization is not different from wild type in Pro$_{PGP1}$:PGP1-cmyc transformants. Bar, 125 µm.

I. Pro$_{PGP1}$:GUS expression increases at the shoot and root apices after 10-day seedlings are treated with 2 µM auxin (+IAA). Bar, 5 mm shoots, 0.2 mm roots. The seedlings were stained for identical amounts of time.

J. Relative promoter activities in Pro$_{PGP1}$:GUS transformants with and without 1 µM IAA treatment.

PGP1 expression is auxin responsive

As is the case for *PGP19* (Noh *et al*., 2001), *PGP1* expression (Pro$_{PGP1}$:GUS) appears to be auxin responsive (Figure 17I, J; Table 1) and the *PGP1* promoter contains auxin response element motifs (ARFAT, ASF-1 and NtBBF1). However, *PGP1* expression in shoot tips did not expand spatially with auxin treatment (Figure 17I). *PGP1* expression was also NPA-sensitive, and NPA treatment reversed increased *PGP1* expression observed in dark- grown wild-type seedlings (Table 1).

PGP1 mediates cellular efflux in Arabidopsis protoplasts

In order to determine whether differences in auxin transport could be observed at the cellular level, efflux from protoplasts under conditions that minimize IAA catabolism was quantified. Protoplasts were isolated from leaf mesophyll cells of wild type, *pgp1*, *pgp19*, and *pgp1 pgp19* plants, but not from *pin1*, *pin2*, *pin3*, or *pin4* mutants, as *PIN1*, *PIN2*, *PIN3* and *PIN4* expression are very low in wild type leaves (Figure 18A).

Wild type protoplasts exhibited ^{3}H-IAA efflux into the media (Figure 18B), and reductions in ^{3}H-IAA efflux from *pgp* protoplasts correlated well with transport reductions seen in whole plants: 72% in *pgp1*, 57% in *pgp19*, and 49% in *pgp1 pgp19* (Figure 18B). *pgp1* mutants transformed with Pro$_{PGP1}$:PGP1-cmyc had efflux levels similar to wild type (Figure 18C). Vacuolar pH, relative protoplast volume and surface area, and chloroplast number per protoplast did not differ significantly between wild type and *pgp* protoplasts excluding indirect effects such as vacuolar trapping (Table 2).

Consistent with ATP-dependence of the process, auxin efflux was diminished in protoplasts isolated from plants kept in the dark for 24h (ATP-depleted) (30% of light-grown wild type) (Figure 18B).

Table 2. Vacuolar pH and morphological features and of leaf mesophyll protoplasts

Line	Protoplast characteristics			
	Vacuolar pH	Relative volume	Relative surface area	Number of chloroplasts
WT	6.40	1	1	37 ± 9
pgp1	6.31	0.976 ± 0.031	0.949 ± 0.015	40 ± 9
pgp19	6.19	0.998 ± 0.028	0.919 ± 0.020	36 ± 5
pgp1 pgp19	6.04	0.724 ± 0.053*	0.514 ± 0.058*	37 ± 9

*Significantly different from WT ($P < 0.05$), ANOVA followed by Tukey's post-hoc analysis.

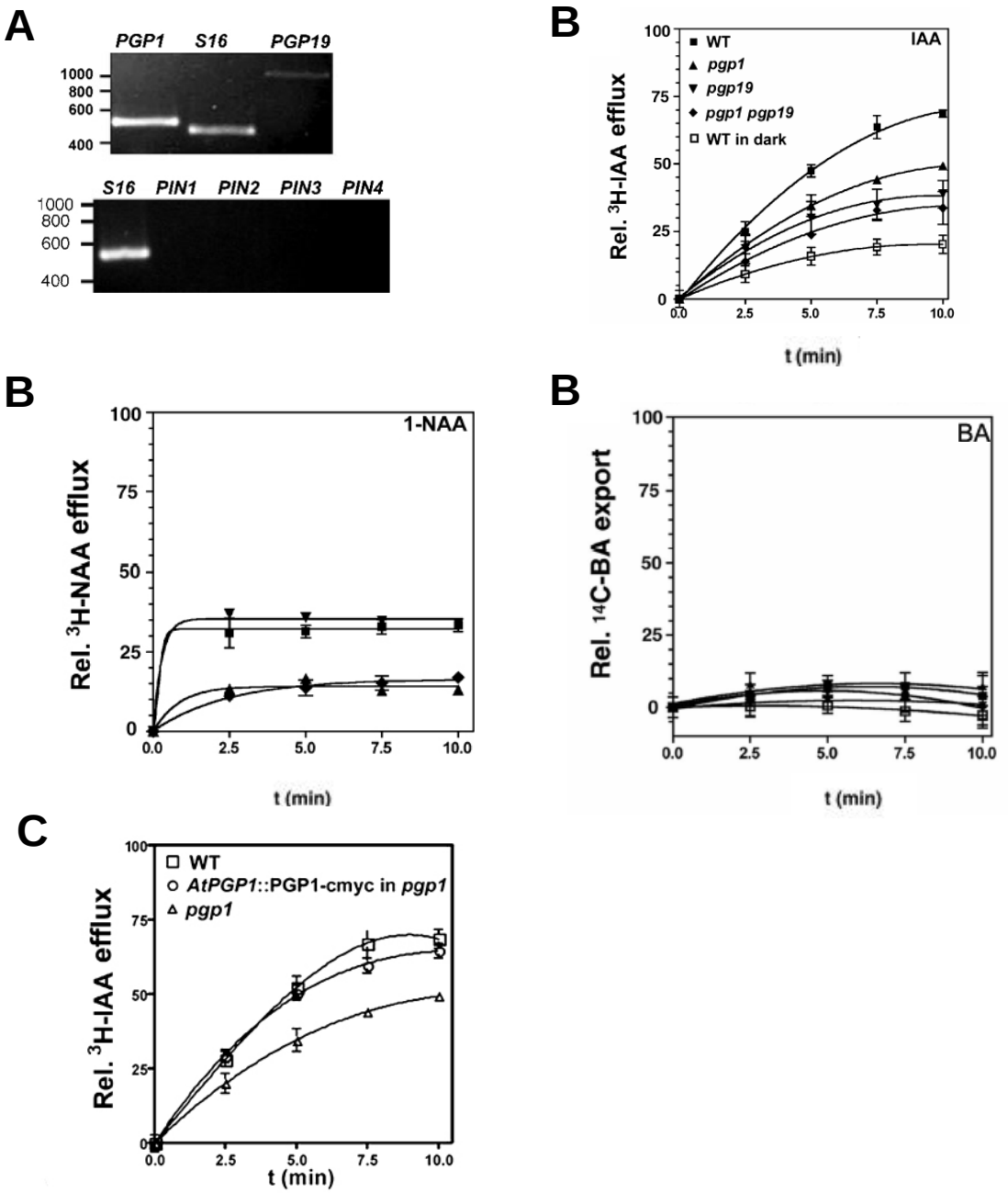

Figure 18. Cellular auxin efflux by PGPs reflects in planta auxin transport.

A. RT-PCR of 40S ribosomal protein *S16* (At2g09990), *PGP1* and *PGP19* (top) and *PIN1*, *PIN2*, *PIN3* and *PIN4* (bottom) in wild type leaf mesophyll protoplasts.

B. ^{3}H-IAA efflux from wild type (WT) leaf mesophyll protoplasts and reduced efflux from *pgp1*, *pgp19*, *pgp1 pgp19* and dark-treated wild type leaf mesophyll protoplasts. ^{3}H-1-NAA efflux was reduced in *pgp1* and *pgp1 pgp19* compared with wild type. No efflux of ^{14}C-BA was observed. Maximum loading of the cells is set at 100%. Values are mean activities ± standard errors from three to five individual measurements, n = 4.

C. Pro$_{PGP1}$:PGP1-cmyc functionally complements *pgp1*. When *pgp1* is transformed with Pro$_{PGP1}$:PGP1-cmyc, auxin efflux in leaf mesophyll protoplasts is not different from wild type.

The synthetic auxin 1-NAA was transported by wild type and *pgp19* protoplasts, but not *pgp1* or *pgp1 pgp19* protoplasts (Figure 18B), suggesting that PGP1 transports this synthetic auxin better than PGP19. Substrate specificity in the protoplast system was investigated further using radiolabeled benzoic acid (^{14}C-BA), a weak acid commonly used as a poorly transported control in plant assays. Negligible efflux of ^{14}C-BA out of wild type, *pgp1*, *pgp19*, *pgp1 pgp19*, and ATP-depleted wild type protoplasts was observed (Figure 18B), demonstrating that IAA efflux from protoplasts reflects the specific auxin transport observed in whole plants.

As the AEI NPA binds MDR/PGPs (Murphy *et al*., 2002; Noh *et al*., 2001) and NPA treatment disrupts membrane protein complexes containing PGPs (Geisler *et al*., 2003), IAA efflux from wild type protoplasts would be expected to be NPA sensitive, and *pgp* mutant protoplasts would be expected to exhibit diminished NPA sensitivity. However, an inactivating NPA amidase activity associated with the membrane aminopeptidase AtAPM1 (Katekar and Geissler, 1979, 1980; Katekar *et al*., 1981; Murphy and Taiz, 1999a,b; Murphy *et al*., 2002) is present in Arabidopsis leaves and is particularly active in leaf protoplasts (Murphy *et al*., 2002; Table 3). Treatment with NPA would be expected to increase initial ^{3}H-IAA loading, but to be less effective in inhibiting ^{3}H-IAA efflux. Treatment with NPA resulted in an 82% increase in ^{3}H-IAA loading of wild type protoplasts (Figure 18D) but only a 24% decrease in efflux. Consistent with even higher levels of NPA amidase activity in protoplasts derived from *pgp1* and *pgp19* (Table 3), measurements of NPA efflux inhibition from *pgp* protoplasts were highly variable.

D

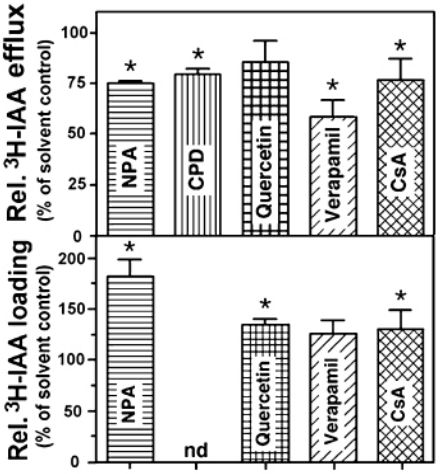

Figure 18. Cellular auxin efflux by PGPs reflects in planta auxin transport.

D. ^{3}H-IAA efflux from *Arabidopsis* wild type protoplasts was significantly reduced by inhibitors of auxin efflux and mammalian MDRs. ^{3}H-IAA efflux from protoplasts (upper panel) and loading into cell suspension cultures (lower panel) in the absence (solvent control) or presence of 10 µM of indicated inhibitors was determined after 10 min. Inhibitors assayed were: 1-N-naphthylphthalamic acid (NPA), 1-cyclopropyl propane dione (CPD), quercitin, verapamyl, and cyclosporine (csA).Values are mean ± and standard deviations (error bars) of three individual measurements, four samples each; export statistically different (Mann-Whitney *U* test, $P < 0.05$) compared with solvent controls is indicated by an asterisk. n.d., not determined.

Table 3. 1-N-naphtylphthalamic acid (NPA) hydrolysis in pgp1/pgp19 protoplasts. NPA hydrolysis is rapid in pgp mutant protoplasts compared with wild type protoplasts.

	a-Naphthylamine formation (naphthylamine equivalents)	
Time (min)	Wild type	*pgp1/pgp19*
0	N.D	N.D.
5	0.4 ± 0.91	3.2 ± 0.51
10	2.6 ± 2.21	6.8 ± 1.20
15	4.7 ± 2.34	7.1 ± 2.03

Chlorophyll-normalized protoplast solutions were incubated with 20 µM NPA. a-Naphthylamine was determined as described previously (Murphy and Taiz, 1999a).

N.D., not determined.

However, when the non-hydrolysable NPA analog, cyclopropyl propane dione (CPD) was substituted for NPA in wild type protoplast assays, mean ^{3}H-IAA efflux was reduced approximately 30% (Figure 18E). In contrast, CPD inhibited ^{3}H-IAA transport from the tips of intact young Arabidopsis rosette leaves approximately 40% (not shown), suggesting that structural characteristics of intact tissues not present in protoplasts contribute to NPA/CPD sensitivity. Low levels of *PIN* expression in leaf protoplasts (Figure 18A) suggest that lower abundance of PIN proteins in mesophyll tissues may be involved in this reduction of AEI sensitivity. As expected, ^{3}H-IAA efflux from CPD-treated protoplasts decreased approximately 12% in *pgp1* and approximately 20% in *pgp19* compared with the respective untreated protoplasts (Figure 18E). These results suggest that PGP19 is less sensitive than PGP1 to AEIs like NPA and CPD, but also confirms that NPA/CPD inhibition requires factors that are altered in protoplasts.

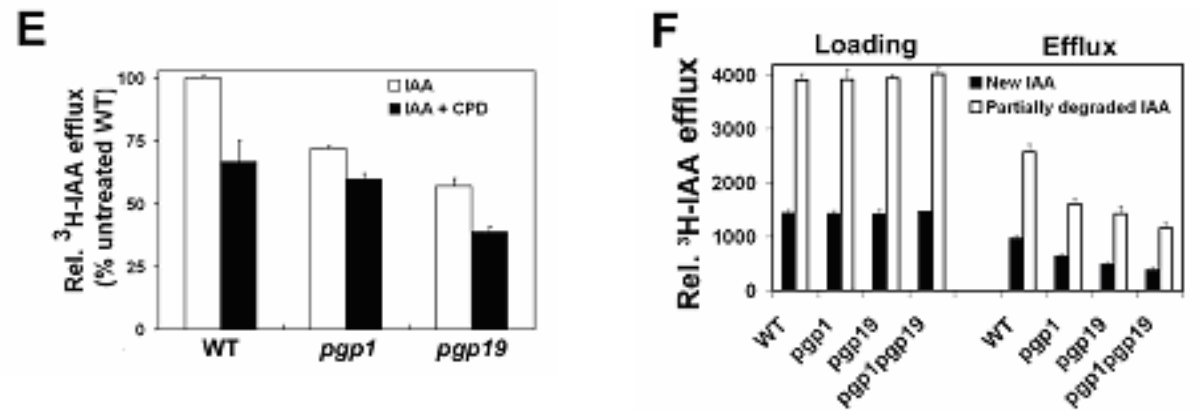

Figure 18. Cellular auxin efflux by PGPs reflects in planta auxin transport.

E. ^{3}H-IAA efflux from wild-type**,** *pgp1* and *pgp19* protoplasts is reduced by the non-hydrolyzable inhibitor cyclopropyl propane dione (CPD). ^{3}H-IAA efflux in the absence and presence of 10 µM CPD was determined after 10 min. Values are mean activities ± standard deviations (error bars) of three individual experiments, four samples each. $P > 0.05$ for *pgp1*.

F. Inclusion of partially degraded ^{3}H-IAA resulted in increase loading of labeled IAA in wild type and *pgp* mutant protoplasts. Apparent rates of efflux appeared to increase as well. However, the relative reduction of efflux seen with fresh ^{3}H-IAA effluence observed in *pgp* mutant protoplasts remained the same.

The strong localization of PGP1 in apical tissues suggests that PGPs might also transport IAA breakdown products produced in these tissues (Kerk *et al*., 2000). Unlabeled, presumably partially degraded IAA is often included in whole-plant radiolabeled auxin transport assays as it enhances measurable transport, possibly by enhancing uptake (Rashotte *et al*., 2000). Protoplast assays were repeated using either >99% radiolabeled IAA or a 1:1 mixture of IAA and oxidative breakdown products (primarily oxindoleacetic acid and indoleacetaldehyde, as determined by LC/MS and GC/MS). Increased loading and efflux was observed with the mixture (Figure 18F), but relative efflux from wild type and *pgp* mutant protoplasts at 10 min was similar with both treatments.

These results suggest that, in leaf cells, uptake and efflux of some IAA metabolites may be mediated by a PGP-dependent mechanism. However, it is not clear how far the specificity of IAA efflux might be enhanced in tissues where *PINs* are strongly expressed.

Analysis of PGP1 and auxin efflux in yeast

Heterologous expression of *PIN2* in yeast was previously used to demonstrate a positive impact on net auxin efflux (Chen *et al*., 1998). Although PGP19 was found to be mistargeted when expressed in a *Saccharomyces. cereviseae* deletion strain (JK93da) with reduced ABC transporter activity (Noh *et al*., 2001), immunohistochemical analyses indicated that PGP1 expressed in JK93da strain was plasma membrane localized (Figure 19A). Yeast expressing PGP1 exhibited time-dependent loading and efflux of radiolabeled IAA, 1-NAA, and BA (Figure 19B). ^{3}H-IAA efflux was temperature- and glucose-dependent (Figure S2A, B), membrane permeability was unaltered (Figure S2C), and the effluent species was determined by GC-MS to be ^{3}H-IAA (Figure 19D). Efflux of ^{3}H-IAA was seven times greater in *PGP1*-transformed yeast than in vector controls, and efflux of ^{3}H-1-NAA was also slightly increased (Figure 19B). However, although no efflux of the weak synthetic auxin 2-NAA was seen (Figure 19C), a lack of specificity was indicated when efflux of ^{14}C-BA was seen to be almost equal to that of ^{3}H-IAA (Figure 19B).

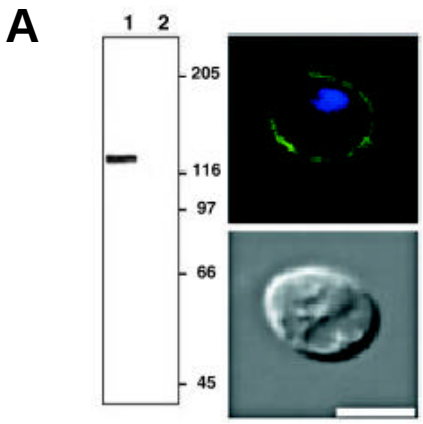

Figure 19. Heterologous expression of PGP1 in yeast cells results in auxin efflux.

A. PGP1-transformed yeast express and correctly target PGP1 to the plasma membrane. Western blot of microsomes from transformed yeast: lane 1, PGP1; lane 2, vector control. Confocal analysis with anti-AtPGP1 antibody (green) and DAPI-stained nucleus (blue) (top), DIC image (bottom). Several hundred yeast cells were examined and >90% showed the pattern. Bar, 5.6 µm.

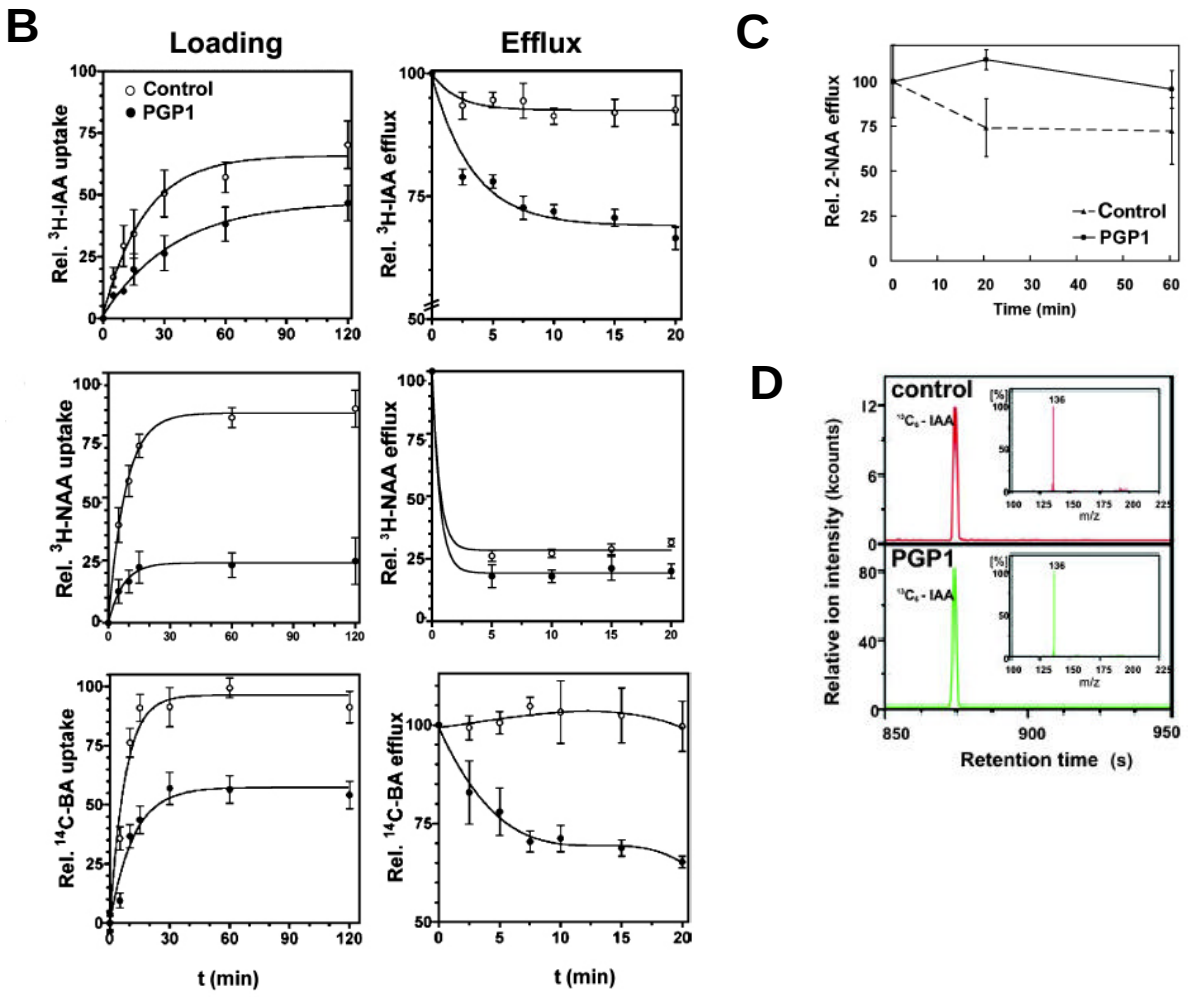

Figure 19. Heterologous expression of PGP1 in yeast cells results in auxin efflux.

B. Yeast cells (strain JK93da, with reduced endogenous ABC transporter activity) expressing *PGP1* effluxed ^{3}H-IAA, ^{3}H-1-NAA, and ^{14}C-BA compared with empty vector control. Mean activities ± standard errors, three to five individual measurements, n = 4. Values presented are relative to the total amount of radiolabeled IAA present in the media.

C. No efflux of 2-NAA was observed in yeast cells expressing *PGP1*.

D. MS/MS analysis of $^{13}C_6$-IAA effluent by yeast.

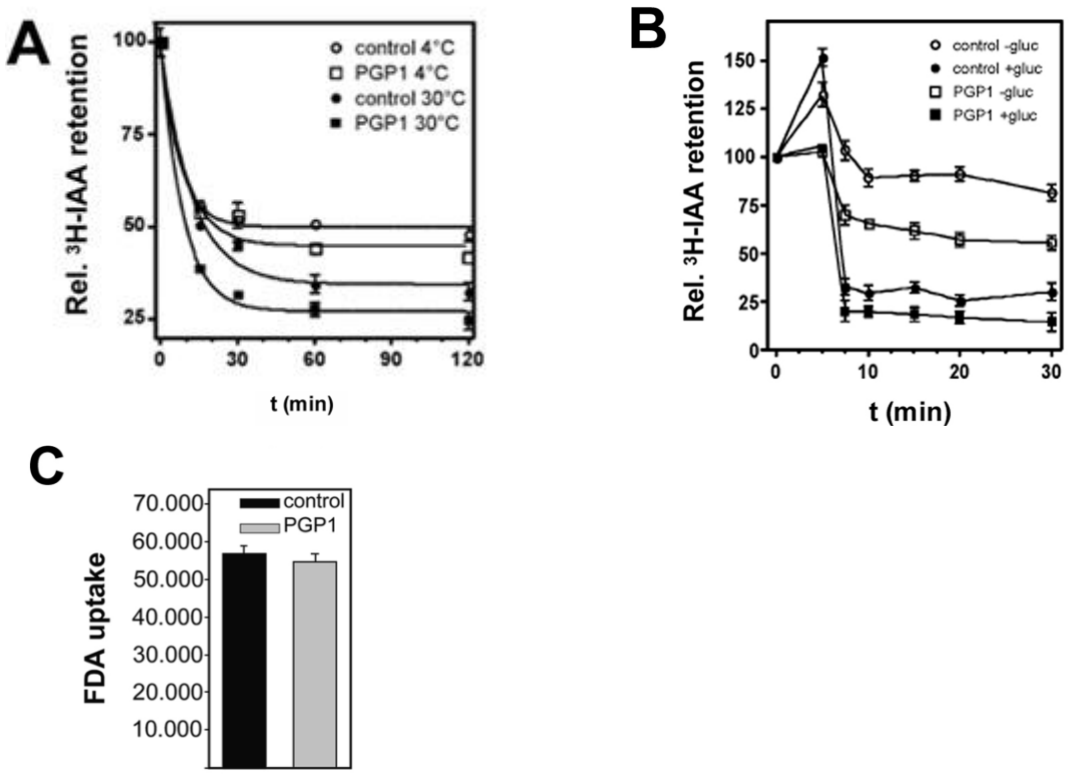

Figure S2. PGP1 expressed in yeast cells with reduced ABC transporter activity.

As might be expected for an energized transport mechanism, PGP1-mediated IAA export in yeast was both temperature- and glucose-dependent (Fig. S2A, B). Yeast cell permeability was similar in cells transformed with either empty vector or *PGP1* (Fig. S2C).

A IAA efflux in yeast is temperature dependent Yeast transformed cell with pNEV-PGPP1 (square) or control plasmid pNEV (circle) were loaded with ^{3}H-IAA and incubated at 4°C and 30 °C. Initial loading was at the same magnitude (+/- 10 %). Presented data represented relative mean activities plus standard deviation.

B IAA efflux in yeast is glucose-dependent. Initial loading was at the same magnitude (+/-10%). Presented data represent relative mean activities plus standard deviations.

C Yeast transformed with pNEV-PGPP1 or empty plasmid pNEV have similar permeabilities. Yeast cells were incubated with the dye FDA and internal fluorescence was measured. Presented data represent relative mean activities of four samples plus standard deviations.

Consistent with PGP1 mediation of auxin efflux, ^{3}H-IAA efflux in PGP1-transformed yeast was significantly reduced by treatment with NPA, the mammalian MDR/PGP inhibitors cyclosporin A and verapamil, and the inhibitor of both auxin transport and mammalian MDR/PGPs, quercetin (Figure. 19E). Further, expression of PGP1 in the hypersensitive *gef1* yeast mutant exhibited increased resistance to the cytotoxic IAA analog 5-fluoroindole which could be reversed by both AEIs and ABC transport inhibitors (M.G., unpublished data) Additionally, yeast *yap1-1* mutants which are hypersensitive to IAA due to increased expression of AUX1-like permeases (Prusty *et al*., 2004) are rescued by AtPGP1 but not by mouse MDR3 (Raymond *et al*., 1992) when grown on IAA (Figure 19F).

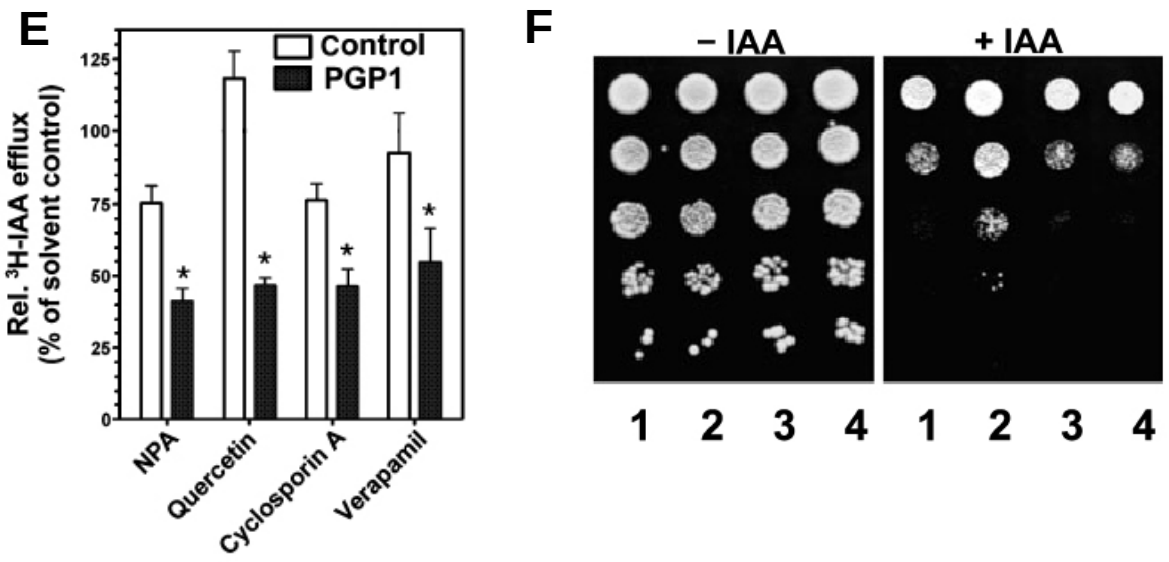

Figure 19. Heterologous expression of PGP1 in yeast cells results in auxin efflux.

E. ^{3}H-IAA efflux by yeast cells expressing *PGP1* was significantly reduced by auxin transport inhibitors and inhibitors of mammalian MDRs. Inhibitor concentrations were 10 µM. Solvent controls were set at 100%. Values presented are relative to total loading at time 0. Mean activities ± standard errors, three to five individual measurements, n = 4.

F. AtPGP1 but not mouse MDR3, functionally rescued a *yap1-1* mutant strain. 10-fold dilutions of yeast cells transformed with AtPGP1 (lane 2), MmMDR3 (lane 4) or corresponding vector controls pNEV (lane 1) and pVT (lane 3) were spotted on control plates or plates supplemented by 10 µM IAA.

Analysis of PGP1-mediated auxin efflux in mammalian cell lines

Vaccinia virus/T7 RNA polymerase expression in human HeLa cells has become a standard system for assaying mammalian PGPs, as it provides efficient heterologous expression of functional eukaryotic plasma membrane proteins and suppression of host protein synthesis (Elroy-Stein and Moss, 1991; Hrycyna *et al*., 1998; Moss, 1991). Protocols to confirm protein functionality and to assay net accumulation of radiolabeled and fluorescent substrates are well established (Hrycyna *et al*., 1998). These protocols were modified to allow loading of ^{3}H-IAA into HeLa cells while maintaining cell viability and substrate integrity.

HeLa cells expressing *PGP1* exhibited significant ^{3}H-IAA efflux compared with empty vector controls (Figure 20A). Although loading of ^{3}H-1-NAA was less than that seen with ^{3}H-IAA, cells expressing *PGP1* exhibited a small net efflux of ^{3}H-1-NAA (Figure 20A).Cells expressing PGP1 exhibited significant ^{3}H-IAA efflux compared with empty vector alone over a sixfold concentration range (Figure 20A, B). No net efflux of 2-NAA could be detected in cells expressing *PGP1* (Figure 20C). However, as seen when PGP1 was expressed in yeast, PGP1-mediated net ^{3}H-BA efflux was also observed when ^{3}H-BA was supplied at higher concentrations (Figure 20B). Background efflux of ^{3}H-BA in empty vector controls was higher than with ^{3}H-IAA, presumably due to endogenous mammalian benzoate / monocarboxylic acid transport activity (Yan and Taylor, 2002). Expression of *PGP1* in HeLa cells resulted in more auxin substrate specificity than when *PGP1* was expressed in yeast, as PGP1-mediated net efflux of ^{3}H-BA decreased to zero when ^{3}H-BA concentration was reduced to 10 nM, while ^{3}H-IAA efflux was unaffected (Figure 20B).

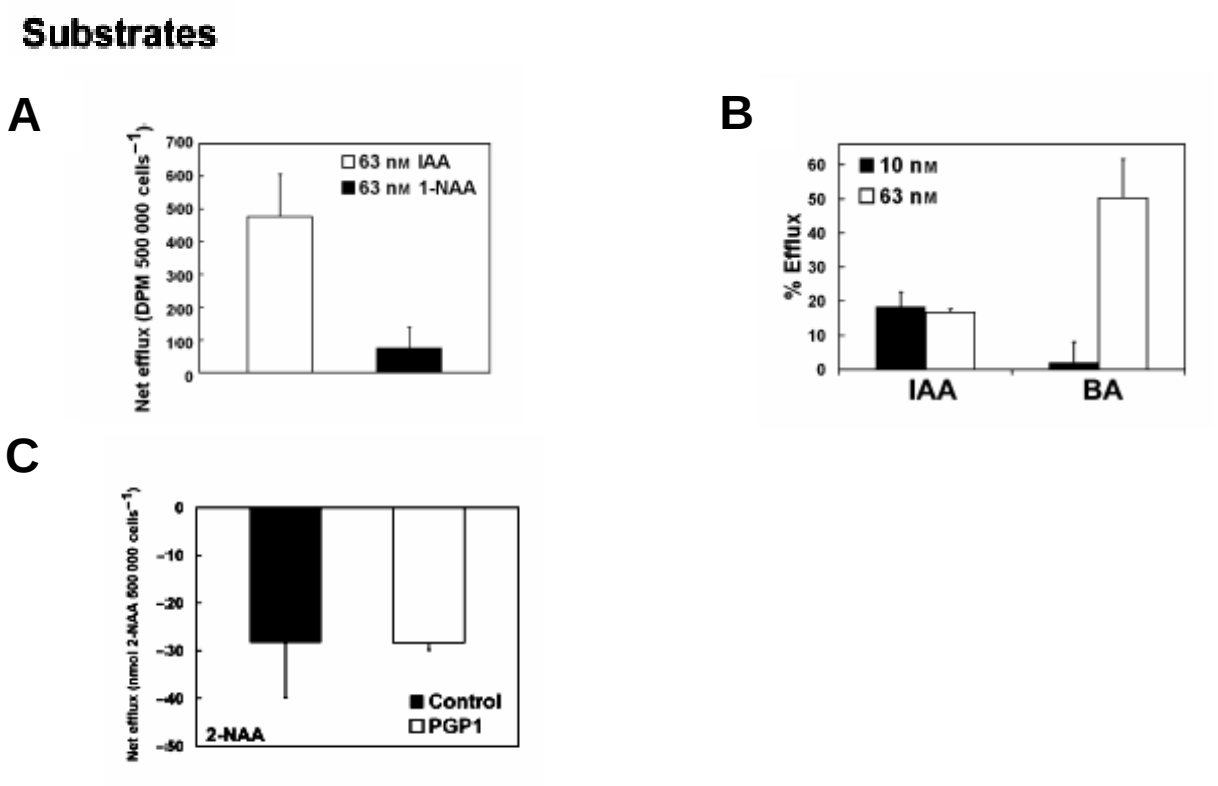

Figure 20. Efflux of radiolabeled substrates from HeLa cells expressing PGP1.

Net efflux is expressed as DPM/500,000 cells: the amount of auxin retained by cells transformed with empty vector minus the amount of auxin retained by cells transformed with gene of interest. Reductions in auxin retention (efflux) in transformed cells are presented as positive values, while increases of auxin retention are presented as negative values. In all cases, expression and localization of expressed *Arabidopsis* proteins were confirmed by RT-PCR (Blakeslee et al, 2004) and Western blotting (Hrycyna et al, 1998) using standard protocols for the system. Cell viability after treatment was confirmed visually and via cell counting. Data points were normalized to the average empty control vector value of 2851.885 DPM/500,000 cells for auxin treatments. Means with sum standard deviations, n = 3.

A. ^{3}H-IAA efflux was increased in HeLa cells expressing *PGP1*. PGP1 also modulated efflux of 1-napthalene acetic acid (^{3}H-1-NAA) and benzoic acid (^{3}H-BA).

B. ^{3}H-IAA efflux remained constant over a six-fold concentration range in cells expressing *PGP1*. Cells expressing *PGP1* transport BA only at high concentrations. Values are presented as percent efflux of empty vector control.

C. 2-NAA was retained in HeLa cells expressing *PGP1*. Cells were incubated with 62.59 nM cold 2-NAA. 2-NAA levels were measured via LC-MS. Data are presented in nanomoles 2-NAA/500,000 cells ± SD, and represent values obtained from two experiments, three replicates each.

Competition assays utilizing 10X more unlabeled BA than ^{3}H-IAA resulted in substantial inhibition of background ^{3}H-IAA efflux (data not shown), and ^{3}H-IAA efflux was reduced 22 ± 12.5% less in cells expressing *PGP1* than in empty vector controls. This suggests that background IAA efflux in HeLa cells is mediated by a monocarboxylic acid transporter, and that PGP1 is a functional transporter when expressed in HeLa cells.

Supporting this conclusion, the monocarboxylate transport inhibitor cardio green reduced background but not PGP1-mediated efflux (not shown). All of the assays were conducted in a buffer solution containing 1-2 mM citrate (see Experimental procedures), indicating that organic acids such as citrate and malate are not substrates for PGP1-mediated transport. Further, no efflux of mammalian MDR/PGP hydrophobic substrates (rhodamine 123, daunomycin, BODIPY-vinblastine) was seen in cells expressing *PGP1* (Figure. S3A-D). These results indicate that PGP1-mediated efflux is specific for active auxins and, to a lesser extent, a subset of aromatic carboxylic acids.

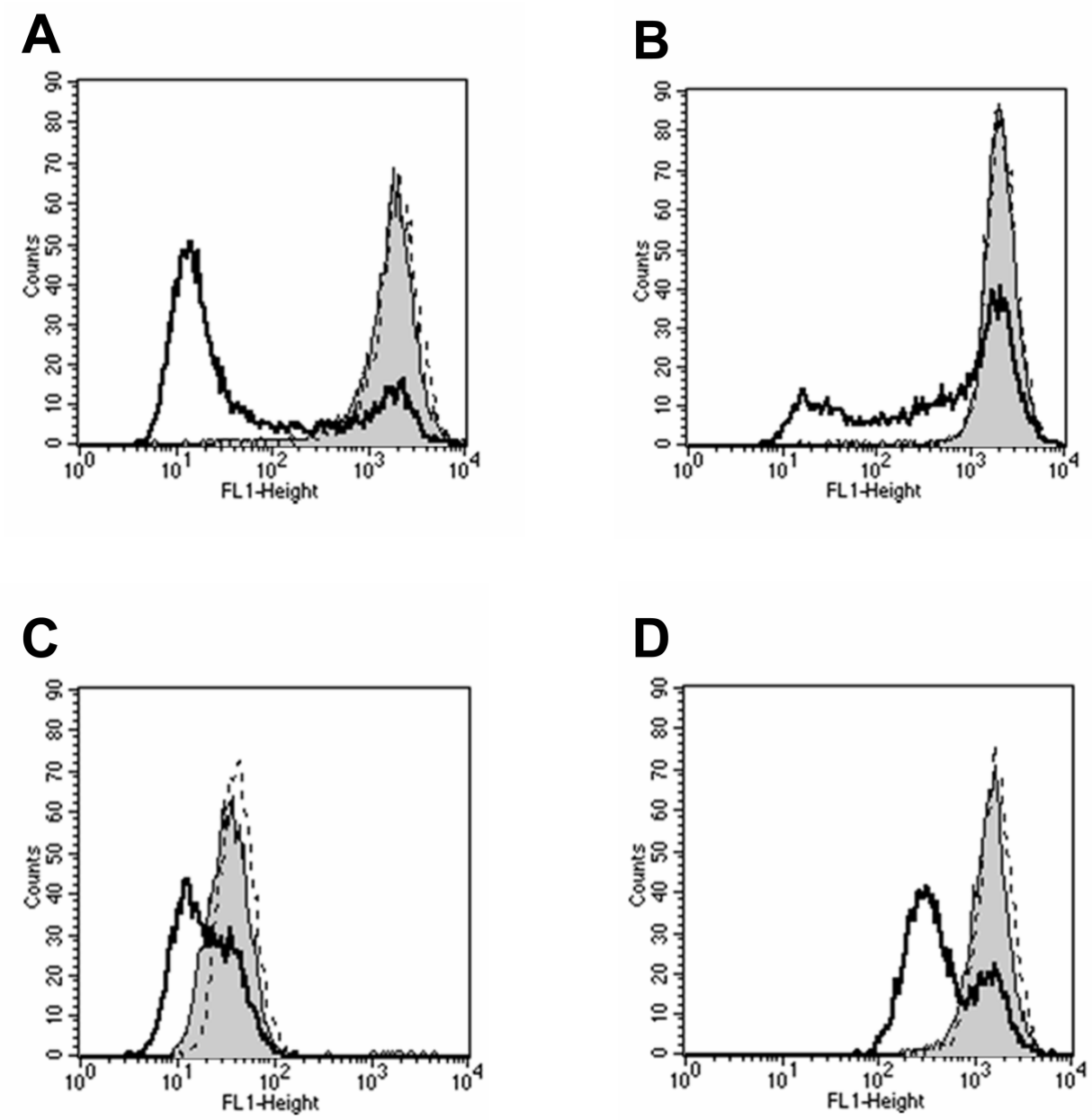

Figure S3. PGP1 expressed in HeLa cells did not transport HsMDR substrates.

A-D. HeLa cells expressing *PGP1* did not transport common mammalian MDR substrates. Grey peak represents cells transformed with pTM1 control vector (negative control). Solid line, *Homo sapiens* MDR1 (positive control); large dashes, PGP1. Shifting of observed peaks to the left indicates transport of the fluorescent substrate. Substrates tested:

A. Rhodamine 123.

B. Rhodamine 123 + cyclosporin A (1 µM).

C. daunomycin.

D. BODIPY -tagged vinblastine.

Assays were performed according previously described protocols (Hrycyna et al., 1998), and substrate retention was analyzed by FACS.

PGP1-mediated efflux of IAA oxidative degradation products in HeLa cells

As protoplast assays suggested that PGP1 may also be involved in efflux of IAA oxidative degradation products (Figure 20F), HeLa cells expressing PGP1 were incubated with a 1:1 mixture of ^{3}H-IAA and oxidative IAA breakdown products. Consistent with protoplast results, incubation of cells with 10 nM (indole equivalents) of the mixture resulted in net loading in transfected cells to levels twice those observed when cells were loaded with 63 nM fresh IAA. PGP1-mediated net ^{3}H-IAA efflux was also twice as high with this treatment (Figure 20D), but, NPA sensitivity observed at lower IAA concentrations was retained. When fresh ^{3}H-IAA was mixed with an equal amount (indole equivalents) of unlabeled oxidative breakdown products, net efflux was reduced (Figure 20D), suggesting competitive inhibition of IAA efflux. These data support a role for PGP1 in the transport of auxin breakdown products *in planta.*

Inhibitor studies of PGP1-mediated efflux in HeLA cells

The effects of inhibitor treatments on PGP1-mediated ^{3}H-IAA efflux were normalized to inhibitor-treated empty vector controls. PGP1-mediated ^{3}H-IAA net efflux was inhibited by treatment with 10 µM NPA (Figure 20E) and efflux was more NPA-sensitive at lower IAA concentrations (Figure 20E, F). Both mammalian and *Arabidopsis* PGPs have been shown to bind the aglycone flavonoid quercetin (Ferte *et al*., 1999; Murphy *et al*., 2002) which decreases mammalian PGP activity and negatively regulates auxin transport in plant tissues where PGPs are expressed (Brown *et al*., 2001; Ferte *et al*., 1999; Peer et al., 2001, 2004). Treatment with flavonoids and mammalian MDR/PGP inhibitors has previously been shown to reverse efflux of numan MDR substrates to the point of net retention in mammalian cells (Zhang and Morris, 2003). Net ^{3}H-IAA efflux by PGP1 was reversed when cells were treated with 200 nM quercetin (Figure 20E, F). Treatment with the MDR/PGP inhibitors verapamil and cyclosporin A increased net retention in cells expressing *PGP1* (Figure 20E, F), suggesting an additive cytotoxicity of these compounds in transfected cells. These data support the hypothesis that PGP1-mediated IAA transport can be regulated by endogenous flavonoids, as well as NPA.

Apparently due to the background activities observed, PGP-mediated efflux exhibited reduced sensitivity to quercetin and standard MDR/PGP inhibitors at lower IAA concentrations (Figure 20E).

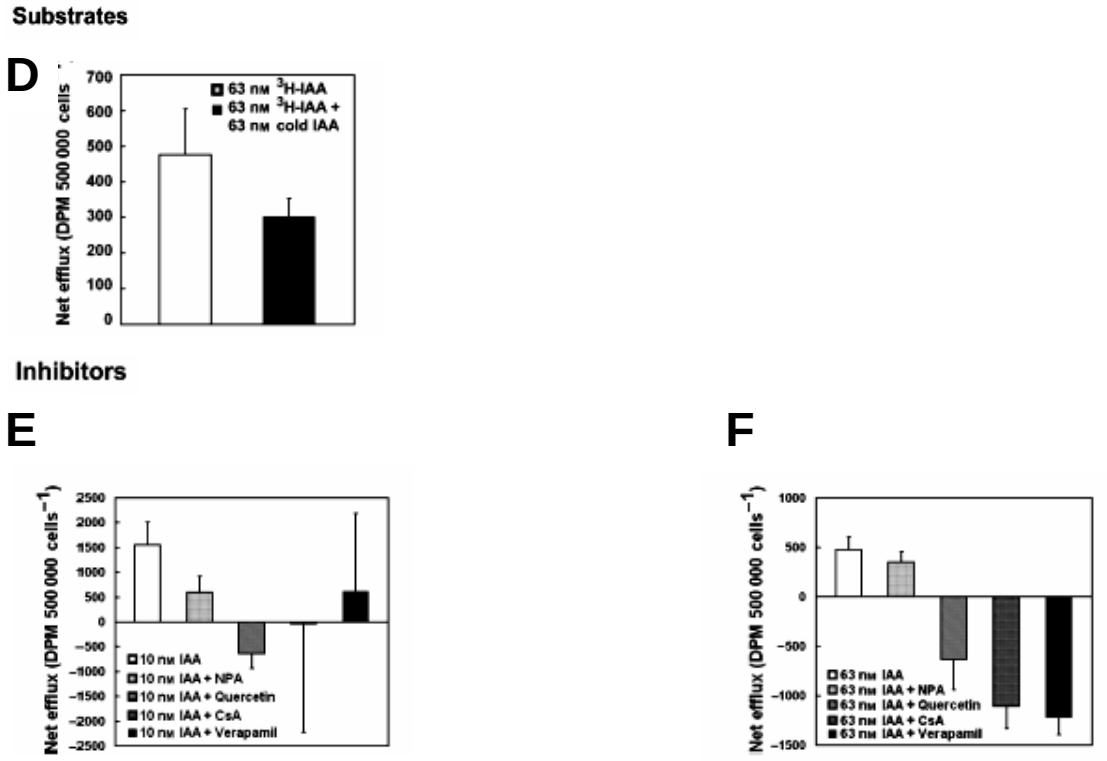

Figure 20. Efflux of radiolabeled substrates from HeLa cells expressing PGP1.

D. Unlabelled auxin degradation products competitively inhibit PGP1-modulated efflux. HeLa cells expression *PGP1* were incubated with a 1:1 mixture of 50.3% ^{3}H-IAA and oxidative IAA breakdown products (20.4% ^{3}H-oxindole-3-acetic acid, 16.8% ^{3}H-oxindole-3-carbinol, 5.7% ^{3}H-indole-3-aldehyde, and 6.8% ^{3}H-methylene oxindole, by LC-MS/MS).

E. ^{3}H-IAA efflux by PGP1 was inhibited by treatment with 10 µM NPA, 200 nM quercetin and by the ABC transport inhibitors cyclosporin A (CsA) and verapamil.

F. ^{3}H-IAA efflux by PGP1 was inhibited by treatment with 10 µM NPA, 200 nM quercetin and by the ABC transport inhibitors cyclosporin A (CsA) and verapamil when cells were loaded with 10 nM radiolabeled substrate.

DISCUSSION

Taken together, these results indicate that, in Arabidopsis, PGP1 can mediate cellular efflux of IAA and some IAA metabolites. Further, protoplast and whole plant transport assays suggest that PGPs are capable of mediating auxin transport *in planta*, although other transport proteins may also function in auxin efflux. As PGP1-mediated auxin efflux in heterologous systems exhibits decreased specificity and AEI sensitivity, other factors present *in planta* are probably required for the high degree of specificity seen in polar auxin transport. Non-polar localization of PGP1 at root and shoot apices suggests that interactions with other proteins are also required to confer directionality to auxin transport in those tissues. In these tissues, where rediffusion of IAA exported from small cells would be expected to impair gradiant-driven transport, additional energy-dependent IAA efflux might be required.

PGP1 localization and inhibition by quercetin are also consistent with its proposed interaction with endogenous flavonoids (Murphy *et al*., 2000; Peer *et al*., 2004). Strong expression of *PGP1* in apical tissues, localized reduction of IAA transport in the root tips of *pgp1* mutants, and PGP-mediated transport of IAA breakdown products suggest that PGP1 functions in regions exposed to high auxin concentrations. Further, the non-polar localization of PGP1 in root apices suggests that, where PIN-PGP interactions might take place, PIN proteins may confer an accelerated vectorial component to PGP-mediated transport.

Specific interactions of the many PIN and PGP family members in discrete tissues would be predicted to provide tight control of transport mechanisms. To elucidate the role of PGP family members in auxin transport, further developmental, and cell biological studies are required.

EXPERIMENTAL PROCEDURES

Plant growth conditions

Plants were grown as described previously (Geisler et al., 2003). For phenotypes of adult plants, Col-0, *pgp1* (At2g36910) and *pgp19* (At3g28860) mutants were grown under short day conditions: 8 hour 100 µmol·m^{-2}·s^{-1} white light, 22°C.

Expression and localization analysis

To construct the PGP1 (At2g36910) cmyc tag line (Pro$_{PGP1}$:PGP1-cmyc), a synthetic double-stranded oligonucleotide (forward primer: 5'*ctag*agcagaagcttatctccgaggaggacct*ctagt*gagct; reverse primer: 5'c*actagt*aggtcctcctcggagata**a**agcttctgct) encoding the 9E10 c-myc epitope was introduced into *Spe*I and *Sac*I sites of construct p4kbPstI (Sidler *et al.*, 1998) leading to p4kbMyc2. The cmyc epitope is thereby inserted at amino acid residue Leu_{14}. In comparison with the original sequence, a base pair was changed (bold letter) leading to introduction of a diagnostic *Hind*III site (underlined) without changing the codon bias. The 5' *Spe*I site of the oligonucleotide (italic) was designed in such a way that it was destroyed upon ligation, thereby allowing us to use the downstream *Spe*I site (italic) for further cloning. To add the 3'-terminal part of the *PGP1* gene, a 6.7 kb *Spe*I fragment was cut out from plasmid pOE and inserted in the correct orientation into p4kbMyc2 predigested with *Spe*I leading to pBSKMdrMyc2. From this a 9kb *Sal*I fragment encompassing *PGP1* was subcloned into the *Sal*I site of binary plant transformation vector pBI101 (Clontech, Palo Alto, USA). The final construct, PGP1cmyc2b (Pro$_{PGP1}$:PGP1-cmyc), containing the full-length genomic fragment of *PGP1*, including the cmyc tag at base pair 980, flanked by the *PGP1* promoter and terminator sequences was introduced into *A. thaliana* (ecotype Columbia) by *Agrobacterium tumefaciens* mediated vacuum-infiltration. Homozygous plants were selected on 0.5 x MS medium containing 50 µg/ml kanamycin and insertion was verified by Southern analysis.

For complementation, *pgp1* mutant plants (Noh *et al.*, 2001) were transformed with the binary vector PGP1cmyc2b (Pro$_{PGP1}$:PGP1-cmyc) via vacuum infiltration and homozygous lines were selected on 0.5 x Murashige and Skoog (MS) medium containing kanamycin.

Arabidopsis seedlings were grown on 1% phytagar plates (0.5x MS basal salts, pH

4.85) under white light (photon flux rate 100 µmol m^{-2} s^{-1}, 14 h light, 22°C) and 5- and 9-day seedlings were prepared for immunolocalization as described in (Friml *et al.*, 2003) with the following modifications: in some cases 0.5-0.8% pectolyase was used in place of drislase, seedlings were incubated overnight (37°C) with mouse anti-cmyc antibody (Santa Cruz Biotechnology) at 1:250 dilution, for 3h at 37°C with rabbit anti-mouse-FITC (whole IgG, Sigma F7506) and for 3h at 37°C with goat anti-rabbit-Alexa 488 at 1:250 in 3% BSA/MTSB, respectively. Immunofluorescence analysis was done using a confocal laser scanning microscope (Nikon, Eclipse 800) equipped with an argon laser (488nm) (Bio-Rad). Images were captured with a SPOT camera and processed using Adobe Photoshop 5.0.

For histochemical GUS staining, 10-d light grown Pro_{PGP1}:GUS transgenic seedlings were incubated in 10 mM HEPES pH 5.2, 500 mM sorbitol containing 2 µM benzoic acid or IAA for 3 hr. For all comparisons between treatments, identical staining conditions were used. For promoter gene quantification, Pro_{PGP1}:GUS transgenic seedlings were transferred for 3h onto 0.5 x MS plates supplemented with 1 µM BA or IAA. Seedlings were washed in MS, separated manually into root and shoot and GUS activity was assayed using 4-ß-4-methylumbelliferone-glucuronide as substrate. For each sample, segments of 40 seedlings were pooled and analyzed.

Protoplast and cell culture efflux experiments

Arabidopsis mesophyll protoplasts were prepared from rosette leaves of plants grown on soil under white light (100 µmol m^{-2} s^{-1}, 8 h light/16 h dark, 22°C). Intact protoplasts were isolated as described (Geisler *et al.*, 2003), and loaded by incubation with 1µl/ml ^{3}H-IAA (specific activity 20 Ci/mmol, American Radiolabeled Chemicals, St. Louis, MO), 7-^{14}C-benzoic acid (53 mCi/mmol, Moravek Biochemicals, Brea, CA) or 4-^{3}H-1-Naphthalene acetic acid (25 Ci/mmol, American Radiolabeled Chemicals, St. Louis, MO) on ice. External radioactivity was removed by separating protoplasts using a 50%/30%/5% percoll gradient. Samples were incubated at 25°C and efflux halted by silicon oil centrifugation. Retained and effluxed radioactivity was determined by scintillation counting of protoplast pellets and aqueous phases. For inhibitor studies, protoplasts were isolated and assayed in the presence of 10 µM of indicated inhibitors or the solvent alone.

Efflux experiments were performed with three to five independent protoplast preparations with 4 replicas for each time point. Protoplast volumes were determined

by the addition of 0.05 µCi ^3H_2O in separate assays; protoplast surfaces were calculated by measuring protoplast diameters.

For inhibitor studies, 50 ml of *Arabidopsis* cell suspension culture (May and Leaver, 1993) was grown in MS basal medium supplemented with 3% sucrose (w/v), 0.5 mg/l naphthalene acetic acid, and 0.05 mg/l kinetin in the presence of 10 µM of indicated inhibitors or the solvent alone for 12 h. Prior to measurements, the culture was centrifuged for 10 min at 800 rpm and 4°C, washed with sterile water and resuspended in 10 ml MCP (500 mM sorbitol, 1 mM $CaCl_2$, 10 mM MES, pH 5.6. 1µl/ml ^{3}H-IAA (specific activity 20 Ci/mmol, American Radiolabeled Chemicals, St. Louis, MO) was added, four 500 µl aliquots were collected after 0 and 10 minutes of incubation at 25°C and filtered on Millipore Durapore 0.22 µm GV filters. Cylcopropyl dione (CPD) was obtained from Caisson Labs (Rexburg, ID).

Transcript detection by RT-PCR

Total RNA from Arabidopsis WT protoplasts was prepared and DNaseI (Qiagen) treatment was performed with column-bound RNA. Oligo-dT primed cDNA from 1 µg of total RNA was synthesized using the Reverse Transcription system (Promega, Madison, USA). Transcripts specific for *PGP1* (At2g36910), *PIN1* (At1g73590), *PIN2* (At5g57090), and 40S ribosomal protein *S16* (At2g09990) were detected by conventional PCR for 30 and 35 cycles at 52°C annealing temperature. Intron-spanning PCR primers were: S16-S 5'ggcgactcaaccagctactga; S16-AS 5'cggtaactctt tggtaacga; PGP1-S 5'gtccctcaagagccgtgcttg; PGP1-AS 5'ccatcatcgatgacagcgatc, PIN1-S 5’tggagctcaagtgcttcgccg; PIN1-AS 5’gagaagagttatgggcaacgc; PIN2-S 5’cacggggtcaacgagtggagc; PIN2-AS 5’ctgagaatatcaggatggacg. Equal volumes of PCR products were separated on 2.5% agarose gels. Negative controls in the absence of enzyme in the RT reaction yielded no products.

RNA Isolation and Quantitative RT-PCR Analysis

RNA isolation and quantitative RT-PCR analysis was carried out as described previously with slight modification (Blakeslee *et al.,* 2004) using the ABI Prism 7000 Sequence Detection System (Applied Biosystems, Foster City, CA) in mixtures of 10 µl of TaqMan Universal PCR Master Mix containing AmpliTaq Gold DNA polymerase, AmpErase uracil-*N*-glycosylase (UNG), deoxynucleoside triphosphates with dUTP, a passive reference dye, optimized buffer components (Applied Biosystems), 500nM

each primer and optimum amount of template DNA in a total volume of 20µl. *ß-Tublin* (At5g12250) forward and reverse primers were 5'ttcccgggtcagctcaac and 5'ggagacgagggaaaggaatga, respectively. Primers used for the *AtPGP1* transcript were 5'tctggcgactagctaaaatgaactc and 5'ccacaaatgacagagcctactga. The A*tPGP19* forward primer sequence was 5'ggaagtttgaggaatctgagctattc, and the reverse primer sequence was 5tcggtcagtctctgcatttga. Transcripts specific for *ß-Tublin*, *AtPGP1*, and *AtPGP19* were detected by PCR; activation of AmpErase UNG (2 min, 50°C) and *Taq* polymerase (10 min, 95°C), 40 cycles of denaturation (15s, 95°C) and elongation (1 min, 60°C).

Analysis of IAA contents and transport

pgp1 mutants expressing the maximal auxin-inducible reporter Pro$_{DR5}$:GUS (Ulmasov *et al.*, 1997) were generated via crossing with wild type Pro$_{DR5}$:GUS plants. Seedlings were grown for five day as described above and stained for GUS expression (Ulmasov *et al.*, 1997).

For endogenous free auxin quantification, seedlings were grown as previously described (Geisler *et al.*, 2003). Nine days after planting seedlings were harvested, the cotyledons were excised, and seedlings were cut in half at the root-shoot transition zone. Roots and shoots were collected in lots of 500, and free auxin was quantitated by GC-MS as previously described (Chen *et al.*, 1988). Data presented are the averages of three lots of 500 seedlings. Auxin quantitations were confirmed by GC-MS after pentafluorobenzyl derivatization (Prinsen *et al.*, 2000).

For additional free auxin quantifications, hypocotyl and root segments of 30-50 seedlings were collected and pooled. The samples were extracted and analyzed by GC-MS. Calculation of isotopic dilution factors was based on the addition of 100 pmol $^2H_2$-IAA to each sample. In some cases, roots of 40 seedlings were manually divided into 2, 8 and 10 mm segments from the root tip and analyzed as described above.

Auxin transport assays on intact light grown Arabidopsis seedlings treated with a 0.1 µL microdroplet of 1 µM auxin at the root apical meristem using techniques described in Geisler *et al.* (2003), and root segments of 2 mm, were collected 2mm, 4 mm and 6 mm from the root tip.

2-NAA quantitation

Triplicate samples were pooled and extracted in methanol/2% HCl with shaking at 4°C for 30 minutes. An equal volume of diethylether/hexane (1:1) was added, the samples were shaken vigorously, and the upper phase was collected. This was repeated twice. Aminopropylsilyl SPE columns (Alltech State College, PA), were preconditioned with hexane before sample extracts were added. Eluate was collected from the application of three bed volumes of diethylether/2% formic acid to the column. The samples were dried prior to resuspension in methanol/1% phosphoric acid. Samples were analyzed by LC-MS using a Waters C18 MS column on a Q-TOF Micro equipped with a collision cell and phosphoric acid lock spray for internal calibration (Waters, Bedford MA) and using naphthalene as an internal standard.

Auxin metabolite characterization

IAA oxidative breakdown products were determined by LC/MS and GC/MS (Ljung *et al*., 2003; 2005).

Yeast assays

The PGP1 cDNA was cut out from plasmid pUCcMDR (Windsor *et al.*, 2003) with *Stu*I and *Hinc*II and cloned into the Klenow filled *Not*I site of yeast shuttle vector pNEV (pNEV-PGP1). pNEV and pNEV-PGP1 were introduced into *S. cerevisiae* strain JK93da or *yap1-1* (Prusty *et al.,* 2004) and single colonies were grown in synthetic minimal medium without uracil, supplemented with 2% glucose (SD-URA). For detoxification assays, transformants grown in SD-URA to an OD_{600} around 0.8 were washed and diluted to an OD_{600} of 1.0 in water. Cells were 5-times 10-fold diluted and each 5 µl were spotted on minimal media plates containing 100 µM $CuSO_4$ supplemented with 750 µM 5-fluoro-indol (5-FI) or 10 µM IAA in the absence or presence of indicated uncouplers and inhibitors. Growth at 30°C was assessed after 3-5 days. Assays were performed with 3 independent transformants.

For loading experiments, cells were grown to an OD_{600} of 1.0, washed and incubated at 30°C with combinations of 1 µl/ml of 5-^{3}H-IAA (specific activity 20 Ci/mmol, American Radiolabeled Chemicals, St. Louis, MO), 7-^{14}C-BA (53 mCi/mmol, Moravek Biochemicals, Brea, CA), 4-^{3}H-1-Naphtalene acetic acid (25 Ci/mmol, American Radiolabeled Chemicals, St. Louis, MO) or 1 µM 2-NAA (Sigma) in SD pH 4.5. Aliquots of 0.5 ml were taken after 0, 5, 10, 30, 60 and 120 min incubation at 30°C.

For efflux experiments, cells were loaded for 10 min on ice, washed 2 times with cold water, and resuspended in 15 ml SD pH 4.5. 0.5 ml aliquots were taken after 0, 2.5, 5, 7.5 10, 15 and 20 min incubation at 30°C.

For assaying permeabilities, yeast were grown to logarithmic phase (OD_{600} 1.25) and were washed with water, FDA-buffer and resuspended in 5 ml FDA-buffer (50 mM HEPES-NaOH pH 7.0, 5 mM 2-deoxy-D-glucose). To 990 µl cell suspension, 10 µl 5 mM fluorescein diacetate (FDA) were added and aliquots were measured at 485 nm excitation and 535 nm emission. In order to determine the temperature dependency of efflux, loaded yeast cells were washed, divided into two aliquots and incubated at 4°C and 30°C, respectively. For assaying ATP dependency of transport, yeast were grown to logarithmic phase, washed with water and FDA-buffer, resuspended in 50 ml FDA-buffer and incubated for 1h at 30°C. Cells were harvested, washed, resuspended in 10.8 ml 20 mM sodium citrate pH 4.5. After temperature equilibration at 30°C, 1 µl/ml of 5-^{3}H-IAA was added, resuspensions were divided into two aliquots followed by addition of 0.6 ml 20% glucose to one aliquot. For inhibitor studies, yeasts were grown for 12 h prior to the measurements and assayed in the presence of 10 µM of indicated inhibitors or the solvent alone.

All aliquots were filtered on Whatman GF/C filters, washed 3 times with cold water and retained radioactivity was quantified by scintillation counting. All transport experiments were performed 3-5 times with independent transformants, with 4 replicas each.

In order to verify the identity of effluxed IAA, yeast cells transformed with pNEV and pNEV-PGP1 were loaded with 10 µM $^{2}H_5$-IAA and 1 µM $^{13}C_6$-IAA in 20 mM sodium citrate pH 4.5. Effluxed IAA was extracted by ethyl acetate and analyzed by MS/MS.

Yeast PGP1 expression and immunolocalization

Yeast cells transformed with pNEV and pNEV-PGP1 were grown to mid-log phase and microsomes were separated via 7.5% PAGE. Western blots were immunoprobed using anti-PGP1 antibody (Sidler *et al.*, 1998). Yeast immunolocalization was performed using standard protocols. Fixed yeast cells were incubated overnight at 30°C with rabbit anti-PGP1 antibody (Sidler *et al.*, 1998) and for 3h with goat anti-rabbit-Alexa 488 at 1:200 in 3% BSA, respectively. Stained cells were incubated in mounting media containinig DAPI and immunofluorescence analysis was done using a confocal laser scanning microscope (Leica, DMIRE2) equipped with argon (488

nm) and UV laser (410 nm). Fluorescence, DIC and DAPI images were processed using Adobe Photoshop 7.0. Vector controls showed no detectable fluorescence with anti-PGP1 antibody.

HeLa cell assays

Radiolabeled substrated accumulation assay: PGP1 (At2g36910) was expressed in mammalian HeLa cells using a vaccinia virus co-transfection system providing several advantages over other heterologous expression systems, including proper glycosylation and suppression of host protein synthesis following vaccinia infection (Elroy-Stein *et al*., 1991). The transient vaccinia expression system was used because stable cells lines develop mutations and express other endogenous drug-resistance mechanisms. Full-length, HA-tagged PGP1 was cloned into the MCS of the pTM1 vector (Hrycyna et al., 1998). For pTM1-PGP1, a *PGP1* PCR fragment containing XmaI/BamHI restriction sites was generated using the following primers: PGP1-S 5'-tcc ccc cgg ggc atg gat aat gac ggt and PGP1-AS 5'-cgc gga tcc agc gta atc tgg tac gtc gta agc atc atc ttc ctt aac. Assays for accumulation of radiolabeled substrates was performed according to the method described in (Hrycyna et al., 1998), with the following modifications: Cells were transfected in 6-well plates with 2 µg of DNA (pTM1 control vector, PGP1) per well. For radiolabeled substrate accumulation assays, gradient conditions were developed wherein radiolabeled auxin was passively accumulated by empty vector control HeLa cells without induction of cellular damage. Confluent cells were transfected in six well plates and 16-24 h after transfection, cells were washed with 3 ml pre-warmed DMEM media, 5% FBS. Each transfection utilized 600,000-1,000,000 cells and equal loading of wells was verified by sampled cell counts. Cells counts were determined both by Coulter counting and microscopic visualization (percent confluence). Cells were then incubated with 2 ml of PBS citrate buffer, pH 5.5, 5% calf sera containing either 10 nM or 62.5 nM of the following radiolabeled substrates: ^{3}H-IAA (specific activity 26 Ci/mmol, Amersham Biosciences, Piscataway, NJ), ^{3}H-benzoic acid (BA) (specific activity 20 Ci/mmol, American Rabiolabeled Chemicals, St. Louis, MO), or ^{3}H-1-NAA (specific activity 20 Ci/mmol, American Radiolabeled Chemicals, St. Louis, MO). Possibly due to buffer compatibility issues, it was difficult to maintain solubilization of 1-NAA in loading assays. For radiolabeled auxin degradation product assays, cells were loaded with 10 nM radiolabeled IAA breakdown products (specific activity 25 Ci/mmol, American

Radiolabeled Chemicals, St. Louis, MO). Cells were incubated with radiolabeled substrates for 40 min at 37°C, 5% CO_2. For inhibitor studies, cells were incubated with radiolabeled IAA in the presence of 10 µM NPA, 200 nM quercetin, 1µM cyclosporin A, or 5 µM verapamil. After incubation, cells were washed 3 times with 3 ml ice-cold PBS, removed from the wells by trypsinization, and added to 18 ml scintillation fluid. Samples were counted in a Perkin-Elmer scintillation counter. Components of the radiolabeled auxin breakdown product mixture were determined and quantified via LC/MS. For cold 2-NAA retention studies, cells were incubated with 62.59 nM cold 2-NAA, harvested, and extracted. 2-NAA was quantified using LC/MS. As with 1-NAA, it proved difficult to keep 2-NAA solubilized for cell loading in the buffer system used. Fluorescent substrate accumulation assays were performed in the HeLa cell system as previously described (Hrycyna *et al*., 1998).

Data points were normalized to the average empty control vector value of 2851.885 DPM/500,000 cells for auxin treatments. Cell viability after treatment was confirmed visually and via cell counting.

Western Blotting of HeLa cells

HeLa cells expressing PGP1 were harvested using a rubber policeman. Proteins were isolated from cells as previously described (Hrycyna *et al*., 1998). Proteins were separated via 7% SDS-PAGE and then transferred onto nylon membrane at 10V, in an ice bath, overnight. After blocking with 5% non-fat dried milk in 1X PBS with 0.1% Tween 20, the nylon membrane was incubated with primary antibody for 2h at 4°C (anti-HA from Sigma). Following washing, membranes were incubated with HRP-conjugated secondary antibody, and developed using the ECL chemiluminescent system, according to the manufacturer's protocols (Amersham Pharmacia Biotech).

Data analysis

Data were analyzed using Prism 4.0b (GraphPad Software, San Diego, CA); statistical analysis was performed using SPSS 11.0 (SPSS Inc., Chicago, Illinois) and SigmaStat (Systat, Point Richmond, CA).

ACKNOWLEDGEMENTS

We thank V. Croy, C. Gaillard, C. Ringli, A. Hopf for technical assistance, S. Plaza for help with statistical analysis, and I. Baxter for microarray data. This publication is dedicated to MD R. Louma (MG) and to the memory of K. Thimann (ASM and WAP).

IV Immunophilin-like TWISTED DWARF1 modulates auxin efflux activities of Arabidopsis MDR/PGP transporters

Rodolphe Bouchard[1], Aurélien Bailly[1], Vincent Vincenzetti[1], Joshua J. Blakeslee[2], Ivan Paponov[3], Klaus Palme[3], Angus. S. Murphy[2], Burkhard Schulz[2] and Markus Geisler[1]

[1] Zurich-Basel Plant Science Center, University of Zurich, Institute of Plant Biology, Molecular Plant Physiology, CH-8008 Zurich, Switzerland

[2] Purdue University, Department of Horticulture, West Lafayette, USA

[3] Institut für Biologie II, Universität Freiburg, D- 79104 Freiburg, Germany

Correspondence to Markus Geisler: markus.geisler@botinst.unizh.ch

ABSTRACT

Previously, the immunophilin-like protein TWD1 (AtFKBP42) from Arabidopsis has been demonstrated to physically interact with MDR/PGP ABC transporters AtPGP1 and AtPGP19 (AtMDR1). Phenotypic and biochemical analysis of overlapping dwarf phenotypes of *atpgp1 atpgp19* and of *twd1* mutant plants suggested a positive regulatory role of TWD1 on AtPGP1 and AtPGP19 transport activities. The latter have recently been shown to control plant development by catalyzing the primary active export of the plant hormone auxin.

Here we show that export of the auxin IAA from *twd1* cells is strongly reduced to similar magnitudes as found for atpgp1 atpgp19 mutants. Overexpression of *AtPGP1* and *AtPGP19* but not of *TWD1* strongly enhances auxin export verifying a regulatory role for TWD1. Secondary effects due to delocalization of auxin efflux components, like PIN1 or PIN2, or AtPGP1 itself were excluded. *atpgp1 atpgp19* and *twd1* mutant roots reveal elevated levels of free IAA in the elongation zone and above that seem to account for agravitrope root behavior and the strong developmental phenotype. Coexpression of TWD1 and AtPGP1 in yeast and mammalian cells demonstrated the specificity of the regulatory effect. Export of the synthetic auxin 1-NAA is strikingly reduced in atpgp1 atpgp19 mutants but surprisingly not in twd1 mutants suggesting that TWD1 defines not only transport activities but also substrate specificities. In summary, we demonstrate a novel mode of MDR/PGP regulation via FKBP-like immunophilins that might offer alternative strategies to overcome multidrug resistance during cancer treatment.

INTRODUCTION

The plant signaling molecule auxin (indole-3-acetic acid, IAA) plays a critical role in plant growth and development (Benkova *et al*., 2003; Friml and Wisniewska, 2004). Moreover, it is currently tested upon its potential to function as beneficial cytotoxin in cancer therapy upon oxidative activation (Folkes and Wardman, 2001). While recent advances support also a morphogen- and neurotransmitter-like concept in plants, (Baluska *et al*., 2003) so far research has mainly concentrated on its hormone-like function. This is linked to so-called polar auxin transport (PAT) from the shoot to the root and up again in cell-to-cell manner (Friml. 2003; Blakeslee *et al*., 2005). PAT apparently provides essential directional and positional information for developmental and physiological processes (Blilou *et al*., 2005). The chemiosmotic model of auxin transport (Raven 1975) was supported by the identification and characterization of candidate proteins for auxin influx (AUX1/LAX family) and efflux (PIN family) (reviewed in Friml and Wisniewska, 2004; Blakeslee *et al*., 2005). While for members of both families clear biochemical verification of their transport activities is still lacking, their role as essential components of auxin influx and efflux complexes has been demonstrated; most strikingly both proteins reveal polar expression pattern that is in line with know routes of PAT (Friml 2003). Evidence has been provided for a model in which multiple PIN proteins co-function in creating a reflux loop (Blilou *et al*., 2005).

Recently, members of the multidrug-resistance/p-glycoprotein (MDR/PGP) family (hereafter referred to as PGPs) have been implicated in auxin transport (Luschnig 2002). Mammalian members of this superfamily of ABC (ATP-binding cassette) transporters are of widely clinical interest as they have been shown to catalyze the ATP-dependent export of chemotherapeutic agents (reviewed in Krishna and Meyer, 2001). In the model plant *Arabidopsis thaliana*, a small subset of - in total 21 - PGPs seems to be involved in auxin transport (Blakeslee *et al*. 2003; Jasinski *et al*., 2003; Martinoia *et al*. 2002). Loss-of function mutants of *AtPGP1* homologs results in reduced auxin transport in intact tissues and growth phenotypes in Arabidopsis (*atpgp1* and *atpgp19* (*atmdr1*); Geisler *et al.,* 2003; Lin and Wang, 2005; Noh *et al*., 2001), maize (*brachytic2*) and sorghum (*dwarf3*, Multani *et al*., 2003). Interestingly, the dwarf phenotype of *atpgp1 atpgp19* is more severe than those of the single knock-outs suggesting overlapping functions (Geisler *et al*., 2003, Lin and Wang,

2005). Recently, AtPGP1 has been demonstrated to catalyze the primary active transport of native and synthetic auxins using plant and heterologous transport systems. AtPGP1 activity was inhibited by diagnostic inhibitors of PAT (like 1-naphthylphtalamic acid (NPA) and flavonols) and anti-cancer drugs (like verapamil and cyclosporin A). AtPGP1 exhibits non-polar plasma membrane locations in small, meristematic cells of the root and shoot apices and polar (mainly basal) expression in longer cells of the elongation zone and above which is inline with mathematical predictions of auxin transport rates (Blakeslee *et al*., 2005). Very recently, in two parallel studies AtPGP4 has been shown to be involved in root and root hair development and to catalyze remarkably influx of auxin (Santelia *et al*., 2005; Terasaka *et al*., 2005). In a model AtPGP1 and AtPGP4 have been proposed to co-function in PAT (Santelia *et al*., 2005).

PGPs seem to function as central catalytic elements of multi-protein auxin transport complexes (Blakeslee *et al*., 2005; Geisler *et al*., 2003; Murphy *et al*., 2002,):

the C-terminus of AtPGP1 has been originally identified in a yeast two-hybrid screen using the soluble portion of the putative GPI-anchored, immunophilin-like protein TWISTED DWARF1 (TWD1, FKBP42) as bait (Geisler *et al*., 2003). Moreover several AtPGPs (among those AtPGP1, AtPGP19 and AtPGP4) have been co-purified with TWD1 from high-affinity NPA-binding complexes with other proteins known to be involved in protein trafficking and cycling (Geisler *et al*., 2003; Murphy *et al*., 2002). *twd1* plants (apparently being isoalelic to ultracurvata2 (ucu2, Pérez-Pérez *et al*., 2004)) show a drastic, pleiotropic auxin-related phenotype that includes dwarfism, circinate leafs, and helical rotation of organs both on the epidermal and whole plant level. Interestingly, plants resemble those of *atpgp1 atpgp19* plants, and accordingly, AtPGP1/AtPGP19/TWD1 interaction has been verified on different levels (Geisler *et al*., 2003). Overlapping phenotypes together with reduced auxin transport in intact hypocotyls has suggested a regulatory role of AtPGP1 and AtPGP19 in auxin transport (Geisler *et al*., 2003; Romano *et al*., 2005).

TWD1 belongs to the FKBP (FK506-binding protein)-type subfamily of immunophilins, ubiquitous proteins known to regulate immunosupression in mammals (Romano *et al*., 2005). Based on drastic phenotypes of transgenic plants with altered expression levels of multidomain FKBPs, like PASTICCINO1/AtFKBP52 (PAS1) and wheat FKBP77 (Kurek *et al*., 2002), have been shown to function as key players in plant development. However, a unique feature of TWD1 is its C-terminal

membrane anchor that fixes it both in the plasma and the vacuolar membrane (Kamphausen *et al*., 2002) where it interacts with the C-termini of MRP-like ABC transporters AtMRP1 and AtMRP2 (Geisler *et al*., 2004). Interestingly, both couples of ABC transporters interact with independent domain of TWD1: AtPGP1/19 with the PPIase (*cis-trans* peptidyl proly isomerase) and AtMRP1/2 with the TPR (tetratricopetide repeat) domain that might account for the specificity of interaction.

For both mirror-like complexes, regulatory roles of TWD1 on individual ABC transporter pairs has been suggested (Geisler *et al*., 2003, 2004) but molecular proof is lacking. Mammalian FKBPs are well known to bind to and to modulate calcium release channels (Cameron *et al*., 1995; Timerman *et al*., 1995). Moreover, FKBP12 has been shown to regulate murine MDR3 but attempts to demonstrate interaction failed so far (Hemenway and Heitman, 1996). Interestingly, FKBP12-dependent regulation of MDR3-mediated drug resistance does not require PPIase activity (Hemenway and Heitman, 1996; Mealey *et al*., 1999). In line with this observation, the PGP interacting PPIase domain of TWD1 is not active (Kamphausen *et al*., 2002) and does not bind FK506 (Schulz and Geisler, unpublished data).

Here, we provide several lines of evidence that TWD1 functions as positive regulator and selectivity filter of AtPGP1 mediated hormone transport suggesting a novel mode of PGP regulation via FKBPs.

RESULTS

Cellular and polar root transport of IAA is reduced in *twd1* and *atpgp1 atpgp19* mutants indicating a regulatory role of TWD1

Recently, functional interaction between Arabidopsis FKBP42 TWD1 and MDR/PGP transporters AtPGP1 and its closest homologue AtPGP19 (Geisler *et al*., 2003) has been demonstrated. Further, several lines of direct and indirect evidence have suggested that TWD1 functions as regulator of auxin transport capacities provided by AtPGP1 and AtPGP19 (Geisler *et al*., 2003, 2005).

In order to demonstrate the physiological impact of TWD1 interaction we measured auxin efflux at the cellular level in plant and heterologous expression systems. Leaf mesophyll protoplasts have been established as ideal system in order to demonstrate PGP-mediated auxin export. In wild-type, IAA efflux is inhibited by known inhibitors of PAT and PGPs of clinical relevance (Geisler *et al*., 2005). *twd1* protoplasts showed strongly reduced ^{3}H-IAA efflux compared to wild-type (66% transport reduction) which was even lower compared to *atpgp1 atpgp19* (49% reduction). This is of interest as it reflects perfectly auxin transport behaviors found for measurements on intact tissues (Geisler *et al*., 2003). Presence of *AtPGP1*, *AtPGP19* and *TWD1* was verified by RT-PCR (Figure 21A) and Western analysis (Figure 21B, C). The impact of indirect factors like vacuolar trapping of IAA or reduced export capacities due to altered vacuolar pH or protoplast surfaces could be exluded (data not shown).

In order to test a regulatory role of TWD1 more rigorously, we measured IAA efflux from plants overexpressing TWD1-HA. Overexpression of TWD1-HA verified by Western blotting did not alter *AtPGP1* or *AtPGP19* expression (inset Figure 21B) and, interestingly, not IAA efflux which was not significantly different from wild-type (Figure 21B). This excludes a direct role of TWD1 in auxin transport. However, constitutive upregulation of *AtPGP1* or *AtPGP19* enhanced strongly IAA export compared to their individual wild-type backgrounds, Arabidopsis RLD and columbia, respectively, that seems to own ecotype–dependent, different efflux capacities. The lower relative stimulation of AtPGP19-mediated IAA export compared to AtPGP1 does not reflect physiological relevance (IAA transport in atpgp1 and atpgp19 was 72% and 57% of wild-type) but differences in expression levels as shown by RT-PCR (relative expression level of wild-type: AtPGP1: 8.0 ± 2.2; AtPGP19: 3.0 ± 0.6).

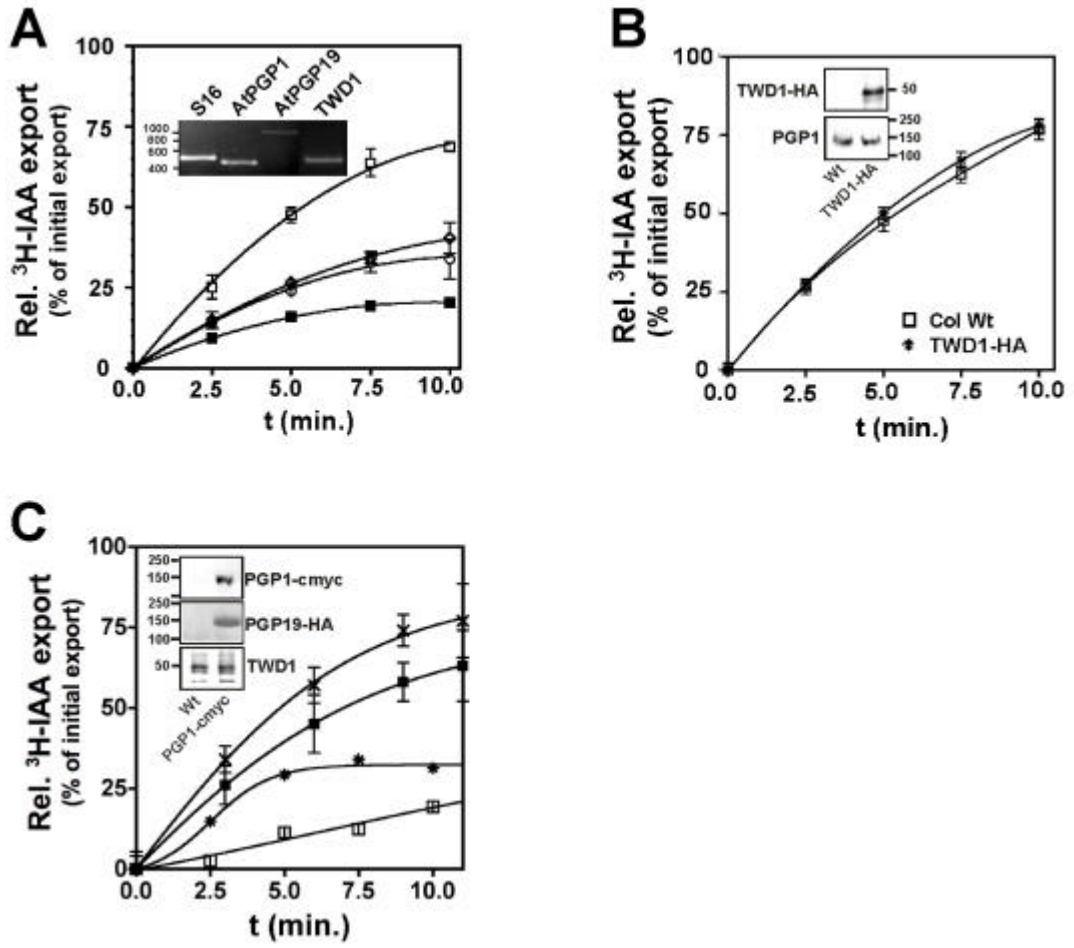

Figure 21: Cellular IAA export is reduced in twd1 but not effected by overexpression of TWD1

A ^{3}H-IAA export from wild-type (□) leaf mesophyll protoplasts is reduced to a similar extend in twd1 (○) and atpgp1 atpgp19 plants (◇). As negative control we used deenergized (dark-treated plant material (■). Presence of AtPGP1, AtPGP19 and TWD1 was verified by semi-quantitative RT-PCT (inset). Efflux is presented as relative export of initial export. Shown are means with standard deviations of 4 individual experiments, n = 4.

B Constitutive overexpression of TWD1 does not alter ^{3}H-IAA export suggesting a regulatory role of TWD1. Overexpression of TWD1-HA in protoplasts was verified by Western blot analysis using anti-HA (Geisler et al. 2005); overexpression of TWD1 does not alter expression of AtPGP1 or AtPGP19 (inset) shown by anti-PGP that does not differentiate between AtPGP1 and AtPGP19 (Geisler *et al.* 2005).

C Constitutive over-expression AtPGP1-cmyc (✳) and AtPGP19 (✕) enhances ^{3}H-IAA export compared to their corresponding wild-type ecotypes, RLD (□) and columbia (■), respectively. Over-expression of AtPGP1 and AtPGP19 in protoplasts was verified by Western blot analysis using anti-cMYC and anti-HA. Over-expression of PGPs does not alter expression of TWD1.

Mammalian FKBPs are known to own chaperone function and to be involved in protein secretion. In order to exclude that loss-of-function of TWD1 did alter targeting of AtPGP1 or other known components of auxin efflux complexes we immunolocalized PIN1 and PIN2, essential components of the auxin efflux complex (Blakeslee *et al*., 2005), in wild-type and twd1 root tips. The ratio to choose PIN1 and PIN2 was that they show partially overlapping expression pattern with AtPGP1 (Geisler *et al*., 2005) and that they co-purified with AtPGP1 and AtPGP19 in an NPA affinity chromatography (Blakeslee *et al*., 2005). Neither PIN1 nor PIN2 were mislocalized in *twd1* (Figure 22A) suggesting that altered PIN localization cannot account for the reduced IAA export in *twd1*. Immunolocalization of Pro_{AtPGP1}:AtPGP1-cmyc in roots and Western analysis of whole plant plasma membranes (data not shown) or microsomes separated by continuous sucrose gradient centrifugation also excluded altered expression or mistargeting of AtPGPs in *twd1*. Further, loss- and gain of function of *TWD1* has no influence on the plant level of *AtPGP1* transcripts shown by RT-PCR (Figure 22B) and gene chip analysis (data not shown).

In summary, our data clearly point to a regulatory role of TWD1 on AtPGP-mediated auxin efflux capacities.

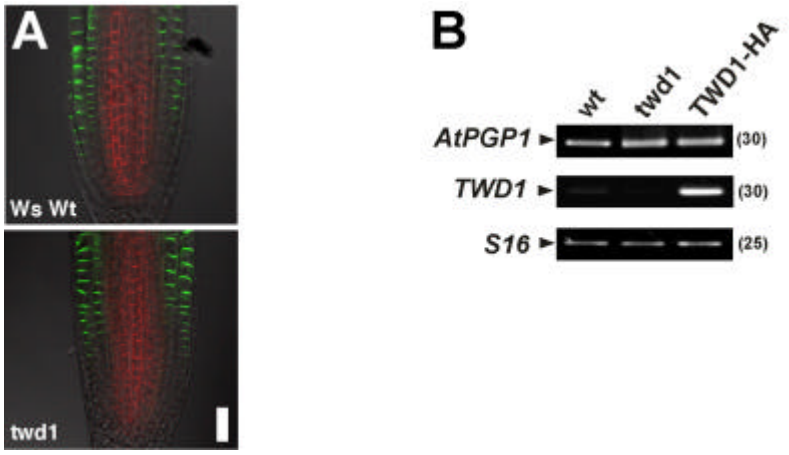

Figure 22: Loss-of-function of *TWD1* does not alter *PIN1*, *PIN2* and *AtPGP1* expression.

A Whole-mount immunolocalization of PIN1 (red) and PIN2 (green), putative components of the auxin efflux complex, shows no significant changes in expression. For orientation, coloured fluorescence images were superimposed with bright field pictures; the bar represents 50 µm.

B Loss- and gain-of-function of *TWD1* has no influence on AtPGP1 expression as shown by semi-quantitative RT-PCR.

twd1 and *atpgp1 atpgp19* roots reveal strongly elevated free auxin levels and altered gravitropism

Previously, basipetal auxin transport from the root tip has been reported to be reduced in atpgp1 and atpgp19 root tips, and as a consequence, to cause reduced IAA levels in 5-days old roots (Geisler *et al*., 2005). We re-analyzed *twd1* free IAA levels in roots and shoots (see Figure 23C for scheme) of nine-day old seedlings (in parallel with atpgp1, atpgp19, atpgp1 atpgp19) and found surprisingly elevated IAA levels in all mutant roots while shoot levels revealed only small differences compared to wild-type (Figure 23A). Interestingly, IAA roots contents in *atpgp1 atpgp19* (308%) and *twd1* (286%) were similarly more drastically altered when compared with *atpgp1* (162%) or *atpgp19* (154%). This again suggests functional redundancy of *AtPGP1* and *AtPGP19*, and a loss-of-function of *AtPGP1/19*-mediated IAA auxin transport.

In order to confirm these data, we analyzed expression of the maximum auxin reporter construct Pro_{DR5}:GFP (Ottenschläger *et al*., 2004) in twd1 and atpgp mutant root tips which allows non-invasive detections in comparison to the Pro_{DR5}:GUS construct. In agreement with previous data using Pro_{DR5}:GUS (Lin and Wang 2005; Geisler *et al*., 2005), atpgp single mutant roots showed reduced reporter gene expression in the root columella (Figure 23B) which was to similar extent also reduced in *atpgp1 atpgp19* and *twd1* roots.

Reduction of auxin levels visualized by the reporter gene constructs seems to be at first view in contradiction to the elevated IAA concentration measured by GC-MS. Fractionation of *twd1* roots as indicated in Figure 23C and determination of free auxin revealed that auxin levels in the “tip” (region 2 mm from the tip) were indeed slightly reduced (89% of wild-type level) while mid (128%) and upper part root fractions (176%) contained higher levels (Figure 23C). The relative contents in this assay were lower which might be due to the drastic manipulation during fractionation. However, these results were confirmed by whole-mount immunodetection of auxin using a monoclonal anti-IAA antibody (Figure 23D) although this antibody cross-reacts as well with auxin conjugates.

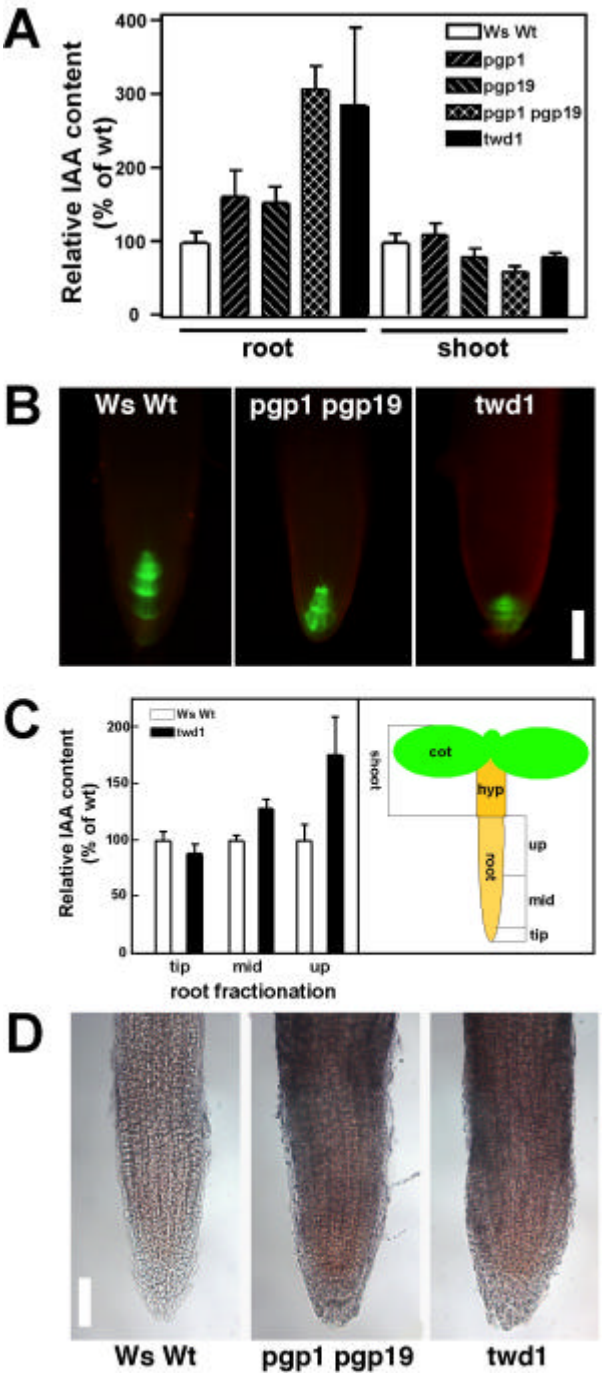

Figure 23: IAA content in twd1 and atpgp1 atpgp19 root is drastically elevated.

A Free IAA content in 9-day seedlings determined by GC-MS.

B Pro_{DR5}::GFP expression in 9-day seedling root tips shows no significant differences.

C Fractionation of 9-day seedling roots indicates elevated free IAA levels in the root elongation zone and above.

D Whole-mount immunolocalization of auxin using monoclonal anti-IAA (Phytodetek) indicates elevated free IAA levels in the root elongation zone and above. Note that a typical columella stain (Benkova et al. 2003) is absent in wild-type root tips due to very short development of all roots; the bar represents 100 µm.

Root gravitropism is known to be dependent on and mediated by PAT (Friml and Palme, 2002; Muday and DeLong, 2001; Teale *et al*., 2005) and therefore an ideal tool to investigate if the elevated auxin levels found in the mutants change gravitropic responses. Using our conditions single mutants exhibited no significant changes in gravitropism (data not shown), but both *atpgp1 atpgp19* and *twd1* exhibited impaired gravitropic responses compared to the wild-type (Figure 24). Consistent with previous results in hypocotyl tissues (Noh *et al*., 2003), the roots of *atpgp1 atpgp19* mutants exhibited slight hypergravitropism, while the roots of *twd1* showed impaired gravitropism without any vectorial preference.

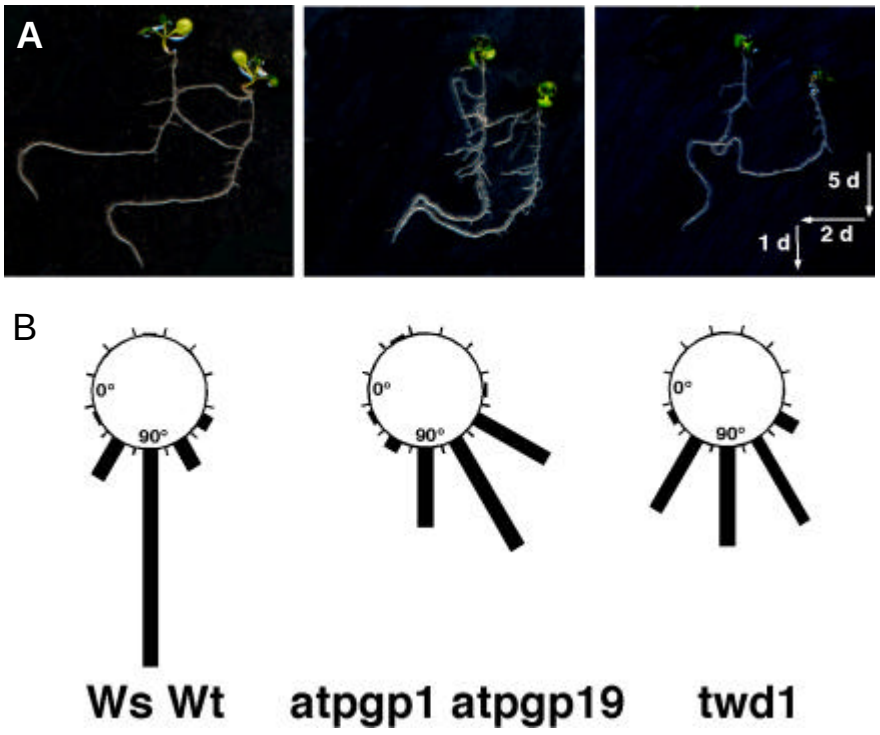

Figure 24: twd1 and atpgp1 atpgp19 seedlings are defective in root gravitropism.

A For analysis of growth plants were grown on vertical plates under continuous white light and pictures were taken after changing the gravity field twice as indicated.

B For quantification of gravitropism plants were grown on vertical plates under controlled light conditions (see Material and Methods). Each gravistimulated root was assigned to one of twelve 30° sectors; the length of each bar reperesents the percentage of seedlings showing the same direction of root growth.

Modulation of AtPGP1-mediated IAA export by TWD1 is specific and has reverse effects in yeast and mammalian cells

In order to investigate the regulatory effect of TWD1 on AtPGP activity in more detail, we coexpressed AtPGP1 and TWD1 in yeast. AtPGP1 and TWD1 colocalize on the plasma membrane as shown by Western and confocal analysis of AtPGP1-YFP and TWD1-CFP (Figure 25A). Expression of AtPGP-YFP and TWD1 N-terminally fused to *Renilla* luciferase (TWD1-rLuc) resulted in a positive BRET ratio verifying the interaction (Bailly and Geisler, unpublished data).

Monitoring time dependent AtPGP1-mediated IAA efflux in yeast revealed that coexpression reverted export drastically to vector control level (Figure 25B). The same tendency was found when loading kinetics were recorded (data not shown).

Inhibition of AtPGP1 by TWD1 in yeast was verified by employing yeast growth assays using the *yap1-1* mutant (Prusty *et al*., 2004). This strain that is hypersensitive to IAA due to transcriptional upregulation of AUX1/LAX-like IAA uptake systems has turned out to be an excellent genetic tool to demonstrate IAA transport (Geisler *et al*., 2005, Santelia *et al*., 2005).

Like shown before (Geisler *et al*., 2005), AtPGP1 complements this mutant providing growth on IAA (Figure 25D), however coexpression with TWD1 reverts detoxification to vector control level. Similarly, TWD1 inhibited AtPGP1-mediated detoxification of the toxic auxin-analogue 5-fluoroindol (Figure 25F) which has been used to demonstrate PIN2/AGR1 function (Luschnig *et al*., 2001).

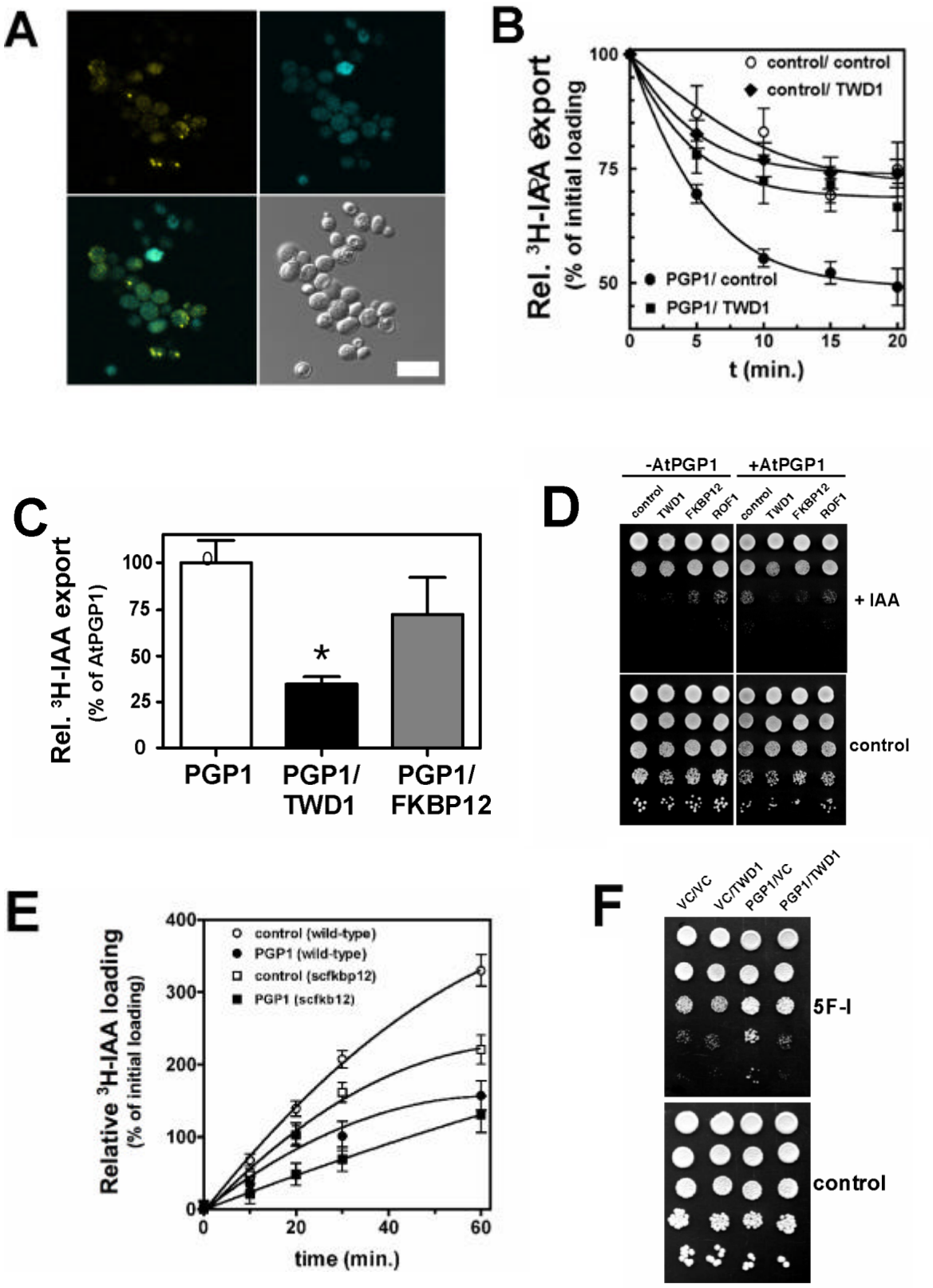

Figure 25: Coexpression of AtPGP1 with TWD1 specifically inhibits IAA export

Figure 25: Coexpression of AtPGP1 with TWD1 specifically inhibits IAA export

A AtPGP-YFP (i) is expressed on the plasma membrane and in raft-like structures (marked with an asterisk) and colocalizes with TWD1-CFP (ii.) in yeast as shown by superimposition (iii.). DIC images of the same cells are shown in (iv.); the bar represents 20 µm.

B Coexpression of TWD1 with AtPGP1 reduces AtPGP1-mediated IAA export to vector control level. Reductions in auxin retention (efflux) after 10 minutes are presented as relative export of initial loading. Data shown are means activities with standard deviations; n = 4.

C Coexpressed AtFKBP12 does not alter AtPGP1-mediated IAA efflux significantly. Reductions in auxin retention (efflux) are presented as relative export of initial loading. Data shown are means activities with standard deviations; n = 3.

D Yeast growth assays on 10 µM IAA show that TWD1 but not AtFKBP12 or ROF1 reverts AtPGP1-mediated complementation of the IAA-hypersensitive yap1-1 mutant.

E AtPGP1-mediated IAA efflux is not dependent on yeast FKBP12 (ScFKBP12/FPR) as shown by assaying IAA efflux in an *fpr1* strain and the corresponding wild type. Reductions in auxin retention (efflux) are presented as relative loading of initial loading. Data shown are means activities with standard deviations; n = 3.

F Yeast growth assays on 10 µM IAA demonstrate inhibition of AtPGP1-mediated detoxification of the cytotoxic auxin analogue 5-fluoro indole.

Inhibition of AtPGP1 by TWD1 in yeast was unexpected as the opposite was found in plant assays. Therefore, we co-expressed AtPGP1 with TWD1 in the mammalian HeLa cells that represents the standard expression system for analyzing mammalian PGPs (Geisler *et al*., 2005). Interestingly, in this system TWD1 conferred stimulation of AtPGP1-mediated auxin efflux (Figure 26) when coexpressed in a 1: 0.5 (AtPGP1: TWD1) ratio while a 1: 1 ratio had only slight effect. The influence of TWD1 on AtPGP19 could not be tested in yeast or HeLa cells as AtPGP19 is inactive in yeast probably due to hyperglycosylation (Geisler *et al*., 2005; Noh *et al*., 2001) while coexpression of AtPGP19 with TWD1 in HeLa cells had destabilizing effects.

However, inhibition of efflux by TWD1 is specific as expression of TWD1 alone had no significant effect on background IAA efflux. Furthermore, AtFKBP12, representing the most basic FKBP consisting essentially of the PPIase domain alone, reduced AtPGP-mediated IAA efflux only slightly compared to TWD1 (Figure 25C). In the *yap1-1* mutant, only TWD1 but not closely related AtFKBP12 or ROF1/AtFKBP59 inhibited AtPGP1-mediated IAA detoxification (Figure 25D). Finally, yeast FKBP12 seems to activate AtPGP1-mediated IAA export resulting in reduced IAA loading in the *S. cerevisiae FKBP12* mutant, however, the same magnitude of stimulation was found also for the vector control (Figure 25E).

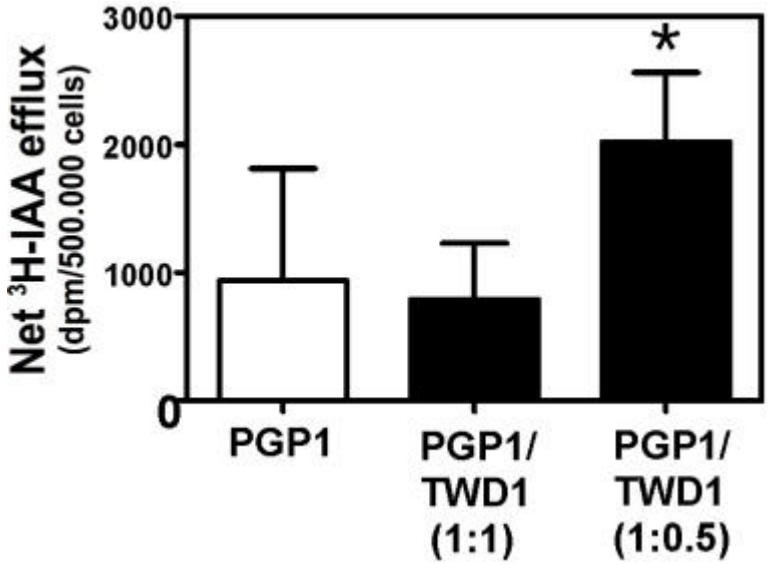

Figure 26: Coexpression of AtPGP1 with TWD1 enhances AtPGP1-mediated IAA export.

Efflux of radiolabelled IAA from HeLa cells expressing AtPGP1 with the indicated ratios of TWD1. Reduction in auxin retention (efflux) is presented as net efflux. Expression an localization of expressed proteins was confirmed by RT-PCR and Western analysis (data not shown). Shown are means with standard deviations, n= 3.

TWD1 defines the substrate specificity of AtPGP1

Assaying efflux of the synthetic auxin 1-NAA from AtPGP mutant protoplasts revealed that 1-NAA is apparently only a substrate for AtPGP1 but not for AtPGP19 (Geisler *et al*., 2005). Surprisingly, AtPGP-mediated 1-NAA export from *twd1* protoplasts was not significantly reduced compared to wild-type (Figure 27A) but in *atpgp1* or *atpgp1 atpgp19* protoplasts. In order to investigate if TWD1 indeed functions as regulator of AtPGP1-mediated IAA- but not of NAA export, we measured NAA export in yeast coexpressing AtPGP1 and TWD1. Indeed, TWD1 had no significant inhibitory effect on NAA export in comparison to IAA (Figure 27B), suggesting that TWD1 defines specificity of AtPGP1.

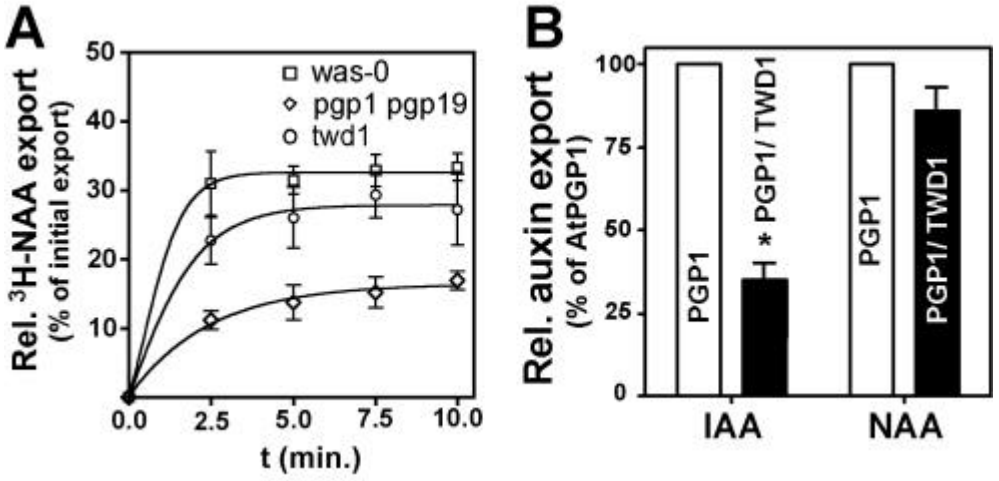

Figure 27: TWD1 modulates the substrate specificity of AtPGP1

A Export of the synthetic auxin ^{3}H-1-NAA from wild-type leaf mesophyll protoplasts is significantly reduced in atpgp1 atpgp19 plants but not in twd1. Efflux is presented as relative export of initial export. Shown are means with standard deviations of 4 individual experiments, n = 4.

B Coexpressed TWD1 does significantly inhibit AtPGP1-mediated IAA efflux but not the export of 1-NAA. Reductions in auxin retention (efflux) are presented as relative activity of AtPGP1-mediated export. Shown are means with standard deviations; n = 3.

DISCUSSION

In order to understand the drastic phenotype that is caused by loss-of-function of the Arabidopsis *FKBP42 TWD1*, we have previously demonstrated interaction between TWD1 and MDR/PGP transporters AtPGP1 and AtPGP19 (Geisler *et al*., 2003); both catalyze export of the plant hormone auxin (Geisler *et al*., 2005). Therefore, a regulatory role of TWD1 on AtPGP1/19 has been suggested accounting for the auxin-related phenotype of *twd1*. An emerging immunophilin function is a role in regulating large membrane proteins, like rhodopsin, the ryanodine receptor or the 1, 4, 5-triphosphate receptor, both integral Ca^{2+} channels (Cameron *et al*., 1995; Timerman *et al*., 1995). Regulation of murine MDR3 by yeast FKBP12 has been shown but verification of the MDR3-FKBP12 complex as well as verification of relevance *in vivo* is lacking (Hemenway and Heitman, 1996).

Here we provide several lines of evidence that TWD1 is an essential component of the auxin efflux complex and that it functions as positive modulator of AtPGP-mediated auxin transport by means of protein-protein interaction. AtPGP1/ AtPGP19/ TWD1 interaction has been previously demonstrated by two-hybrid analysis, affinity chromatography and pull-down assays (Blakeslee *et al*., 2005; Geisler *et al*., 2003; Murphy *et al*., 2002).

(1) Cellular efflux of IAA from twd1 is reduced compared to wild-type in the order *pgp1* > *pgp19* >> *pgp1 pgp19* ≥ *twd*. The magnitude of reduction reflects *in planta* transport (Geisler *et al*., 2003) and is inline with mutant phenotypes (Geisler *et al*., 2003; 2005). Overexpression of *TWD1* has no effect on IAA export while up-regulation of the export catalysts *AtPGP1* or *AtPGP19* strongly enhances efflux.

(2) Expression and localization of AtPGP1, or PIN1 and PIN2, essential components of the auxin efflux complex, is not altered in twd1 excluding reduced auxin export to be a consequence of indirect factor as altered expression or mistargeting. This makes also a chaperone function for TWD1 unlikely that has been demonstrated for some FKBPs (Romano *et al*., 2004).

(3) The modulation by TWD1 is specific as closely related AtFKBP12 (Faure *et al*., 1998) or ROF1/AtFKBP59 (Vuccich and Gasser, 1996) have only slight effects on AtPGP1 IAA transport compared to TWD1 when coexpressed in yeast. Surprisingly, coexpression in yeast and mammalian cells have opposite effects on AtPGP1 activity (inhibition in yeast *versus* stimulation in HeLa cells) suggesting that plant-specific

components are absent in the lower eukaryote *S. cerevisiae*. Currently, we are trying to identify the identity of these factors that seems to determine the direction of modulation. Reversible protein phosphorylation by protein kinases might be a good guess as mammalian PGPs are well-known to be phosphorylated and regulated by protein kinases like PKC (Sananes *et al*., 1999). However, the mechanism of modulation is till unclear and reports differ in their direction of modulation (Castro *et al*., 1999). Interestingly, AtPGP1 has been recently shown to be phosphorylated in a so-called regulatory linker domain (Nühse *et al*., 2004).

(4) Regulation of transport activity by TWD1 is apparently restricted to the most abundant native auxin IAA but not found for AtPGP1-mediated export of the synthetic auxin 1-NAA that can substitute IAA in many respects. 1-NAA export is not significantly reduced in *twd1* and upon coexpression in yeast suggesting that TWD1 functions beside its role as positive regulator as specificity filter. This effect is limited to AtPGP1 as AtPGP19 has been demonstrated to be unable to export 1-NAA (Geisler *et al*., 2005).

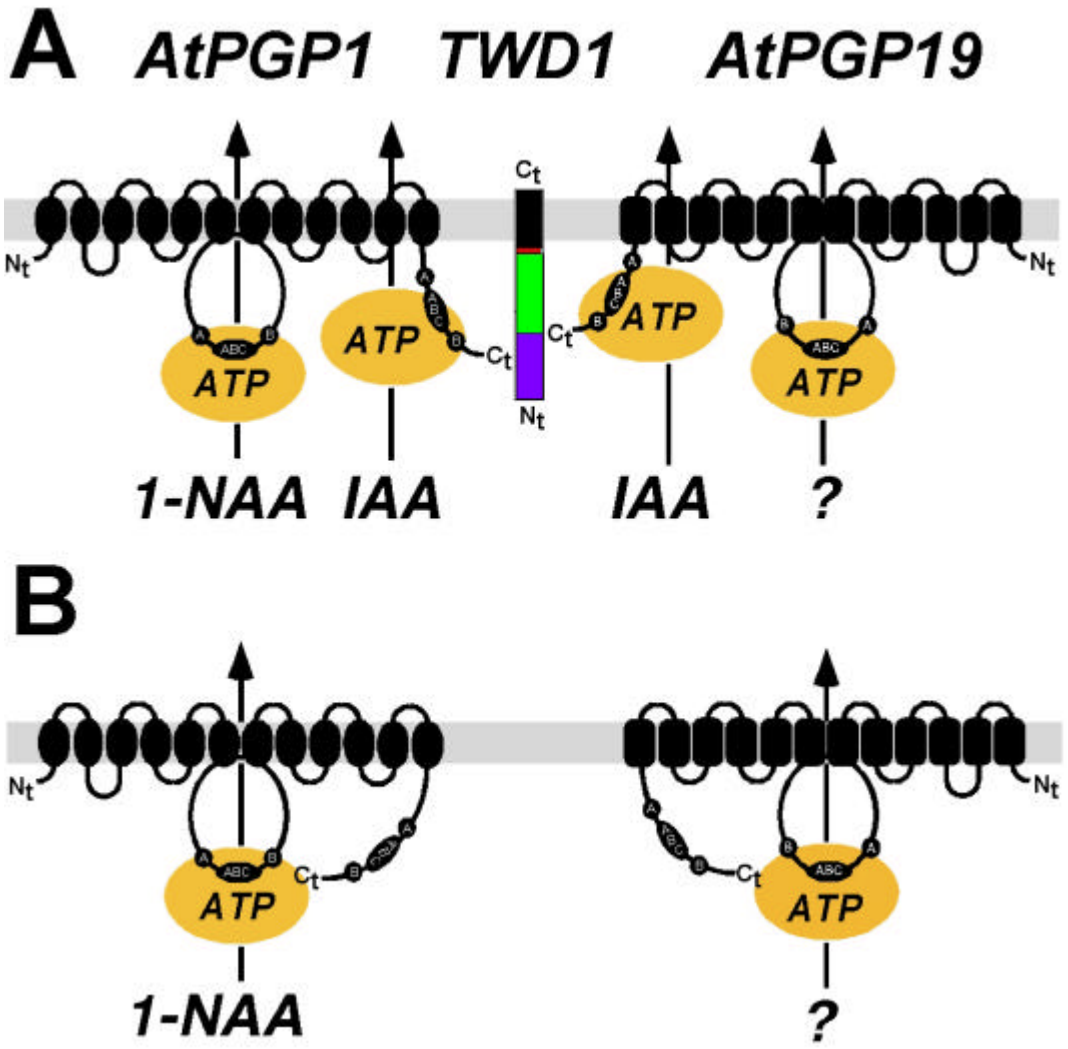

Figure 28: Model for the positive regulation of PGP-mediated auxin efflux by means of protein-protein interaction via TWD1

A Interaction of the Gtermini of AtPGP1 and AtPGP19 with interacting sites of TWD1 provides access of the substrate (IAA) or ATP to sofar non-identified unknown substrate binding site or the Gterminal nucleotide binding folds, respectively.

B In the absence of TWD1, either access of IAA and/or ATP to the substrate binding domain or NBF is blocked leading to inhibition of transport.

In this hypothetical model export of the synthetic auxin 1-NAA would be mediated by the N-terminal NBF of AtPGP1, which is inline with current models of two independent drug binding sites for mammalian PGPs. AtPGP19 seems not to transport 1-NAA; therefore the substrate transported by the N-terminal NBF is not known.

Functional domains of TWD1 are colored: black, membrane anchor; red, calmodulin-binding domain; green, tetratrico peptide repeat domain; violet, PPIase domain.

Figure 28 depicts our current understanding of an AtPGP1/TWD1/AtPGP19 auxin efflux complex. Interaction takes place between the C-terminal nucleotide binding fold (NBF2) of AtPGP1 and the N-terminal PPIase-like domain of TWD1; AtPGP19 apparently requires the full TWD1 enzyme for interaction as has been mapped recently (Geisler *et al*., 2003). The NBFs of the PGPs do not interact with each other (Bouchard and Geisler, unpublished data), which is of interest as mammalian ABC transporters have been suggested to function as heterodimers (Ramaen *et al*., 2005). Therefore, we postulate that TWD1 functions as linker between both PGPs.

The simplest mechanistic model that is inline with our data is that the C-termini of AtPGP1 and AtPGP19 perform TWD1-induced conformational changes that offer ATP access to the C-termini forming the NBF2 (Figure 28A). However, we cannot exclude that this domain shift allows alternatively or additionally substrate (IAA) binding. Binding of so many diverse drugs to PGPs as substrate is still not fully understood (Ambuidkar *et al*., 2003). In the absence of TWD1, these ATP- or/and auxin-binding sites would be blocked leaving AtPGP1/19 in an inactive state (Figure 28B). For mammalian PGPs both ATP-binding sites have been shown to be catalytically active (Urbatsch *et al*., 1995) and are required for the protein to function as transporter (Azaria *et al*., 1989). Therefore, in order to fit into this model one had to postulate that the NBF1 of AtPGP1/19 would be not involved in IAA export. The NBF1 of AtPGP1/19 do not interact with TWD1 (Geisler *et al*., 2003) and would therefore consequently be able to take over this function which would result in transport in the presence of TWD1.

As already mentioned, AtPGP1 but not AtPGP19 catalyzes the export of 1-NAA. Photoaffinity drug labeling studies have identified two major drug binding regions, corresponding to regions in and around trans membrane domains (TMD) 5 and 6 and 11 and 12, respectively. Moreover, there is evidence for two non-identical drug-interaction sites in the human PGP (Dey *et al*., 1997). Transfer of this finding into our model suggests that NBF1 is involved in 1-NAA export, while NBF2 would be responsible for IAA. In agreement, there is no interaction between NBF1 and TWD1 that might need no stabilization as it is fixed between TMD5 and 6 compared to the more flexible C-terminus.

Further, the fact that overexpression of *AtPGP1/19* results in increased IAA efflux argues that either TWD1 is not yet saturated by AtPGP1/19 or that activation is a transient event. The later has been suggested to be responsible for lack of

demonstration of the murine MDR3/FKBP12 complex in yeast (Hemenway and Heitman, 1996). However, overexpression of TWD1 has no significant effect on IAA efflux suggesting that TWD1 is already saturated which favours the transient model.
Our current data also provide further evidence that the PPIase acitivity, harboured by the FKBP domain, is not the essential *in vivo* function of TWD1. TWD1 has no PPIase activity (Kamphausen *et al*., 2002), does not complement yeast FKBP12 (Geisler, unpublished data) and interaction with AtPGP1 does not require immunosuppressant drugs (Geisler *et al*., 2003). Therefore, PPIase activity of TWD1 is neither essential for interaction nor for activation. This has been found also for other regulation of transport complexes by FKBP via protein-protein interaction (Hemenway and Heitman, 1996; Kurek *et al*., 2002; Timerman *et al*., 1995) which therefore seems to be phenomenon which is well conserved between plants and mammals.

Beside this novel role for FKBPs, we demonstrate a direct involvement of TWD1 in auxin transport that, at least partially, is able to explain the drastic, overlapping developmental phenotype of both *twd* and *atpgp1 atpgp19* plants. Loss-of-function of *AtPGP1*- /*AtPGP19*-mediated auxin export in *twd1* blocks basipetal polar auxin transport (shown for *atpgp1* and *atpgp19* (Geisler *et al*., 2005)) resulting in elevated free IAA in upper parts of the roots. This correlates with a polar (dominantly basal) expression of AtPGP1 in the corresponding regions of the root. Reduction of IAA in *twd1* and *atpgp* columella regions demonstrated using the DR5 reporter gene might be contributed by non-polar expression in the epidermis of the root apex as shown for AtPGP1. This further verifies an involvement of AtPGP1/19 and TWD1 in PAT, as has been suggested (Geisler *et al*., 2005; Shi and Wu 2005).
Agravitropic roots and many aspects of the strong developmental phenotype of *twd1* and *atpgp1 atpgp19* plants are in good agreement with altered PAT and elevated auxin concentrations in the roots. Other growth defects especially in the shoot might be a consequence of altered reflux of auxin into the shoot or due to secondary effects. However, the “twisted syndrome” not found in *atpgp1 atpgp19* plants suggests that other TWD1-mediated functions are additionally defect in *twd1*. In this respect it is important to keep in mind that the multi-domain FKBP TWD1 interacts additionally with hsp90, calmodulin and MRP-like ABC transporters, AtMRP1 and

AtMRP2 (Kamphausen *et al*., 2003; Geisler *et al*., 2003; 2004) that might account for the more severe phenotype by loss-of additional functions.

The precise expression pattern of *TWD1* and *AtPGP19* is still not known and co-immunolocalization of all components has failed so far due to the extremely low abundance of TWD1. Attempts to localize TWD1 using antisera (Vincenzetti, Popanov, Palme, Schulz and Geisler, unpublished data) or CFP fusions (Vincenzetti and Geisler, unpublished data) have failed so far. The low expression of *TWD1* compared to the *AtPGP*s as shown by RT-PCR (Figure 22B) and *in silico* data (data not shown) further supports the transient mode of action. However, careful gene chip analysis reveals that TWD1, despite its low abundance, is co-expressed in virtually all tissues with AtPGP1/19 and that all three are induced by various stresses (https://www.genevestigator.ethz.ch; data not shown).

FK506 and rapamycin (and analoga) partially overcome multidrug resistance which raised several possibilities to explain reversal effects (Hemenway and Heitman, 1996): immunosuppressant drugs might inhibit PGPs directly, calcineurin, a PP2A protein phosphatase being inhibited by cyclophilin- and FKBP-drug binding complexes, positively regulate PGPs, or immunosupressant drugs interfere with FKBP-mediated PGP function. Our data clearly further support the third option demonstrating PGP upregulation by physical interaction with the FKBP TWD1. This is further supported by the fact that immunosuppressant concentrations required for MDR reversal are significantly higher than for immunosuppression (Epand and Epand, 1991). Although immunosuppressant drugs apparently are not involved in AtPGP activation, our data provide evidence that the cellular targets of FK506 and rapamycin, thus FKBPs, do regulate PGP function. In agreement, using pharmaceutical antagonists it has been reported that PGP inhibition is independent of calcineurin and PPIase function (Mealey *et al*., 1999).

Therefore, transfer of this novel FKBP function might have direct benefit on the development of novel strategies for cancer therapy via FKBP-mediated down-regulation of drug efflux. A mammalian putative GPI-anchored FKBP homologue of TWD1 exists also in mammals and might be an interesting target of genetic or chemical manipulation.

MATERIALS AND METHODS

Plant growth conditions

Plants were grown as described previously (Geisler *et al*., 2003). For gravitropism analysis, Ws Wt, *pgp1* (At2g36910) and *pgp19* (At3g28860), *pgp1 pgp19* and *twd1-1* mutants were grown under long day conditions (16 hour 100 µmol·m^{-2}·s^{-1} white light, 22°C). For quantitation of gravitropism, seeds were surface sterilized and grown on 1/2 Murashige and Shoog medium, 0.7% phytagar (Gibco Invitrogen Corporation, Paisley, UK) as specified in Lariguet and Fankhauser (2004)

Analysis of IAA contents

Arabidopsis thaliana ecotype Wassilewskija (Ws-2), *pgp1, pgp19, pgp1 pgp19 and twd1* mutants (all in Ws-2) expressing the maximal auxin-inducible reporter Pro_{DR5}:GFP (Ottenschlager *et al*., 2003) were generated by Agrobacterium-mediated transformations using plasmid *DR5-GFPm* construct. Single-locus insertion lines were selected in T2. Homozygous T3 was used for all experiments described. Seedlings were grown vertically for 5 days as described above, stained with 10 µM propidium iodide before microscopy and analyzed by DIC (Leica DMR microscope equipped with a Leica DC300 F charge coupled device (CCD) and confocal laser scanning (CLS) microscope () using a 530 ± 15-nm band pass filter for GFP detection and a 580 ± 15-nm band pass filter for detection of propidium iodide and tissue autofluorescence. For histological signal localization both images were electronically overlaid and further processed with photoshop (Adobe Systems, Mountain View, CA). IAA immunolocalization using monoclonal anti-IAA (http://agdia.com) was done as described in Benkova *et al*., (2003).

For endogenous free auxin quantification, shoot and root segments of 30-50 seedlings were collected and pooled. The samples were MeOH extracted and analyzed by GC-MS. Calculation of isotopic dilution factors was based on the addition of 100 pmol $^{2}H_{2}$-IAA to each sample. In some cases, roots of 40 seedlings were manually divided into root segments (see Figure 23C) from the root tip and analyzed as described above. Data presented are the averages of three independent lots of each 30-50 seedlings.

IAA transport

Auxin transport assays on intact light grown Arabidopsis seedlings treated with a 0.1 µL microdroplet of 1 µM auxin at the root apical meristem using techniques described in Geisler *et al*., (2003), and root segments of 2 mm, were collected 2 mm, 4 mm and 6 mm from the root tip.

Expression and localization analysis

In order to localize AtPGP1 in twd1, Arabidopsis *twd1* was transformed with construct PGP1cmyc2b (Pro_{PGP1}:PGP1-cmyc, Geisler *et al*., 2005) using *Agrobacterium tumefaciens* mediated vacuum-infiltration. Homozygous plants were selected on 0.5 x MS medium containing 50 µg/ml kanamycin and insertion was verified by Southern analysis. AtPGP1-cmyc, PIN1 and PIN2 were whole-mount immunolocalized in *twd1* using anti-cmyc (Roche, Buchs, Switzerland), anti-PIN1 and anti-PIN2 as described elsewhere.

Transcript detection by RT-PCR

Total RNA from Arabidopsis WT protoplasts was prepared and DNaseI (Qiagen, Hilden, Germany) treatment was performed with column-bound RNA. Oligo-dT primed cDNA from 1 µg of total RNA was synthesized using the Reverse Transcription system (Promega, Madison, USA). Transcripts specific for *AtGP1* (At2g36910) *TWD1* (At3g21640) and 40S ribosomal protein *S16* (At2g09990) were detected by conventional PCR for 25 and 30 cycles at 52°C annealing temperature. Intron-spanning PCR primers were: S16-S 5'ggcgactcaaccagctactga; S16-AS 5'cggtaactctt tggtaacga; PGP1-S 5'gtccctcaagagccgtgcttg; PGP1-AS 5'ccatcatcgatgacagcgatc, TWD1-S 5' cca tag cat aca tgg ggg acg, TWD1-AS 5' tct gtg gcg tcg aaa gat acg. Equal volumes of PCR products were separated on 2.5% agarose gels. Negative controls in the absence of enzyme in the RT reaction yielded no products.

Protoplast efflux experiments

Intact Arabidopsis mesophyll protoplasts were prepared from rosette leaves of plants grown on soil under white light (100 µmol m^{-2} s^{-1}, 8 h light/16 h dark, 22°C) as described (Geisler *et al.*, 2003). Auxin efflux experiments were performed exactly as shown elsewhere (Geisler *et al*., 2005) with three to five independent protoplast

preparations with 4 replicas for each time point. Protoplast volumes were determined by the addition of 0.05 µCi ^3H_2O in separate assays; protoplast surfaces were calculated by measuring protoplast diameters.

Yeast assays

Arabidopsis TWD1 (At3g21640), FKBP12 (At1g58450) and ROF1 (At3g25230) was cloned by PCR into BamHI and SalI sites of copper-inducible yeast shuttle vector pRS314CUP. pNEV, pNEV-PGP1 (Geisler *et al*., 2005), pRS314CUP, pRS-FKBP12 and pRS-ROF1 were introduced into *S. cerevisiae* strains JK93da (Hemenway and Heitman, 1996), SMY87-4, PJ69-4a (Cruz *et al*., 1999) or *yap1-1* (Prusty *et al.,* 2004) and single colonies were grown in synthetic minimal medium without uracil and tryptophane, supplemented with 2% glucose and 100 µM $CuCl_2$ (SD-UT). For detoxification assays, transformants grown in SD-UT to an OD_{600} around 0.8 were washed and diluted to an OD_{600} of 1.0 in water. Cells were 5-times 10-fold diluted and each 5 µl were spotted on minimal media plates supplemented with 10 µM IAA or 750 µM 5-fluoro indole. Growth at 30°C was assessed after 3-5 days. Assays were performed with 3 independent transformants.

IAA efflux and loading experiments were performed as in Geisler *et al*. (2005).

Yeast AtPGP1 and TWD1 expression and immunolocalization

YFP and CFP were amplified by PCR from plasmids pEYFP and pECFP (Clontech) inserted in-frame into *Asc*I sites generated in the coding regions of pNEV-PGP1 (bp 2674) and pRS-TWD1 (bp 64) using the QuikChange XLsite-directed mutagenesis kit (Stratagene). That like, YFP and CFP were inserted into the cyctoplasmic loop between transmembrane domain 10 and 11 of AtPGP1 and into the very N-terminus of TWD1.

Cells coexpressing AtPGP1-YFP and TWD1-CFP were incubated in mounting media containinig DAPI and immunofluorescence analysis was done using a confocal laser scanning microscope (Leica, DMIRE2) equipped with argon (488 nm) and UV laser (410 nm). Fluorescence, DIC and DAPI images were processed using Adobe Photoshop 7.0. Vector controls showed no detectable fluorescence.

Yeast cells transformed coexpressing AtPGP1 and TWD1 were grown to mid-log phase and microsomes were separated via continuous sucrose gradient centrifugation (Geisler *et al*., 2004). Plasma membrane fractions were subjected to

7.5% PAGE and Western blots were immunoprobed using anti-PGP1 antibody (Sidler *et al.*, 1998) and anti-TWD1 (Geisler *et al*., 2003)

HeLa cell assays

Radiolabeled substrated accumulation assay after transient coexpression of AtPGP1 (At2g36910) and TWD1 (At3g21640) Data points were normalized to the average empty control vector value of 2851.885 DPM/500,000 cells for auxin treatments. Cell viability after treatment was confirmed visually and via cell counting and expression was verified by Western blotting.

Data analysis

Data were analyzed using Prism 4.0b (GraphPad Software, San Diego, CA) and statistical analysis was performed using SPSS 11.0 (SPSS Inc., Chicago, Illinois).

ACKNOWLEDGEMENTS

We are grateful to Drs. C. Fankhauser for technical support during gravity assays, A. Müller for analyzing free IAA contents, and E. Martinoia for financial and intellectual support.

Abbreviations list

ABC, ATP binding cassette; NPA, 1-*N*-naphthylphthalamic acid; IAA, 3- indole-acetic acid; NAA, naphthalene acetic acid; NBF, nucleotide binding fold; FKBP, FK506-binding protein; PGP, p-glycoprotein; MDR, multidrug resistance; TWD1, TWISTED DWARF1.

V DISCUSSION

TWISTED DWARF1, a unique plasma membrane-anchored immunophilin-like protein, interacts with *Arabidopsis* multidrug resistance-like transporters AtPGP1 and AtPGP19

The starting point of this work was the challenging, pleiotropic developmental phenotype that is caused by loss-of-function of the FKBP-like TWD1/AtFKBP42 gene in Arabidopsis. As mentioned in the introduction, FKBPs are known to function either as chaperones or as molecular switches of transport complexes. However, the *twd1* phenotype could hardly directly be related to the putative domain structure of TWD1. An interesting point was the presence of a TPR (tetra tricopeptide repeat) domain in TWD1 known to mediate protein-protein interaction and that promised the identification of putative target proteins. Results of a cDNA library screening with the yeast two-hybrid system using the soluble, N-terminal part of TWD1 as bait, brought first pieces of evidence that TWD1 mediates an interaction with the C-terminus of AtPGP1. This *in vitro* interaction between TWD1-PGP1, later verified as well for TWD1-PGP19, is specific among the PGP/MDR subfamily of plant ABC transporters. This interaction between the three plasma membrane localized proteins was further confirmed by co-immunoprecipitation and affinity chromatography assays. Surprisingly the interaction TWD1-PGP1 and TWD1-PGP19 is not mediated by the TPR domain of TWD1. Noteworthy is the difference in the domains of TWD1 required to mediate interaction with both PGPs: PGP1 recognizes the N-terminal PPIase domain of TWD1, while AtPGP19 needs more than the PPIase domain of TWD1 for the interaction.

The interaction between TWD1 and both ABCs does apparently not require the PPIase activity nor the presence of immunosuppressant compounds. The PPIase-independent interaction between yeast FKBP12, and a mouse ABC transporter, MDR3, as well as a calcium channel, inositol 1, 4, 5 triphosphate and a ryanodin receptor, has been already demonstrated. An amino acid sequence comparison between animal and plant immunophilins revealed that amino acids suggested as important in mediating drug binding, such as FK506 or rapamycin, in animals are poorly conserved in plants. Such changes would explain the insensibility of the TWD1-PGP interaction to immunosuppressiva.

Genetical and biochemical data published by Noh *et al*. (2001) linked PGPs, AtPGP1 and AtPGP19, and TWD1 to auxin transport. These three proteins were found among other proteins in plant microsomal extracts purified by NPA affinity chromatography. Affinity assays on one hand confirmed TWD-PGP interaction and on the other hand revealed that NPA might modulate the TWD1-PGPs interaction as excess of NPA disrupting both interactions.

The measurement of auxin transport activity in hypocotyls of *pgp1*, *pgp19*, *pgp1 pgp19* and *twd1* mutants correlated first the more or less pronounced deficiency in auxin transport to the mutant phenotype. This auxin assay revealed that PGP19 affected, to a greater extent than PGP1, auxin transport. Moreover concordance of drastic phenotype and auxin transport deficiency of double mutant *pgp1 pgp19* suggested that both PGPs seem to function in redundancy in regards to auxin transport. Similar to PGP19 and PGP1, but with emphasized effect, TWD1 seemed to play a crucial role in polar auxin transport, probably through the interaction with PGP1 and PGP19. Based on *pgp1 pgp19* and *twd1* mutant phenotypes it was suggested that both transporters might be directly or indirectly involved in auxin transport. In analogy to ion channels and mouse MDR3, for which it was shown that immunophilins are essential for their activity, it was proposed that TWD1 is required for a proper and functional auxin transport complex.

Cellular efflux of auxin mediated catalyzed by the Arabidopsis MDR/PGP transporter AtPGP1

Noh *et al*. (2001) reported that AtPGP1, in comparison to PGP19, had apparently no significant effect on auxin transport. This was in contrast to a suggested role of AtPGP1 in light intensity-dependent elongation of hypocotyls (Sidler *et al*., 1998). To reconcile these two contradictory statements we showed that depending on light condition and growth stage *pgp1* exhibits an intermediate dwarf phenotype but not as severe as *pgp19*. This slight phenotype, compared to wild type, was observed for mature plants under short day conditions. 5 days seedlings under both short and long day conditions displayed a similar phenotype as described by Noh *et al*. (2001) but measurement of polar auxin transport on hypocotyls (Geisler *et al*., 2003) reported a relatively small deficiency in basipetal auxin transport for *pgp1*, which is in concordance with the intermediate *pgp1* phenotype. Measurement of auxin transport activity in hypocotyls of *pgp1*, *pgp19* and *pgp1 pgp19* mutants correlated well with

determination by GC-MS of relative IAA content in the whole root. Determination of reduced root IAA contents using the DR5:GUS reporter system in the primary root gave consistent results with whole root data analyzed by GC-MS.

These data were inline with basipetal root transport deficiencies and consistent with the expression ratio between PGP1 and PGP19 in the root. In the root apex PGP1 is predominantly expressed, in contrast to non-apical root tissue where PGP19 is in the majority expressed. As no mislocalization of PIN1 and PIN2 in *pgp1* root tips has been reported, improper PIN1 and PIN2 localization as reason for the observed basipetal deficiency could be excluded.

A non-polar localization in root and shoot apical cells suggests a role in non-directional auxin export from apical cells, where PGP1 may complement PIN protein function. In contrast, in mature cortical and endodermal cells at the upper boundary of the distal elongation zone an apparent polar localization was observed. In endodermal cells PGP1 displays always a basal localization, whilst in cortical cells the localization is predominantly basal. This basal localization suggests and reinforces the role of PGP1 in root basipetal auxin movement in these tissues.

The demonstration of auxin transport activity of PGP1 using plant protoplast, yeast cells and Hela cells clearly demonstrated AtPGP1 to transport auxin. Moreover transport assays in protoplast and Hela cells suggested that PGP1 mediates transport of auxin breakdown product. Reduction of IAA efflux for *pgp1*, *pgp19* and *pgp1 pgp19* protoplasts correlated well with auxin transport deficiencies observed for plant tissues. Transport assays demonstrated high auxin specificity for PGP1 and PGP19 and that PGP1 owns a higher affinity for 1-NAA compared to PGP19.

This IAA efflux activity of AtPGP1 was shown to be inhibited in yeast, HeLa as well as in plant cells by endogenous and synthetic AEIs as well as mammalian PGP inhibitors. Comparison of yeast and HeLa cells data for IAA and BA transport assays suggest that a protein, present in plant cells, should confer IAA transport specificity to PGP1.

Determination of the PGP1 localization brought precious information concerning PAT. Non-polar localization in root and shoot apices suggested that directional auxin transport in these regions required other proteins. Polar localization of PGP1 in certain tissues of the elongation zone is in line with the basipetal IAA transport deficiency observed for pgp1. Subsequent, interaction with other proteins, such as PINs, might play a prominent role in auxin transport.

Immunophilin-like TWISTED DWARF1 modulates auxin efflux activities of Arabidopsis MDR/PGP transporters

So far the drastic phenotype caused by loss-of-function of the *TWD1* gene encoding the plasma membrane TWD1 was looking like a puzzle. We first demonstrated the physical interaction between TWD1 and the two ABC transporters *AtPGP1* and *AtPGP19* using several approaches. Later on, using yeast and HeLa cells as heterologous expression system, we demonstrated that PGP1 mediates a primary energized IAA efflux. Unfortunately heterologous expression of PGP19 failed likely due to hyperglycosylation of the protein. However, either measurement of basipetal auxin transport using hypocotyl and root or measurement of auxin efflux capacity of plant protoplast, strongly suggest that PGP19 catalyses auxin transport as well. The phenotype and related auxin transport activity of *twd1* mutant were strongly suggesting TWD1 as a modulator of the auxin transport machinery, probably through protein interaction with both PGPs.

We provided several pieces of evidence demonstrating the positive modulation of PGP1- and likely also of PGP19-mediated auxin transport, exerted by TWD1. IAA root contents were determined using three different methods: GC-MS, DR5:GFP reporter gene analysis and immunodetection. The “micro” and “macro” measurements of root IAA content allowed to demonstrate that *twd1* mutant, as well as pgpg1 *pgp19*, contain less IAA in the root tip columela, but higher level in the elongation zone. This difference, in comparison to wild type, of the root content attests a deficiency in basipetal auxin transport that is inline with the phenotype. Another trait related to the phenotype is the gravitropic behaviour of the root. Both *pgp1 pgp19* and *twd1* displayed agravitropic behaviour. This abnormal phenotype and related auxin transport deficiencies observed for *twd1* is independent of a mislocalization of PIN1 and PIN2, essential proteins of the efflux complex.

To address the question how TWD1 modulates auxin transport and whether this modulation depends on the interaction with the ABC transporters AtPGP1 and AtPGP19, we co-expressed PGP1 and TWD1 in yeast and Hela cells. In yeast TWD1 was demonstrated as a negative regulator of PGP1 activity. In Hela cells, interestingly, TWD1 displayed like in plants a stimulation of PGP1 activity, which depends on the expression rate ratio between PGP1 and TWD1. Comparison of transport data between yeast on one hand and Hela and protoplast cells on the other

suggested the existence of a plant-specific factor, responsible for the regulation and specificity of transport activity. Reversible protein phosphorylation might be a likely one. Mammalian PGPs have been shown to be regulated through PKC like-dependent phosphorylation. This parallel is supported by the fact that PGP1 has been recently shown to be phosphorylated in the so-called linker domain (Nühse *et al*., 2004).

To confirm the modulation of PGP1 activity by TWD1 in natural environment we used three overexpressing plant construct for TWD1, PGP1 and PGP19. Comparison of auxin transport activity of these three overexpressing lines allowed to demonstrate, that TWD1 itself does not directly influence auxin transport but rather act as a modulator, and that increase of auxin transport activity displayed by PGP1 and PGP19 overexpressing lines is suggested to be related to TWD1.

Furthermore, we demonstrated using the yeast expression system that the regulatory effect of TWD1 on PGP1 transport activity is specific. FKBP12 and ROF1, close homologues of TWD1, did not revert the PGP1-mediated IAA resistance of the *yap1-1* mutant, while yeast FKBP12 seemed to have a positive, but unspecific effect on IAA efflux activity of PGP1.

In summary, these data are strongly suggesting a modulator role of TWD1 on AtPGP1 (and AtPGP19)-mediated auxin transport. TWD1 seems to further fulfill a selectivity function, in regards of the transported substrates, which is limited to AtPGP1.

VI GENERAL DISCUSSION

Auxin is transported throughout the whole plant from its main synthesis sites, the shoot apical meristem and young leaves. Similarly to other plant hormones auxin is transported via a non-polar transport pathway but - being specific to auxin - also via a polar transport pathway (Raven, 1975; Went, 1974; Rubery and Sheldrake, 1974). The phloem transport is non-directional and characteristic for auxin conjugates and derivates. Through this pathway, auxin is transported up and down between the shoot apical meristem and the root tip. The second pathway, the polar auxin transport (PAT) is in contrast to the phloem transport directional and specific for free auxin.
Along these concentration gradients auxin is transported in a cell-to-cell manner. The first concentration gradient stretches from the auxin source tissues, meristem and young leaves, in direction to the root tip. The second concentration gradient redistributes auxin from the root tip, considered as an auxin sink, backwards to the root elongation zone. Both auxin concentration gradients are of importance for developmental processes such as apical dominance, organs development, gravi- and photo-tropisms (Benkova *et al.*, 2003; Blakeslee *et al.*, 2005; Friml and Palme, 2002; Muday and Delong, 2001; Rashotte *et al.*, 2000; Reinhardt *et al.*, 2000).
Recent results indicate that so-called PIN proteins (PIN1, 2, 3, 4, and 7) function as putative mediators of auxin transport. The polar localization of PINs proteins in maxima auxin concentration regions, the alteration of auxin distribution in *pin* mutants, the growth and maintenance defects of root meristem observed in *pin* mutants, the influence of PIN activities on both expansion and elongation of meristem and elongation zone cells, jointly suggested the five PIN gene products to collectively control auxin distribution and consequently regulating primary root development (Blilou et al., 2005).

At the time point of this work, putative PIN-like auxin efflux carriers were suggested as the efflux component of the auxin chemiosmotic model. Each of the five members of the PIN protein family characterized so far display, in Arabidopsis, a unique and tissue-specific expression pattern. Furthermore the growth phenotype of the some *pin* mutant is in line with a loss of directional auxin transport in the tissue where the PIN protein is expressed, respectively (Blilou *et al.*, 2005; Friml *et al.*, 2002, 2003;

Galweiler *et al.*, 1998; Luschnig *et al.*, 1998; Palme and Galweiler, 1999). However, to date PIN proteins have not been clearly demonstrated to catalyze directly auxin transport. Only PIN2 has been shown to stimulate auxin efflux when expressed in a heterologous system (Luschnig *et al.*, 1998).

The auxin transport deficiency-related phenotype of the loss-of-function mutation of the *FKBP42* gene, encoding for the immunophilin-like TWD1, constituted the starting point of this work (Kamphausen *et al.*, 2003). A more conceivable link to auxin transport was proposed when, based on the presence of a TPR motif characteristic of protein-protein interaction, suggested TWD1 to function in protein-protein interaction. A yeast-two hybrid screen revealed the interaction of TWD1 with two closely related ABC transporters, PGP1 and PGP19, suggested auxin transport components. This interaction was further confirmed *in vivo* (Geisler *et al.*, 2003)
As a common characteristic, *pgp1*, *pgp19*, *pgp1 pgp19* and were displaying a gradual deficiency in polar auxin transport in the hypocotyls suggesting a direct involvement of PGP1 and PGP19 in auxin transport. Based on the auxin transport deficiency of *twd1*, TWD1 was suggested to be required for the formation of a functional auxin transport complex. In analogy to existing animal models Hemenway and Heitman, 1996), TWD1 was further proposed, within a putative auxin transport complex, to regulate the putative activity of the associated PGPs.

The growth phenotype associated with the single mutation of P-glycoproteins, *pgp1* and *pgp19*, does not *a priori* suggest an implication of the two closely-related PGPs in auxin transport. In contrast, the *pgp1 pgp19* double mutant, shows characteristics of auxin transport deficient mutants, suggesting for both PGP1 and PGP19 an implication, if not a redundant function, in auxin transport
(Geisler *et al.*, 2004; Noh *et al.,* 2001).
A significant progress in understanding the role of PGP1 in auxin transport was achieved by its heterologous expression. Expression of PGP1 in yeast and mammalian HeLa cells allowed demonstrating that PGP1 is catalyzing IAA efflux. Growth phenotypes, reduction of polar auxin transport activity in root and hypocotyl sections, reduction of auxin efflux from mesophyl protoplasts, reduced root and hypocotyl IAA content were consistant with a role in PAT as suggested by immunolocalization pattern of PGP1. The polar/basal localization of PGP1 in the

epidermis of the mature root suggested that PGP1 acts as an auxin efflux transporter in the basipetal auxin stream of the root (Geisler *et al.*, 2005).
The non-polar localization of PGP1 in root and shoot apices suggested that in such tissue, where auxin concentration is high, other proteins are required to confer directionality of the transport (Geisler *et al.*, 2005; Geisler and Murphy, 2006). As candidate, PINs might interact with the PGPs to direct auxin transport, avoiding hence re-diffusion, an impediment to gradient-driven transport.
An auxin transport activity for PGP19 could unfortunately not be demonstrated at that time point, due to the impossibility to functionally express PGP19 in yeast. However, the characteristics related to auxin transport deficiency being more pronounced for *pgp19* plants compared to *pgp1* plants, suggests a likely implication of PGP19 in polar auxin transport.

The demonstrated interaction with the two ABC transporters, together with the mutant phenotypes of *twd1*, suggested TWD1 to function as a regulator of PGP1 and PGP19 transport activity.
Interestingly, in animals the regulation of transporter proteins by FKBP-type immunophilins has been already demonstrated. Two independent studies (Cameron *et al.*, 1995; Timmerman *et al.*, 1995) have shown that FKBP12 regulates the activity of two different membrane integral Ca^{2+} channels. Further, it was shown that in yeast, multidrug resistance activity of murine MDR3 is dependent on yeast FKBP12 (Hemenway and Heitman, 1996). The authors suggested that FKBP12 is required for the drug extrusion activity of the MDR transporter. The positive regulation of FKBP12 on the MDR3 activity was shown to be PPIase activity-independent. The same is apparently also true for TWD1-mediated regulation of PGP1: all attempts to measure a PPIase/rotamase activity using purified protein failed sofar. Moreover, TWD1 - unlike other Arabidopsis FKBPs - failed to complement the yeast fkbp12 mutant (Geisler, personal communication). This suggests that some FKBPs have apparently lost their original chaperone function toward an altered function in protein modulation. In their model, the Heitman group proposed, that the drug can either be competitively transported by the active MDR-immunophilin complex reverting hence the drug resistance, or can bind to the immunophilin what subsequently dissociates the active complex immunophilin-ABC transporter and revert the drug resistance ABC transporter-mediated. However co-immunoprecipitation or affinity chromatography

assays failed to demonstrate the FKBP12-MDR3 interaction. Hence the dissociation of the complex immunophilin-MDR subsequent to drug binding has not been demonstrated.

In contrast to MDR3, *in vitro* and in *vivo* data demonstrated the interaction between TWD1 and the two MDR transporters, PGP1 and PGP19. Furthermore, yeast growth assays and BRET data from our group (Bailly and Geisler, results not shown) indicate that the TWD1-PGP1 complex, expressed in yeast, upon treatment with either synthetic or endogenous ATI is dissociated what subsequently reverts the inhibition of PGP1-mediated auxin transport activity. Moreover, none of the TWD1 closest homologous, FKBP12 and ROF1, were regulating PGP1 transport activity as TWD1 does, indicating that TWD1 specifically regulates PGP1 transport activity.

In plants, this regulatory role of TWD1 on auxin transport activity, was demonstrated using over-expressing plants. In TWD1 over-expressing lines, in contrast to PGP1 and PGP19 over-expressing plants, no increase of IAA export activity was reported, excluding hence a direct role of TWD1 in auxin transport. To confirm the hypothesis that TWD1 acts as a regulator of auxin transport we have shown that loss of function of TWD1 did not alter a targeting of auxin efflux component (PIN1, PIN2, PGP1 and PGP19) as well as that both loss- and gain-of-function of *TWD1* did not influenced the expression rate of *PGP1*. Together these data underline that TWD1 functions as a regulator of PGP-mediated auxin efflux activity.

Outlook

The results of the three sets of experiments established new elements in auxin transport, especially auxin efflux. We demonstrated that ABC transporters, PGP1 and also likely PGP19, are catalyzing auxin efflux. Furthermore, we demonstrated that the interacting partner of both ABC transporters, the immunophilin-like protein TWD1, via protein-protein interaction modulates PGP1, and most likely also PGP19, activity. One might hypothesize that auxin efflux would be mediated by a ternary complex.

An intriguing point found with our protoplast system, was the difference in the auxin substrate specificity observed between PGP1 and PGP19, however, the mechanism how substrate specificities of PGPs are defined is not known.

TWD1 has been shown to be an interacting protein of both PGPs and furthermore a regulatory component of their transport activities. In our model, TWD1 is thought to

be a linker between PGP1 and PGP19. Such an activation would be fulfilled through interaction of TWD1 with the NBF2 of the PGPs. Detailed structure analysis of mammalian PGPs revealed that tertiary structure of the two NBDs of a full ABC molecule, obtained by association of two half ABC molecules, would present different substrate affinity properties (Dey *et al.*, 1997). The likely difference in the tertiary structure, supported by the difference in amino acid sequence, would explain directly the difference in substrate specificity through TWD1 interaction.

The regulation of the PGPs by TWD1 might be transient as over-expression of TWD1, in contrast to over-expression of PGP1 and PGP19, did not increase auxin transport capacities, respectively. This is surprising as *TWD1* expression is several folds lower than those of *PGP1* and *PGP19*. In our model TWD1 would "jump" on freshly provided PGP1 and PGP19 by over-expression. The latter has been suggested to be responsible for the unsuccessful demonstration of a murine MDR3/FKBP12 complex in yeast (Hemenway and Heitman, 1996).

This model would furthermore suggest that in the situation of requirement of increasing auxin transport capacities, first, an activation of auxin transport units through PGP1/TWD1/PGP19 interaction would take place. Second, expression of *PGP1* and *PGP19* would be increased; induction of both has been shown to be IAA-dependent.

All data are inline with the concept that all three proteins are gathered within a ternary complex. All attempts to demonstrate it by co-immunolocalisation failed so far. The difference in growth phenotypes between *pgp1* and *pgp19* plants is also not in accordance with the existence of this ternary complex. The immunolocalization pattern of PGP1 which correlates with the mild effect of the PGP1 loss of function indicates that PGP1 is implicated in the root basipetal transport. The more severe phenotype of *pgp19* in comparison with *pgp1* plants suggests that PGP19 would more affect an auxin gradient what induces a stronger development default. This dissociation in auxin gradient affected suggests that PGP1 and PGP19 are localized in different tissues.

Although reductions of PGP-mediated auxin transport in *twd1* are in agreement with dwarfism and other auxin-related phenotypes, loss-of TWD1 action does not directly explain the "twisted syndrome". However, many helical orientations caused by

mutations are due to misassembly of microtubuli. Interestingly, mammalian multi-domain FKBPs have been shown to bind dynein via the N-terminal PPIase domain.

Finally, it remains to be solved why *twd1* mutant plant show more pronounced phenotypes at later stages compared to pgp1/pgp19 plants. One possibility is that other TWD1-interactors contribute to the full twisted phenotype. These might be MRP1/MRP2, but unfortunately their *in vivo* substrate is hard to guess and quadruplet knock-out lines are hard to get due to chromosomal distances. Other obvious candidates include interacting partner HSP90, a well-known developmental regulator and calmodulin.

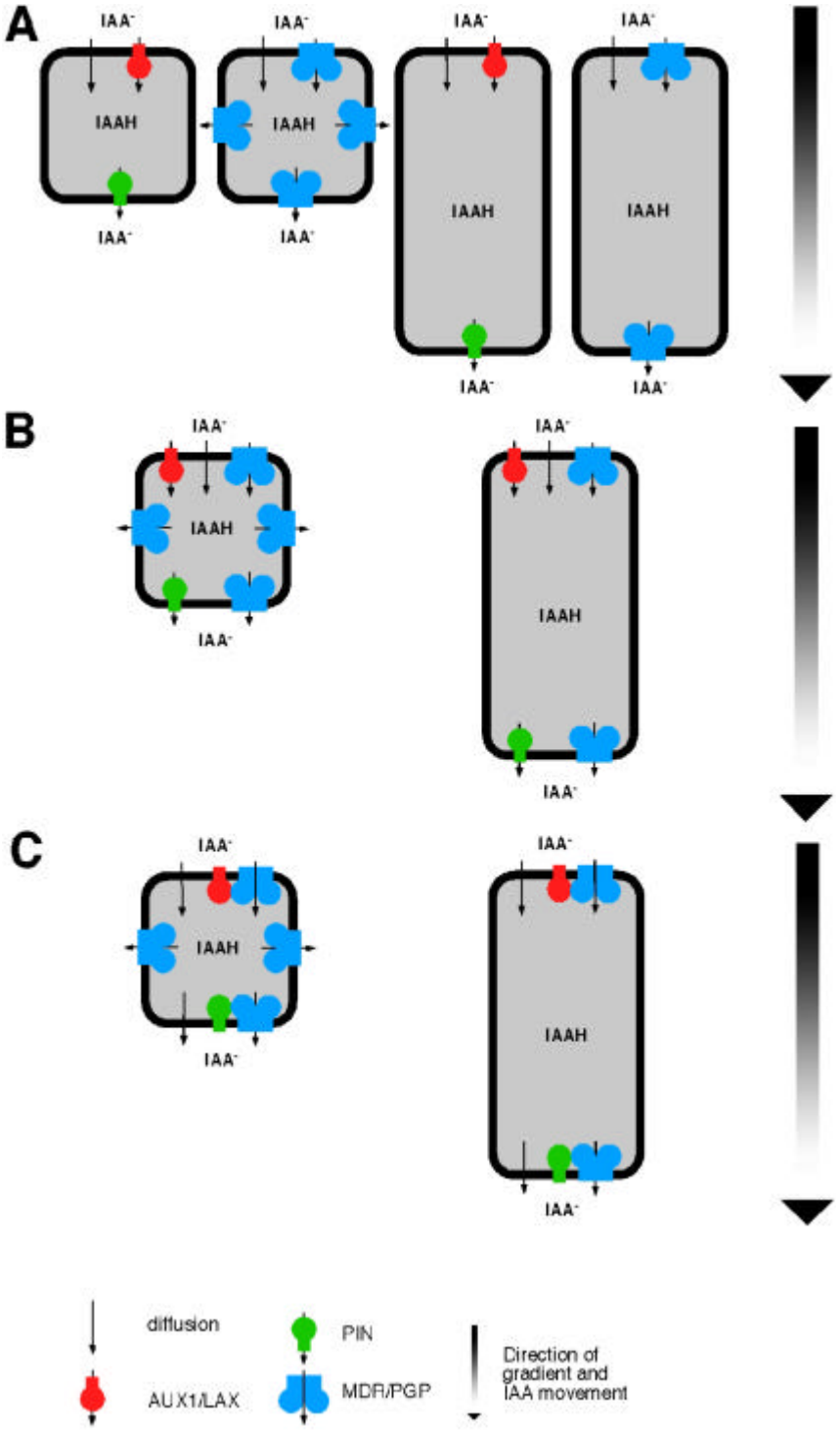

Fig. 29: Three scenarios describing how identified components of auxin influx (AUX1/LAX) and efflux (PGP/MDR and PIN) might function either alternatively (A), additive (B) or synergistic (C) in polar auxin transport (taken from Geisler and Murphy, 2007).

As described above, it has been suggested that PINs and PGPs work independently or together in auxin transport. Figure 29 is depicting how; depending on the nature of the tissue and local IAA concentration, PINs and PGPs would mediate auxin efflux.

In this model auxin enters the cell through either diffusion or catalyzed import, via the auxin symporter AUX1 or P-glycoprotein PGP4. Auxin is exported out of the cell via a PIN or PGP-mediated efflux mechanism (Santelia *et al.*, 2005). Three scenarios can be considered: (A.) an alternative model in which depending on the tissue and the cell size either PINs or PGPs would catalyze auxin export. PIN-mediated auxin efflux is likely in more mature tissue in which the cells are longer and the rate of auxin re-diffusion is not too important. This alternative model fits with polar localization of PIN2 in the epidermis and PGP1 in the cortex, respectively.

A mathematical model (Kramer, 2004) suggests that, based on cell size and auxin concentration criteria, in meristematic cells PIN proteins are not on their own sufficient to explain the rate of auxin transport seen *in planta*. Polar expression of PIN proteins would not be able to overcome a high auxin re-diffusion, phenomenon, which would inhibit the polar auxin transport. In an additive model (B.), both PINs and PGPs would independently mediate auxin transport activity.

A synergetic model (C.) may also support auxin transport in such cells where PINs would function as a regulator of PGPs activity. The non-polar localization of PGP1 in the root tip would be in line with the additive or synergetic auxin transport model.

Both the synergetic and additive models fulfill the requirements for the auxin transport rates in meristematic cells, in particular the non polar- localization of an auxin exporter. To date the influence of PINs on PGPs activity or *vice versa* is not yet established. Interaction analysis between PINs and PGPs should allow to discriminating the model corresponding to the cellular context.

VII ACKNOWLEDGEMENTS

I would like to thank the following persons for their respective contribution to this PhD

Prof. Enrico Martinoia for giving me the opportunity to perform this PhD within his laboratory

Dr. Markus Geisler for his supervision, the nice working atmosphere in his group and the fun we had all along

Members of Markus Geisler's group: Dr. Yoichiro Fukao, Aurélien Bailly, Vincent Vincenzetti, Sophie Oehring and Sonia Plaza for discussion and critics as well as for their contribution to the nice atmosphere in the laboratory

Dr. Michal Jasinski and Prof. Shiratake Katsuhiro for sharing their experience and the fun we had together within the group of Markus Geisler

Prof. Angus Murphy and Dr. Wendy Peer for their collaboration

Dr. Patricia Lariguet and Prof. Christian Fankhauser for helping in performance of phototropism experiments

To members of Enrico Martinoia's laboratory in Neuchâtel and Zurich for their help and good humour

VIII REFERENCES

Aghdasi, B., Ye, K., Resnick, A., Huang, A., Ha, H.C., Guo, X., Dawson, T.M., Dawson, V.L., and Snyder, S.H. (2001) FKBP12, the 12-kDa FK506-binding protein, is a physiological regulator of the cell cycle. Proc. Natl. Acad. Sci. USA **98**: 2425-2430

Ambudkar, S.V., Kimchi-Sarfaty C., Sauna, Z.E., Gottesman, M.M. (2003) P-glycoprotein: from genomics to mechanism. Oncogene **22**: 7468-7485

Arabidopsis Genome Initiative (2000) Analysis of the genome sequence of the flowering plant *Arabidopsis thaliana*. Nature **408**: 796-815

Axelos, M., Curie, C., Mazzolini, L., Bardet, C., and Lescure, B. (1992) A protocol for transient gene expression in *Arabidopsis thaliana* protoplasts isolated from cell suspension cultures. Plant Physiol Biochem **30**: 123-128

Baluska, F., Barlow, P.W., Baskin, T., Chen, R., Feldamn, L., Forde, B.G., Geisler, M., Jernstedt, J., Menzel, D., Muday, G., Murphy, A.S., Samaj, J., and Volkmann D. (2005) What is apical and what basal in plant root development? Trends Plant Sci **10**: 409-411

Benkova, E., Michniewicz, M., Sauer, M., Teichmann, T., Seifertova, D., Jurgens, G., and Friml, J. (2003) Local, efflux-dependent auxin gradients as a common module for plant organ formation. Cell **115**: 591-602

Berardini, T.Z., Bollmann, K., Sun, H., and Poethig, S. (2001) Regulation of vegetative phase change in *Arabidopsis thaliana* by cyclophilin 40. Science **291**: 2405-2407

Bisbal, C., Silhol, M., Laubenthal, H., Kaluza, T., Carnac, G., Milligan, L., Le Roy, F. and Salehzada, T. (2000) The 2'-5' oligoadenylate/ RNase L/ RNase L inhibitor pathway regulates both MyoD mRNA stability and muscle cell differentiation. Mol. Cell. Biol. **20**: 4959-4969

Blakeslee, J.J, Peer, W.A., and Murphy, A.S. (2005) Auxin transport. Curr. Opin. Plant Biol. **8**:1-7

Blilou, I., Xu, J., Wildwater, M., Willemsen, V., Paponov, I., Friml, J., Heidstra, R., Aida, M., Palme, K., and Scheres, B. (2005) The PIN auxin efflux facilitator network controls growth and patterning in *Arabidopsis* roots. Nature **433**: 39-44

Brown, D.E., Rashotte, A.M., Murphy, A.S., Normanly, J., Tague, B.W., Peer, W.A., Taiz, L., and Muday, G.K. (2001) Flavonoids act as negative regulators of auxin transport in vivo in Arabidopsis. Plant Physiol. **126**: 524-535

Cameron, A.M., Steiner, J.P., Roskams, A.J., Ali, S.M., Ronnett, G.V., and Snyder, S.H. (1995) Calcineurin associated with the inositol 1,4,5-trisphosphate receptor-FKBP12 complex modulates Ca2+ flux. Cell **83**: 463-472

Cardenas, M.E., Cruz, M.C., Del Poeta, M., Chung, N., Perfect, J.R., and Heitman, J. (1999) Antifungal activities of antineoplastic agents: *Saccharomyces cerevisiae* as a model system to study drug action. Clin. Microbiol. Rev. **12**: 583-611

Cardenas, M.E., Hemenway, C., Muir, R.S., Ye, R., Fiorentino, D., and Heitman, J. (1994) Immunophilins interact with calcineurin in the absence of exogenous immunosuppressive ligands. EMBO J **13**: 5944-5957

Casimoro, I., Marchant, A., Bhalerao, P.R., Beeckman, T., Dhooge, S., Swarup, R., Graham, N., Inzé, D., Sandberg, G., Casero, P.J., and Bennett, M. (2001) Auxin transport promotes Arabidopsis lateral root initiation. Plant Cell **13**: 843-852

Castro, A.F., Horton, J.K., Vanoye, C.G., Altenberg, G.A. (1999) Mechanism of Inhibition of P-glycoprotein-Mediated Drug Transport by Protein Kinase C Blockers. Biochem. Pharmacol. **58**: 1723-1733

Chakraburtty, K. (2001) Translational regulation by ABC systems. Res Microbiol. **152**:391-399

Chambraud, B., Radanyi, C., Camonis, J.H., Shazand, K., Rajkowski, K., and Baulieu, E.E. (1996) FAP48, a new protein that forms specific complexes with both immunophilins FKBP59 and FKBP12. Prevention by the immunosuppressant drugs FK506 and rapamycin. J. Biol Chem **271**: 32923-32929

Chambraud, B., Radanyi, C., Camonis, J.H., Rajkowski, K., Schumacher, M., and Baulieu, E.E. (1999) Immunophilins, Refsum disease, and lupus nephritis: the peroxisomal enzyme phytanoyl-COA alpha-hydroxylase is a new FKBP-associated protein. Proc. Natl. Acad. Sci. USA **96**: 2104-2109

Chen, R.J., Hilson, P., Sedbrook, J., Rosen, E., Caspar, T., and Masson, P.H. (1998) The Arabidopsis thaliana AGRAVITROPIC 1 gene encodes a component of the polar-auxin-transport efflux carrier. Proc. Natl. Acad. Sci. USA **95**: 15112-15117

Chen, Y-G., Liu, F. and Massagué J. (1997) Mechanism of TGFß receptor inhibition by FKBP12. EMBO J. **16**:3866-3876

Ciesielski T. (1872) Untersuchungen über die Abwärtskrümmung der Wurzel. Beitrage zur Biologie der Pflanzen **1**:1-30

Cohen, J.D. and Bandurski, R.S. (1982) Chemistry and physiology of the bound auxins. Annu. Rev.plant Physiol., **33**:403-430

Cruz, MC., Cavallo, LM., Gorlach, JM., Cox, G., Perfect, JR., Cardenas, ME., Heitman, J. (1999) Rapamycin antifungal action is mediated via conserved complexes with FKBP12 and TOR kinase homologs in Cryptococcus neoformans. Mol Cell Biol. **19**: 4101-12

Darwin, C., and Darwin, F. (1881) The power of movement in plants. Darwins gesammelte Werke, Vol. 13, Schweizer-bart'sche Verlagsbuchhandlung, Stuttgart, Germany

Das, A.K., Cohen, P.T.W., and Barford, D. (1998) The structure of the tetratricopeptide repeats of protein phosphatase 5: implications for the TPR-mediated protein-protein interactions. EMBO J **17**: 1192-1199

Dassa, E. (2003) Phylogenetic and functional classification of ABC (ATP-binding Cassette) systems. *In*: S.P:C. Cole, K. Kuchler, C.F Higgins, I.B.Holland eds, ABC Transporters: from Bacteria to Man, Elsevier, Amsterdam, pp 3-35.

Davies, T.G.E., Theodoulou, F.L., Hallahan, D.L. and Forde, B.G. (1996) Cloning and characterization of a novel P-glycoprotein homologue from barley. Gene **199**:195-202

Delbarre, A., Muller, P., and Guern, J. (1998) Short-lived and phosphorylated proteins contribute to carrier-mediated efflux, but not to influx, of auxin in suspension-cultured tobacco cells. Plant Physiol. **116**: 833-844

Dey, S., Ramachandra, M., Oastan, I., Gottesman, M. (1997) Evidence for two nonidentical drug-intercation sites in the human P-glycoprotein. Proc. Natl. Acad. Sci. USA **94**: 10594-10599

Dolinski, K., Muir, S., Cardenas, M., and Heitman, J. (1997) All cyclophilins and FK506 binding proteins are, individually and collectively, dispensable for viability in *Saccharomyces cerevisiae*. Proc. Natl. Acad. Sci. USA **94**: 13093-13098

Dornan, J., Page, A.P., Taylor, P., Wu, S-Y., Winter, A.D., Husi, H., Walkinshaw, M.D. (1999) Biochemical and structural characterization of a divergent loop cyclophilin from *Caenorhabditis elegans*. J. Biol. Chem **274**:34877-34883

Dudler, R., and Hertig, C. (1992) Structure of an *mdr*-like gene from *Arabidopsis thaliana* J. Biol. Chem. **267**: 5882-5888

Epand, RF., Epand, RM. (1991) The new potent immunosuppressant FK-506 reverses multidrug resistance in Chinese hamster ovary cells. Anticancer Drug Des. **6**: 189-93

Elroy-Stein, O., and Moss, B. (1991) Gene Expression Using the Vaccinia Virus/T7 RNA Polymerase Hybrid System. In Current Protocols in Molecular Biology, (F.M. Ausubel, R. Brent, R.E. Kinston, D.D. Moore, J.A. Smith, J.C. Seidman, and K. Struhl, eds) p. 16.19.11-16.19.19. John Wiley & Sons, Inc. New York, 1991

Faure J.D., Vittorioso P., Santoni V., Fraisier V., Prinsen E., Barlier I., Van Onckelen H., Caboche M., and Bellini C. (1998) The PASTICCINO genes of *Arabidopsis thaliana* are involved in the control of cell division and differentiation. Development **125**: 909-918

Fath, M.J., and Kolter, R. (1993) ABC transporters –bacterial exporters. Microbiol. Rev. **57**:995-1017

Ferte, J., Kuhnel, J.M., Chapuis, G., Rolland, Y., Lewin, G., and Schwaller, M.A. (1999) Flavonoid-related modulators of multidrug resistance: Synthesis, pharmacological activity, and structure-activity relationships. Journal of Medicinal Chemistry **42**: 478-489

Fischer G., Bang, H., Mech C.(1984) Nachweis einer enzymkatalyse die *cis-trans* isomerisierung der peptidbindung in prolinhaltigen peptiden. Biomedica Biochemica Acta **43**:1101-1111

Folkes, L.K., and Wardman, P. (2001) Oxidative activation of indole-3-acetic acids to cytotoxic species-a potential new role for plant auxins in cancer therapy. Biochem. Pharmacol. **61**: 129-126

Friml. J. (2003) Auxin transport - shaping the plant. Curr. Opin. Plant Biol. **6**: 7-12

Friml, J., and Palme, K. (2002) Polar auxin transport - old questions and new concepts? Plant Molecular Biology **49**: 273-284

Friml, J., and Wisnieswska J. (2004) Auxin as an intercellular signal. Annual Plant Reviews, **16**: 1-26

Friml, J., Wisniewska, J., Benkova, E., Mendgen, K., and Palme, K. (2002) Lateral relocation of auxin efflux regulator PIN3 mediates tropism in Arabidopsis. Nature **415**: 806-809

Friml, J., Benkova, E., Blilou, I., Wisniewska, J., Hamann, T., Ljung, K., Woody, S., Sandberg, G., Scheres, B., Jurgens, G., and Palme, K. (2002) AtPIN4 mediates sink-driven auxin gradients and root patterning in Arabidopsis. Cell **108**: 661-673

Fuglsang, A.T., Visconti, S., Drumm, K., Jahn, T., Stensballe, A., Mattei, B., Jensen, O.N., Aducci, P., and Palmgren, M.G. (1999) Binding of 14-3-3 protein to the plasma membrane H(+)-ATPase AHA2 involves the three C-terminal residues Tyr(946)-Thr-Val and requires phosphorylation of Thr(947). J. Biol. Chem. **274**: 36774-36780

Gaedeke, N., Klein, M., Kolukisaoglu, U., Forestier, C., Muller, A., Ansorge, M., Becker D., Mamnun, Y., Kuchler, K., Schulz, B., Mueller-Roeber, B., Martinoia, E. (2001) The *Arabidopsis thaliana* ABC transporter AtMRP5 controls root development and stomatal movement. EMBO J. **20**: 1875-1887

Galweiler, L., Guan, C.H., Muller, A., Wisman, E., Mendgen, K., Yephremov, A., and Palme, K. (1998) Regulation of polar auxin transport by AtPIN1 in Arabidopsis vascular tissue. Science **282**: 2226-2230

Garcia, O., Bouigue, P., Forestier, C., and Dassa E. (2004) Inventory and comparative analysis of rice and Arabidopsis ATP-binding cassette (ABC) systems. J. Mol: Biol. **343**:249-265

Geisler, M., Blakeslee, J.J., Bouchard, R., Lee, O.R., Vincenzetti, V., Bandyopadhyay, A., Titapiwatanakun, B., Peer, W.A., Bailly, A., Richards, E.L., Ejendal, K.F.K., Smith, A.P., Baroux, C., Grossniklaus, U., Müller, A., Hrycyna, C.A., Dudler, R., Murphy, A.S., and Martinoia, E. (2005) Cellular efflux of auxin catalyzed by the Arabidopsis MDR/PGP transporter AtPGP1. Plant J. **44**:179-94

Geisler, M., Frangne, N., Gomès, E., Martinoia, E., and Palmgren, M.G. (2000) The ACA4 gene of *Arabidopsis* encodes a vacuolar membrane calcium pump that improves salt tolerance in yeast. Plant Physiol. **124**: 1814-1827

Geisler, M., Girin, M., Brandt, D., Vincenzetti, V., Plaza, S., Paris, N., Kobae, Y., Maeshima, M., Billion, K., Kolukisaoglu, U.H., Schulz, B., Martinoia, E. (2004) Arabidopsis Immunophilin-like TWD1 Functionally Interacts with Vacuolar ABC Transporters. Mol. Biol. Cell. **15**: 3393-3405

Geisler, M., Kolukisaoglu, H.U., Bouchard, R., Billion, K., Berger, J., Saal, B., Frangne, N., Koncz-Kalman, Z., Koncz, C., Dudler, R., Blakeslee, J.J., Murphy, A.S., Martinoia, E., and Schulz, B. (2003) TWISTED DWARF1, a unique plasma membrane-anchored immunophilin-like protein, interacts with Arabidopsis multidrug resistance-like transporters AtPGP1 and AtPGP19. Mol. Biol. Cell. **14**: 4238-4249

Geisler, M and Murphy, A.S. (2006) The ABC of auxin transport: the role of p-glycoproteins in plant development. FEBS Lett. (in press)

Geldner, N., Friml, J., Stierhof, Y.D., Jurgens, G., and Palme, K. (2001) Auxin transport inhibitors block PIN1 cycling and vesicle trafficking. Nature **413**: 425-428

Goel, M., Garcia, R., Estacion, M., Schilling, WP. (2001) Regulation of Drosophila TRPL channels by immunophilin FKBP59. J. Biol. Chem **276**:38762-38773

Gopalan, G., He, Z., Balmer, Y., Romano, P., Gupta, R., Héroux, A., Buchanan, B.B., Swaminathan, K., and Luan S. (2004) Structural analysis uncovers a role for redox in regulating FKBP13, an immunophilin of the chloroplast thylakoid lumen. Proc. Natl. Acad. Sci. USA **101**: 13945-13950

Gil, P., Dewey, E., Friml, J., Zhao, Y., Snowden, K.C., Putterill, J., Palme, K., Estelle, M., and Chory, J. (2001) BIG: a calossin-like protein required for polar auxin transport in *Arabidopsis*. Genes Dev **15**: 1985-1997

Gupta, R., Mould, R.M., He, Z., and Luan, S. (2002) A chloroplast FKBP interacts with and affects the accumulation of Rieske subunit of cytochrome *bf* complex. Proc. Natl. Acad. Sci. USA **99**: 15806-15811

Harrar, Y., Bellec, Y., Bellini C., and Faure J. D. (2003) Hormonal Control of Cell Proliferation Requires *PASTICCINO* Genes. Plant Physiol. **132**:1217-1227

Harrar, Y., Bellini, C., and Faure, J.D. (2001) FKBPs: at the crossroads of folding and transduction. Trends Plant Sci. **6**: 426-431

He, Z., Li, L., and Luan, S. (2004) Immunophilins and Parvulins. Superfamily of peptidyl prolyl isomerases in arabidopsis. Plant Physiol. **134**: 1248-1267

Hemenway, C.S., and Heitman, J. (1996) Immunosuppressant target protein FKBP12 is required for P-glycoprotein function in yeast. J. Biol. Chem. **271**: 18527-18534

Hrycyna, C.A., Ramachandra, M., Pastan, I., and Gottesman, M.M. (1998) Functional expression of human P-glycoprotein from plasmids using vaccinia virus-bacteriophage T7 RNA polymerase system. In Methods in Enzymology: ABC Transporters: Biochemical, Cellular, and Molecular Aspects, S.V. Ambudkar and M.M. Gottesman, eds (San Diego, CA: Academic Press), pp. 456-473

Holland, B.I., Cole, S.P.C., Kuchler, K., and Higgins, C.F. (2003) ABC proteins. From bacteria to men. Academic press

Jasinski, M., Ducos, E., Martinoia, E., and Boutry, M. (2003) The ATP-binding cassette transporters: Structure, function, and gene family comparison between rice and Arabidopsis. Plant Physiol. **131**: 1169-1177

Jasinski, M., Stukkens, Y., Degand, H., Purnelle, B., Marchand-Brynaert, J. and Boutry, M. (2001) A plant plasma membrane ATP-binding cassette-type transporter is involved in antifugal terpenoid secretion. Plant Cell **13**:1095-1107

Jones, A.M. (1998) Auxin transport: down and out and up again. Science **282**: 2201-2202

Jones, S.E., DeMeo, J.S., Davies, N.W., Noonan, S.E., and Ross, J.J. (2005) Stems of the *Arabidopsis* pin1-1 mutant are not deficient in free indole-3-acetic acid. Planta **222(3)**: 530-534

Kamphausen, T., Fanghänel, J., Neumann, D., Schulz, B., and Rahfeld, J.-U. (2002) Characterisation of *Arabidopsis thaliana At*FKBP42 that is membrane bound and interacts with Hsp90. Plant J. **32**: 263-276

Kerk, N., Jiang, K.N., and Feldmann, K.A. (2000) Auxin metabolism in the root apical meristem. Plant Physiol **122**: 925-932

Kramer EM (2004) PIN and AUX/LAX: their role in auxin accumulation. Trends Plant Sci **9**:578-582

Krishna, R., and Mayer, L.D. (2001) Modulation of P-glycoprotein (PGP) mediated multidrug resistance (MDR) using chemosensitizers: recent advances in the design of selective MDR modulators. Curr. Med. Chem. Anti-Canc. Agents **1**: 163-174

Kurek, I., Pirkl, F., Fischer, E., Buchner, J., and Breiman, A. (2002) Wheat FKBP73 functions in vitro as a molecular chaperone idenpendently of ist peptidyl-prolyl cis-trans isomerase activity. Planta **215**: 119-126

Lamb, J. R., Tugendreich, S., and Hieter, P. (1995) Tetratrico-peptide repeat interactions: to TPR or not to TPR? Trends Biochem. Sci. **20**: 257-259

Leonhardt, N., Marin, E., Vavasseur, A., and Forestier, C. (1997) The evidence for the existence of a sulfonylurea-receptor-like proteins in plants: modulation of stomatal movements and guard cells potassium channels by sulfonylureas and potassium channel openers. Proc. Natl. Acad. Sci. USA **94**: 14156-14161

Leyser, O. (2005) Auxin distribution and plant pattern formation: how many angels can dance on the point of PIN? Cell **121**: 819-822

Lin, R., and Wang, H. (2005) Two Homologous ATP-Binding Cassette Transporter proteins, AtMDR1 and AtPGP1, Regulate Arabidopsis Photomorphogenesis and Root Development by Mediating Polar Auxin Transport. Plant Physiol. **138**: 949-964

Lomax, T.L., Mehlhorn, R.J., and Briggs, W.R. (1985) Active Auxin Uptake by Zucchini Membrane-Vesicles - Quantitation Using Electron-Spin-Resonance Volume and Delta-Ph Determinations. Proc. Natl. Acad. Sci. USA **82**: 6541-6545

Lomax, T.L., Muday, G.K., and Rubery, P.H. (1995) Auxin Transport. In Plant hormones: physiology, biochemistry, and molecular biology, P.J. Davies, ed (Dordrecht, Netherlands: Kluwer Academic Press), pp. 509-530

Luan, S., Kudla, J., Gruissem, W., and Schreiber, S.L. (1996) Molecular characterization of a FKBP-type immunophilin from higher plants. Proc. Natl. Acad. Sci. USA **93**: 6964-6969

Luschnig, C. (2002) Auxin transport: ABC proteins join the club. Trends Plant Sci. **7**: 329-32

Luschnig, C., Gaxiola, R., Grisafi, P., and Fink, G. (1998) EIR1, a root specific protein involved in auxin transport, is required for gravitropism in *Arabidopsis thaliana.* Genes Dev. **12**: 2175-2187

Mancuso S., Marras AM., Magnus V., Baluska F. (2005) Non invasive and continuous recordings of auxin fluxes in intact root apex with a carbon nanotube-modified and self-referencing microelectrode. Anal Biochem. **341**: 344-51

Martinoia, E., Klein, M., Geisler, M., Bovet., L., Forestier, C., Kolukisaoglu, U., Muller-Rober, B., and Schultz, B. (2002) Multifunctionality of plant ABC transporters - more than just detoxifiers. Planta **214**: 345-355

Mealey, K.L., Barhoumi, R., Burghardt, R.C., McIntyre, B.S., Sylvester, P.W., Hosick, H.L., and Kochevar, D.T. (1999) Immunosuppressant inhibition of P-glycoprotein function is independent of drug-induced suppression of peptide-prolyl isomerase and calcineurin activity. Cancer Chemother Pharmacol. **44**: 152-158

Moss, B. (1991) Vacinia Virus-A Tool for Research and Vaccine Development. Science **252**: 1662-1667

Muday, G., and DeLong, A. (2001) Polar auxin transport: controlling where and how much. Trends Plant Sci. **6**: 535-542

Muday, G.K., and Murphy, A.S. (2002) An emerging model of auxin transport regulation. Plant Cell **14**: 293-299

Muller, A., Guan, C.H., Galweiler, L., Tanzler, P., Huijser, P., Marchant, A., Parry, G., Bennett, M., Wisman, E., and Palme, K. (1998) AtPIN2 defines a locus of Arabidopsis for root gravitropism control. EMBO J **17**: 6903-6911

Multani, D.S., Briggs, S.P., Chamberlin, M.A., Blakeslee, J.J., Murphy, A.S., and Johal, G.S. (2003) Loss of an MDR transporter in compact stalks of maize br2 and sorghum dw3 mutants. Science **302**: 81-84

Murphy, A., Peer, W.A., and Taiz, L. (2000) Regulation of auxin transport by aminopeptidases and endogenous flavonoids. Planta **211**: 315-324

Murphy, A.S., Hoogner, K.R., Peer, W.A., and Taiz, L. (2002) Identification, purification, and molecular cloning of N-1-naphthylphthalmic acid-binding plasma membrane-associated aminopeptidases from Arabidopsis. Plant Physiol. **128**: 935-950

Moss, B. (1991) Vacinia Virus-A Tool for Research and Vaccine Development. Science **252**: 1662-1667

Nelson, E.J., Zinkin, N.T., and Hinkle, P.M. (1998) Fluorescence methods to assess multidrug resistance in individual cells. Cancer Chemother. Pharmacol. **42**: 292-299

Németh, K., Salchert, K., Putnoky, P., Bhalerao, R., Koncz-Kálmán, Z., Stankovic-Stangeland, B., Bakó, L., Mathur, J., Okrész, L., Stabel, S., Geigenberger, P., Stitt, M., Rédei, G.P., Schell, J., and Koncz, C. (1998) Pleiotropic control of glucose and hormone responses by PRL1, a nuclear WD protein, in *Arabidopsis*. Genes Dev. **12**: 3059-3073

Noh, B., Murphy, A.S., and Spalding, E.P. (2001) Multidrug resistance-like genes of Arabidopsis required for auxin transport and auxin-mediated development. Plant Cell **13**: 2441-2454

Noh, B., Bandyopadhyay, A., Peer, W.A., Spalding, E.P., and Murphy, A.S. (2003) Enhanced gravi- and phototropism in plant mdr mutants mislocalizing the auxin efflux protein PIN1. Nature **423**: 999-1002

Nuhse TS, Stensballe A, Jensen ON, Peck SC. (2004) Phosphoproteomics of the Arabidopsis plasma membrane and a new phosphorylation site database. Plant Cell **16**: 2394-405

Ottenschlager I, Wolff P, Wolverton C, Bhalerao RP, Sandberg G, Ishikawa H, Evans M, Palme K. (2003) Gravity-regulated differential auxin transport from columella to lateral root cap cells. Proc. Natl. Acad. Sci USA **100**: 2987-91

Owens-Grillo, J.K., Stancato, L.F., Hoffmann, K., Pratt, W.B., and Krishna, P. (1996) Binding of immunophilins to the 90 kDa heat shock protein (hsp90) via a tetratrico-peptide repeat domain is a conserved protein interaction on plants. Biochemistry **35**: 15249-15255

Paciorek, T., Zazimalova, E., Ruthardt, N., Petrasek, ,J., Stierhof, Y-D., Kleine-Vehn, J., Morris, D.A., Emans, N., Jürgens, G., Geldner, N., and Friml, J. (2005) Auxin inhibits endocytosis and promotes its own efflux from cells. Nature **435**: 1251-1256

Palme, K., and Galweiler, L. (1999) PIN-pointing the molecular basis of auxin transport. Curr. Opin. Plant Biol.**2**: 375-381

Patterson, E.C., Schaub, T., Coleman, E. J., and Davis, E.C. (2000) Developmental regulation of FKBP65 an ER-localized extracellular matrix binding-protein. Mol. Biol. Cell. **11**: 3925-3935

Pedersen, K.M., Finsen, B. Celis, J.E., and Jensen N.A. (1999) muFKBP38: A novel murine immunophilin homolog differentially expressed in Schwannoma cells and central nervous system neurons in vivo. Electrophoresis **20**: 249-255

Peer, W.A., Brown, D.E., Tague, B.W., Muday, G.K., Taiz, L., and Murphy, A.S. (2001) Flavonoid accumulation patterns of transparent testa mutants of Arabidopsis. Plant Physiol. **126**: 536-548

Peer, W.A., Bandyopadhyay, A., Blakeslee, J.J., Makam, S.N., Chen, R., Mason, P., and Murphy, A. (2004) Variation in expression and protein localization of the PIN family of auxin efflux facilitator proteins in flavonoid mutants with altered auxin transport in Arabidopsis thaliana. Plant Cell **16**: 1898-1911

Pérez-Pérez, J.M., Ponce, M.R., and Micol, J.L. (2004) The ULTRACURVATA2 gene of Arabidopüsis encodes an FK506-binding protein involved in auxin and brassinosteroid signaling. Plant Physiol **134**: 101-117

Pratt, W.B., Krishna P., and Olsen L.J. (2001) Hsp90-binding immunophilins in plants: the protein movers. Trends Plant Sci. **6**: 54-58

Prusty, R., Grisafi, P., and Fink, G.R. (2004) The plant hormone indoleacetic acid induces invasive growth in Saccharomyces cerevisiae. Proc. Natl. Acad. Sci. USA **101**: 4153-4157

Ramaen, O., Sizun, C., Pamlard, O., Jaquet, E., and Lallemand, J.Y. (2005) Attempts to characterise the NBD heterodimer of MRP1: transient complex formation involves G771 of the ABC signature sequence but does not enhance the intrinsic ATPase activity. Biochem J. (in press)

Rashotte, A.M., Brady, S., Reed, R., Ante, S., and Muday, G.K. (2000) Basipetal auxin transport is required for gravitropism in roots of *Arabidopsis*. Plant Physiol. **122**: 481-490

Rashotte, A.M., DeLong, A., and Muday, G.K. (2001) Genetic and chemical reductions in protein phosphatase activity alter auxin transport, gravity response and lateral root growth. Plant Cell **13**: 1683-1697

Raven, J.A. (1975) Transport of indoleacetic acid in plant cells in relation to pH and electrical potential gradients, and its significance for polar IAA transport. New phytol, **74**:163-172

Raymond, M., Gros, P., Whiteway, M., and Thomas, D.Y. (1992) Functional complementation of yeast ste6 by a mammalian multidrug resistance mdr gene. Science **256**: 232-234

Rea, A.P., Ze-Sheng, L., Yu-Ping, L., Drozdowicz, Y.M., and Martinoia, E. (1998) From vacuolar GS-X pumps to multispecific ABC transporters. Annu. Rev. Plant Physiol. **49**: 727-760

Reddy, R.K., Kurek, I., Silverstein, A.M., Chinkers, M., Breiman, A. and Krishna, P. (1998) High-molecular-weight FK506-binding proteins are components of heat-shock protein 90 heterocomplexes in wheat germ lysate. Plant Physiol. **118**: 1395-1402

Reinhardt, D., Mandel, T., and Kuhlemeier, C. (2000) Auxin regulates the initiation and radial position of plant lateral organs. Plant Cell **12**: 507-518

Riggs, D.L., Roberts, P.J., Chirillo, S.C., Cheung-Flynn, J., Prapapanich, V., Ratajczak, T., Gaber, R., Picard, D., and Smith, D.F. (2003) The Hsp90-binding peptidylprolyl isomerase FKBP52 potentiates glucocorticoid signaling in vivo. EMBO J **22**: 1158-1167

Rokka, A., Aro, E-M., Herrmann, R.G., Andersson, B., and Vener, A.V. (2000) Dephosphorylation of photosystem II reaction center proteins in plant photosynthetic membranes as an immediate response to abrupt elevation of temperature. Plant Physiol. **123**: 1525-1535

Romano, P., Gray, J., Horton, P., and Luan S. (2005) Plant immunophilins: functional versatility beyond protein maturation. New Phytologist. **166**: 753-769

Romano, P.G.N., Horton, P., Gray, J.E. (2004) The Arabidopsis cyclophilin gene family. Plant Physiol. **134**:1268-1282

Rubery, P.H and Sheldrake, A.R. (1974) Carrier-mediated auxin transport. Planta **188**:101-121

Ruegger, M., Dewey, E., Hobbie, L., Brown, D., Bernasconi, P., Turner, J., Muday, G.K., and Estelle M (1997) Reduced naphthylphtalamic acid binding in the tir3 mutant of Arabidopsis is associated with a reduction in polar auxin transport and diverse morphological defects. Plant Cell **9**: 745-757

Sabatini, S., Beis, D., Wolkenfelt, H., Murfett, J.,Guilfoyle, T., Malamy, J., Benfey, P., Leyser, O., Bechtold, N., Weisbeek, P., and Scheres, B. (1999) An auxin-dependent distal organizer of pattern and polarity in the *Arabidopsis* root. Cell **99**: 463-472

Samaj, J., Read, N., D., Volkmann, D., Menzel, D., and Baluska, F. (2005) The endocytic network in plants. Trends in cell biology **15**: 425-433

Sananes, N., Baulieu, E.E., Le Goascogne, C. (1998) Stage-specific expression of the immunophiln FKBP59 messenger ribonucleic acid and protein during differentiation of male germ cells in rabbits and rats. Biol Reprod. **58**: 353-60

Sanchez-Fernandez, R., Davies, T.G.E., Coleman, J.O.D., and Rea, P.A. (2001) The *Arabidopsis thaliana* ABC protein superfamily, a complete inventory. J. Biol. Chem. **276**: 30231-30244

Santelia, D., Vincenzetti, V., Bovet, L., Fukao, Y., Düchtig, P., Martinoia, E., and Geisler, M. (2005) MDR-like ABC transporter AtPGP4 is involved in auxin-mediated lateral root and root hair development. FEBS Lett. **579(24)**: 5399-5406

Schiene, C., and Fischer, G. (2000) Enzymes that catalyse the restructuring of proteins. Curr. Opin. Struct. Biol. **10**: 40-45

Schmid, M., Davison, T. S., Henz, S. R., Pape, U. J., Demar, M., Vingron, M. Schölkopf, B. Weigel, D., and Lohmann, J. (2005) A gene expression map of Arabidopsis development. Nature Genetics **37**: 501-506

Schnell, D.J. (1998) Protein targeting to the thylakoid membrane. Annu. Rev. Plant. Physiol. Plant Mol. Biol. **49**: 97-126

Schubert, M., Petersson, U.A., Haas, B.J., Funk, C., Schroder, W.P., and Kieselbach, T. (2002) Proteome map of the chloroplast lumen of *Arabidopsis thaliana*. J. Biol. Chem. **277**: 8354-65

Shi, J., Kim, K.N., Ritz, O., Albrecht, V., Gupta, R., Harter, K., Luan, S., and Kudla, J. (1999) Novel protein kinases associated with calcineurin B-like calcium sensors in *Arabidopsis*. Plant Cell **11**: 2393-2406

Sidler, M., Hassa, P., Hasan, S., Ringli, C., and Dudler, R. (1998) Involvement of an ABC transporter in a developmental pathway regulating hypocotyl cell elongation in the light. Plant Cell **10**: 1623-1636

Silverstein, A.M., Galigniana, M.D., Kanelakis, K.C., Radanyi, C., Renoir, J.M., and Pratt, W.B. (1999) Different regions of the immunophilin FKBP52 determine its association with the glucocorticoid receptor, hsp90, and cytoplasmic dynein. J. Biol. Chem. **274**: 36980-36986

Smart, C.C. and Fleming, A.J. (1996) Hormonal and environmental regulation of a plant PDR5-like ABC transporter. J. Biol. Chem. **271**:19351-19357

Swarup, R., Friml, J., Marchant, A., Ljung, K., Sandberg, G., Palme, K., and Benett, M. (2001) Localisation of the auxin permease AUX1 suggests two functionally distinct hormone transport pathways operate in the *Arabidopsis* root apex. Genes Dev. **15**: 2648-2653

Swarup, R., Kargul, J., Marchant, A., Zadik, D., Rahman, A., Mills, R., Yemm, A., May, S., Williams, L., Millner, P., Tsurumi, S., Moore, L., Napier, R.M., Kerr, I., and Bennett, M.J. (2004) Structure-function analysis of the presumptive Arabidopsis auxin permease AUX1. Plant Cell **16**: 3069-3083

Teale, W.D., Paponov, I.A., Ditengou, F., and Palme, K (2005) Auxin and the developing root of Arabidopsis thaliana. Physiol. Plantarum. **123**: 130-138

Terasaka, K., Blakeslee, J.J., Titapiwatanakun, B., Peer, W.A., Bandyopadhyaay, A., Makam, S.N., Lee, O.R., Richards, E., Murphy, A.S., Sato, F., and Yazaki, K. (2005) PGP4, an ATP-binding cassette p-glycoprotein, catalyzes auxin transport in Arabidopsis thaliana roots. Plant Cell (in press)

Theodoulou, F. L. (2000) Plant ABC transporters. Biochimica and Biophysica Acta **1465**: 79-103

Thimann KV. (1977) Hormone action in the whole life of plants. Amherst: University of Massachusetts Press

Thomas, C., Rajagopal, A., Windsor, B., Dudler, R., Lloyd, A., and Roux, S.J. (2000) A role for ectophosphatase in xenobiotic resistance. Plant Cell **12**: 519-533

Timerman, AP., Wiederrecht, G., Marcy, A., Fleischer, S. (1995) Characterization of an exchange reaction between soluble FKBP-12 and the FKBP ryanodine receptor complex. Modulation by FKBP mutants deficient in peptidyl-prolyl isomerase activity. J. Biol. Chem. **270**: 2451-2459

Tyzack, J.K., Wang, X.M., Belsham, G.J. and Proud C.G. (2000) ABC50 interacts with eukaryotic initiation factor 2 and associates with the ribosome in an ATP-dependant manner. J. Biol. Chem. **275**:34131-34139

Überlacker, B, and Werr, W. (1996) Vectors with rare-cutter restriction enzyme sites for expression of open reading frames in transgenic plants. Mol. Breeding **2**: 293-295

Urbatsch, I.L., Sankaran, B., Bhagat, S., Senior, A.E. (1995) Both P-glycoprotein nucleotide-binding sites are catalytically active. J Biol Chem. **270**: 26956-61

Van Duyne, G.D., Staendaert, R.F., Karplus, P.A., Schreiber, S.L., and Clardy, J. (1991) Atomic structure of FKBP-FK506, an immunophilin-ligand complex. Science **252**: 839-842

Vittorioso, P., Cowling, R., Faure, J.D., Caboche, M., and Bellini, C. (1998) Mutation in the *Arabidopsis PASTICCINO1* gene, which encodes a new FK506-binding protein-like protein, has a dramatic effect on plant development. Mol. Cell. Biol. **18**: 3034-3043

Vucich, V.A., and Gasser, C.S. (1996) Novel structure of a high molecular weight FK506 binding protein from *Arabidopsis thaliana*. Mol. Gen. Genet. **252**: 510-517

Wang, W., Takezawa, D. and Pooviah, B.W. (1997) A potato cDNA encodes a homologue of mammalian multidrug resistance P-glycoprotein. Plant Mol. Biol. **31**: 683-687

Weixel, K.M., and Bradbury, N.A. (2000) The carboxyl terminus of the cystic fibrosis transmembrane conductance regulator binds to AP-2 clathrin adaptors. J. Biol. Chem. **275**: 3655-3660

Went, F.W. (1974) Reflections and speculations. Annu. Rev. Plant Physiol. **25**: 1-26

Windsor, B., Roux S.J., and Lloyd A. (2003) Multiherbicide tolerance conferred by AtPGP1 and apyrase overexpression in *Arabidopsis thaliana*. Nature Biotech. **21**: 428-433

Woodward, A.W., and Bartel B. (2005) Auxin: regulation, action and interaction. Annals of botany **95**: 707-735

Xu, Q., Liang, S., Kudla, J., and Luan, S. (1998) Molecular characterization of a plant FKBP12 that does not mediate action of FK506 and rapamycin. Plant J. **15**: 511-519

Yan, R., and Taylor, E.M. (2002) Neotrofin is transported out of brain by a saturable mechanism: Possible involvement of multidrug resistance and monocarboxylic acid transporters. Drug Metabolism and Disposition **30**: 513-518

Zhang, S.Z., and Morris, M.E. (2003) Effects of the flavonoids biochanin A, morin, phloretin, and silymarin on P-glycoprotein-mediated transport. Journal of Pharmacology and Experimental Therapeutics **304**: 1258-1267

Curriculum vitae

Name	BOUCHARD
First name	Rodolphe
Date/City of birth	24th October 1975 in Vierzon, France
Nationality	French

Education

October 2001-December 2005	University of Neuchâtel, University of Zurich, Switzerland PhD thesis under supervision of Prof. Enrico Martinoia and Dr. Markus Geisler
1999-2000	University of Orléans, Orléans, France Postgraduate degree (D.E.A) in Biology and Molecular and cellular Biophysics
1998-1999	University of Orléans, Orléans, France Maîtrise de biochimie equivalent to a Master's Degree in Biochemistry
1992-1993	Lycée Agricole de Chateauroux, Chateauroux, France Baccalaureat D'